Topics in String Geometry

Ismail Achmed-Zade

München 2020

Topics in String Geometry

Ismail Achmed-Zade

Dissertation
an der Physik
der Ludwig–Maximilians–Universität
München

vorgelegt von
Ismail Achmed-Zade
aus Altötting

München, den 18.02.2020

Erstgutachter: Dieter Lüst
Zweitgutachter: Michael Haack
Tag der mündlichen Prüfung: 24.4.2020

Contents

Zusammenfassung

Diese Arbeit besteht aus drei unabhängigen Teilen: Der erste beschäftigt sich mit T-Dualität, der zweite mit F-Theorie und der letzte mit Ricci-flachen Kähler Metriken auf nicht-kompakten Calabi-Yau Mannigfaltikeiten.

In dem ersten Kapitel konstruieren wir T-folds. In unserem Fall sind diese lokal durch Torusbündel, welche mit T-dualitätstransformationen verklebt sind, gegeben. Wir betrachten Fasern mit reellen Dimensionen $n = 2, 3, 4$. Insbesondere betrachten wir ein Model das durch einen, über eine durchstochene S^2 gefaserten, T^3 gegeben ist. Diese Faserung kann durch das Einfügen singulärer T^3 über den Löchern vervollständigt werden. Lokal unterzieht sich die Faser einer $SO(3, 3; \mathbb{R})$ Monodromie. Dadurch wird ein Beispiel einer globalen T-fold mit T^3 Fasern beschrieben. Wir geben einen kleinen Ausblick auf den Fall mit T^4 Fasern.

In dem zweiten Kapitel betrachten wir ein F-Theorie Model, welches zu einer $SU(5) \times U(1)$ Eichgruppe in vier Dimensionen führt. Das Model is durch eine singuläre, komplex 4-dimensionale, elliptisch gefaserte Calabi-Yau Varietät gegeben. Wir sprechen folgende Probleme an: Erstens ist das Model, aufgrund von $\mathbb{Q}$-faktoriellen terminalen Singularitäten, nicht krepant auflösbar. Diese liegen nicht auf der GUT-Brane und führen zu ungeladenen Hypermultiplets.

Das zweite und bei weitem schwerere Problem is das Auftreten eines nicht-flachen Punktes nach der Auflösung. Dies ist ein Punkt auf der GUT-Brane über welchem die Faser komplex zwei dimensional ist. Er liegt an dem Schnittpunkt verschiedener Materiekurven und sollte konventionell zu Yukawainteraktionen führen. Man findet den gewünschten Term im Superpotential im schwach gekoppelten Limit. Da der Ausdruck holomorph ist, bleibt der Term durch den gesamten Moduliraum erhalten.

In dem letzten Teil konstruieren wir explizit Ricci-flache Kähler Metriken in allen Kähler Klassen auf den Totalräumen gewisser Vektorbündel V über Fahnenmannigfaltigkeiten. Diese können nur geformt werden, wenn die kanonische Klasse der Mannigfaltigkeit $\mathscr{F}$ durch q teilbar ist. Dann gilt $V = \left(K_{\mathscr{F}}\right)^{1/q}\Big)^{\oplus q}$, wobei $K_{\mathscr{F}}$ das kanonische Bündel beschreibt. Man findet die gewünschten Metriken durch das Lösen einer Verallgemeinerung des Calabi Ansatzes.

Summary

This thesis is comprised of three independent parts: The first deals with T-duality, the second with F-theory and the final part with Ricci-flat Kähler metrics on non-compact Calabi-Yau manifolds.

In the first chapter we construct T-folds. In our case these are locally torus bundles glued together via T-duality transformations. We consider fibers of real dimensions $n = 2, 3, 4$. We in particular consider a model given by a T^3 fibered over a punctured S^2. The fibration can be completed by inserting singular T^3 fibers over the punctures. Locally around any puncture the fiber undergoes an $SO(3, 3; \mathbb{R})$ monodromy. Thus an example of a global T-fold with T^3 fibers is provided. We further provide a brief outlook on the case with T^4 fibers.

In the second chapter we study an F-theory model leading to an $SU(5) \times U(1)$ gauge theory in four dimensions. The model is given by a singular complex 4-dimensional elliptically fibered Calabi-Yau variety. We address two problems: Firstly the model is not crepantly resolvable, due to $\mathbb{Q}$-factorial terminal singularities. These lie away from the GUT brane and lead to uncharged hypermultiplets.

The second and more severe problem is the appearance of a non-flat point upon resolution. This is a point on the GUT brane over which the fiber is actually complex two dimensional. It lies at the intersection of various matter curves and should conventionally lead to a Yukawa-interaction. Taking the weak coupling limit we indeed find the desired part of the superpotential. Since the expression is holomorphic it survives throughout moduli space.

In the final part we construct explicitly Ricci-flat Kähler metrics in all Kähler classes on the total spaces of certain vector bundles V over flag manifolds. These can only be formed when the canonical class of the flag $\mathscr{F}$ is divisible by q. Then $V = \left(K_{\mathscr{F}}\right)^{1/q}\Big)^{\oplus q}$, where $K_{\mathscr{F}}$ denotes the canonical bundle. One finds the desired metrics by solving a generalization of Calabi's Ansatz.

Chapter 1

T-folds with higher rank fibers

This chapter deals with the results presented in [1]. We first give a brief introduction to T-duality. Then local examples of T-folds over circles and punctured disks are provided. Finally we construct a global example with T^3 fibers and finish we an ansatz for T^4 fibers.

1.1 Introduction to T-duality

We say that two Lagrangians L_1, L_2 are dual if they are different but lead to equation of motions whose solutions can be identified in a one to one manner. An elementary example is the harmonic oscillator with

$$L_1 = \frac{m}{2}\dot{x}^2 + \frac{k}{2}x^2 \tag{1.1}$$

$$L_2 = \frac{1}{2k}\dot{x}^2 + \frac{1}{2m}x^2. \tag{1.2}$$

We see that $(m, k) \mapsto (k^{-1}, m^{-1})$ leaves the solutions

$$x(t) = A\cos\left(\sqrt{\frac{k}{m}}t\right) + B\sin\left(\sqrt{\frac{k}{m}}t\right) \tag{1.3}$$

invariant.

In string theory a number of non-trivial dualities arise, due to the extended nature of the strings. Such dualities do not appear in regular quantum field theory, but can sometimes lead to surprising relations between fields theories that are seemingly unrelated. These dualities relate all observables in a one to one manner between dual theories.

One such duality is called T-duality as it arises in torus compactifications. Excellent reviews can be found in [2] [3]. The strings wrapping the torus can 'trade' their momentum in order to wrap non-trivial homology cycles, as we will explain now.

Let us start with the closed bosonic string compactified on a D-dimensional torus $T^D = \mathbb{R}^D/2\pi\Lambda_D$. Here $\Lambda_D = \langle e_i \rangle$ and its dual lattice is $\Lambda_D^* = \langle e^{*i} \rangle$. We choose the metric $e^i e^j = g_{ij} = \delta_{ij}$. Neglecting the dilaton the string sigma model is given by

$$S = -\frac{1}{4\pi\alpha'} \int_\Sigma d\sigma d\tau \;\; \eta^{ij} G_{\mu\nu} \partial_i X^\mu \partial_j X^\nu + \epsilon^{ij} B_{\mu\nu} \partial_i X^\mu \partial_j X^\nu, \tag{1.4}$$

where η is a Minkowski metric on the world sheet Σ and $\epsilon^{01} = -1$. If we consider the closed string we enforce for the uncompactified directions $\mu = D, ..., 25$:

$$X^\mu(\sigma + l, \tau) = X^\mu(\sigma, \tau) \tag{1.5}$$

where l is the string length. The solutions to the equations of motion of (1.4) can be decomposed into left and right movers $X^\mu(\tau, \sigma) = X_L^\mu(\tau + \sigma) + X_R^\mu(\tau - \sigma)$:

$$X_L^\mu(\sigma + \tau) \;\; = x_L^\mu + \frac{\pi\alpha'}{l}(\tau + \sigma) p_L^\mu + \sqrt{\frac{\alpha'}{l}} \sum_{n \neq 0} \frac{1}{n} \alpha_n^\mu \exp(-i \frac{2\pi}{l}(\tau + \sigma)) \tag{1.6}$$

$$X_R^\mu(\tau - \sigma) \;\; = x_R^\mu + \frac{\pi\alpha'}{l}(\tau - \sigma) p_R^\mu + \sqrt{\frac{\alpha'}{l}} \sum_{n \neq 0} \frac{1}{n} \bar{\alpha}_n^\mu \exp(-i \frac{2\pi}{l}(\tau - \sigma)) \tag{1.7}$$

Here $x^\mu = x_L^\mu + x_R^\mu$ parametrizes the center of mass position of the string. If we consider the compactified directions $I = 0, ..., D-1$ we have to satisfy

$$X^I \sim X^I + 2\pi L^I, \tag{1.8}$$

where $L^I = \sum n^i e_i^I$ is a lattice vector in Λ_D. This means that strings wrapping cycles on the T^D must satisfy in turn $X^I(\sigma + 2\pi, \tau) = X^I(\sigma, \tau) + 2\pi L^I$. The solutions to the equation of motion now take the form $X^I = \left(\sqrt{\frac{\alpha'}{2}}\right)(X_L^I + X_R^I)$:

$$X_L^I(\sigma + \tau) \;\; = x_L^I + (\tau + \sigma) p_L^I + \sum_{n \neq 0} \frac{1}{n} \alpha_n^I \exp(-in(\tau + \sigma)) \tag{1.9}$$

$$X_R^I(\tau - \sigma) \;\; = x_R^I + (\tau - \sigma) p_R^I + \sum_{n \neq 0} \frac{1}{n} \bar{\alpha}_n^I \exp(-in(\tau - \sigma)) \tag{1.10}$$

Canonically conjugate to the X^I we have

$$\Pi_I = G_{IJ} \partial_\tau X^J + B_{IJ} \partial_\sigma X^J. \tag{1.11}$$

The center of mass momentum is then

$$\pi_I = \int_0^{2\pi} \frac{1}{2\pi\alpha'} \Pi_I = G_{IJ} p^J + B_{IJ} L^J. \tag{1.12}$$

It generates translations in the center of mass position x_I and in order for the wavefunction $\exp(ix_I p_I)$ to be single valued we require

$$\pi_I = \sum m_i e_I^{*i}. \tag{1.13}$$

The mass operators $\alpha' m_{L,R}^2$ depend on the momenta $p_{L,R}^I$ which can be expressed in terms of the π_I:

$$\begin{aligned} p_{L,R}^I &= \sqrt{\frac{\alpha'}{2}}\pi_I \pm \frac{1}{\sqrt{2\alpha'}}(G_{IJ} \mp B_{IJ})L^J & (1.14)\\ &= \left(\sqrt{\frac{\alpha'}{2}}m_i \pm \sqrt{2\alpha'}(g_{ij} \mp b_{ij})n^j\right) e_I^{*i}, & (1.15)\end{aligned}$$

where $g_{ij} = e_i^I G_{IJ} e_j^J$ and similarly for b_{ij}. If we introduce the vector notation $\vec{m} = (m_i), \vec{n} = (n_i)$ we can rewrite the mass operators as

$$\begin{aligned} \alpha' m_{L,R}^2 &= (p_{L,R}^I)^2 + 2(N_{L,R} - 1) = \\ &\quad (\vec{m}, \vec{n})^T \mathcal{M}(\vec{m}, \vec{n}) \pm \vec{n}^T \vec{m} + 2(N_{L,R} - 1). \end{aligned} \tag{1.16}$$

where

$$\mathcal{M} = \begin{pmatrix} G^{-1} & G^{-1}B \\ -BG^{-1} & G - BG^{-1}B \end{pmatrix} \in O(D, D; \mathbb{R}). \tag{1.17}$$

It is well known that the spectrum (1.16) is left invariant by T-duality transformations in the group $O(D, D; \mathbb{Z})$.

We note here that T-duality can easily be extended to the superstring by including the transformation [2]

$$(\Psi_L, \Psi_R) \to (\Psi_L, -\Psi_R). \tag{1.18}$$

When taking into account the GSO projection, one can infer that for D odd, T-duality exchanges IIA and IIB string theory, whereas for D even it maps the theories into themselves.

1.1.1 Buscher Rules

T-duality can be extended to any target space manifold with a $U(1)$ isometry. Let the corresponding Killing vector field be k. We assume in addition to $\mathcal{L}_k G = 0$

$$\mathcal{L}_k \Phi = 0, \qquad \mathcal{L}_k B = d\Lambda. \tag{1.19}$$

Then if the direction associated with k is called x and i, j denote coordinates not equal to x, we obtain the rules

$$\begin{aligned} &\tilde{G}_{xx} = \tfrac{1}{G_{xx}},\ \tilde{G}_{ix} = \tfrac{B_{ix}}{G_{xx}},\ \tilde{B}_{ix} = \tfrac{B_{ix}}{G_{xx}} \\ &\tilde{G}_{ij} = G_{ij} - \tfrac{1}{G_{xx}}(G_{ix}G_{jx} - B_{ix}B_{jx}) \\ &\tilde{B}_{ij} = B_{ij} - \tfrac{1}{G_{xx}}(G_{ix}B_{jx} - B_{ix}G_{jx}). \end{aligned} \tag{1.20}$$

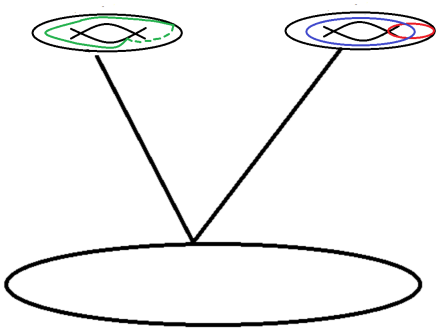

Figure 1.1: An example of a mapping torus of T^2. The monodromy leaves the red cycle invariant while sending the blue to the sum of the red and blue cycles depicted in green.

Implicit in these equations is a change in topology in the target space. A discussion can be found in [4] and subsequent papers.

1.2 Examples of T-folds

A manifold can be viewed as a collection of connected open subsets with gluing functions. By T-fold we understand a space glued together from solutions of the supergravity equations via T-dualities.

While this notion is not rigorous in general, we focus on spaces that locally are T^n bundles, with $n = 2, 3, 4$. The T-duality transformations act on the fiber.

In the case of a T^2 fiber an extensive classification has been carried out in [5]. We will mimic that approach for higher rank bundles.

1.2.1 Generalities for T-folds over the circle

The easiest way to construct a T-fold $\mathcal{X}$ with T^n fibers is by modifying the so-called mapping torus of T^n. By this we mean the manifold

$$\mathcal{X} = \frac{T^n \times [0, 2\pi]}{(x, 0) \sim (M(x), 1)} \,. \tag{1.21}$$

Here $M \in SL(n; \mathbb{Z})$ is the monodromy. Its action is defined on the n-dimensional vector space $H_1(T^n; \mathbb{Z})$ by matrix multiplication. Let the coordinate θ parametrize the S^1. Then a well-defined metric on $\mathcal{X}$ is given by

$$ds^2 = d\theta^2 + G_{ab}(\theta) dx^a dx^b \,, \quad a, b = 1, ..., n \,. \tag{1.22}$$

where

$$M^T G(0) M = G(1). \tag{1.23}$$

If we now only consider monodromies $M \in SL(n;\mathbb{Z}) \cap \exp(\mathfrak{sl}(n;\mathbb{R}))$, we can specify $G_{ab}(\theta)$ as

$$G(\theta) = \left[\exp(\theta \log M)\right]^T G(0) \left[\exp(\theta \log M)\right]. \tag{1.24}$$

The way to generalize this to certain monodromies in the full T-duality group $O(n,n;\mathbb{Z})$ is as follows: Consider $M \in O(n,n;\mathbb{Z}) \cap \exp(\mathfrak{o}(n,n;\mathbb{R}))$. Now we need to define a metric G and a two-form B-field on the space

$$T^n \times [0, 2\pi]. \tag{1.25}$$

They will both depend on θ and should satisfy

$$M \cdot (G(0), B(0)) = (G(2\pi), B(2\pi)), \tag{1.26}$$

where M acts via T-duality. We will explain this action below in detail.

Then we can say that the 'space' or T-fold $\mathcal{X}$ is well-defined. To this end we consider the so-called background matrix $E(\theta) = G(\theta) + B(\theta)$. It is well-known that an $O(n,n;\mathbb{Z})$ element acts on it by generalized fractional linear transformations [3], as exploited below. One recovers B and G as the (anti-)symmetric parts respectively. Denoting by X, Y, Z, W $n \times n$ matrices, we can define

$$\exp(\theta \log M) := \begin{pmatrix} X(\theta) & Y(\theta) \\ Z(\theta) & W(\theta) \end{pmatrix}. \tag{1.27}$$

From this notation we see that an $O(n,n;\mathbb{Z})$ invariant way of writing E is given by

$$E(\theta) = \exp(\theta \log M) \cdot E(0) \equiv \frac{X(\theta)E(0) + Y(\theta)}{Z(\theta)E(0) + W(\theta)}. \tag{1.28}$$

This means that $E(0)$ determines $G(\theta)$ and $B(\theta)$ completely.

There are different types of $O(n,n;\mathbb{Z})$ monodromies and not all of them are in the image of the exponential map. Note that $\exp : \mathfrak{o}(n,n;\mathbb{R}) \to O(n,n;\mathbb{R})$ is a subset of $SO(n,n;\mathbb{R})^+$, i.e. a subset of the identity component[1]. The generators of $O(n,n;\mathbb{Z})$ are:

- Large diffeomorphisms. They take the form and lead to $\mathcal{X}$ being a smooth manifold

$$\begin{pmatrix} (R^{-1})^T & 0 \\ 0 & R \end{pmatrix}, \quad R \in GL(n;\mathbb{Z}). \tag{1.29}$$

  They act on E by conjugation.

[1] Be aware that given an element outside the image of the exponential map, but path-connected to the identity we can still define $\mathcal{X}$ and $G(\theta), B(\theta)$.

- B-shifts and β-transformations. B-shifts have the structure

$$\begin{pmatrix} \mathbb{E}_n & \Theta \\ 0 & \mathbb{E}_n \end{pmatrix}, \quad \Theta^T = -\Theta, \tag{1.30}$$

  and lead to gauge transformations of the B-field, $B_{ij} \mapsto B_{ij} + \Theta_{ij}$. β-transformations are of the form

$$\begin{pmatrix} \mathbb{E}_n & 0 \\ \omega & \mathbb{E}_n \end{pmatrix}, \quad \omega^T = -\omega, \tag{1.31}$$

  and lead to so-called non-geometric backgrounds, as they mix B-field with metric.

- Factorized dualities. These take the form

$$\begin{pmatrix} \mathbb{E}_n - E_{ii} & E_{ii} \\ E_{ii} & \mathbb{E}_n - E_{ii} \end{pmatrix} \tag{1.32}$$

  where E_{ii} is an elementary matrix, meaning $(E_{ii})_{kl} = \delta_{ik}\delta_{il}$. Note that these are not path-connected to the identity.

For shifts and large diffeomorphisms $\mathcal{X}$ is a smooth manifold. In such cases $\mathcal{X}$ is called *geometric*, i.e. M is a product of shifts and diffeomorphisms.

Other monodromies lead to *non-geometric* $\mathcal{X}$. Factorized dualities will not be considered here.

1.2.2 T-folds over the (punctured) disk

Of course it is desirable to have more complicated base manifolds than the circle. The above construction is extended to the punctured disk $D^2 \setminus \{0\}$ by foliating the latter by copies of the T-folds over S^1. Now the metric and B-field also depend on the radius of the disk. We also introduce the holomorphic coordinate $z = re^{i\theta}$ on the base.

For $n = 2$ i.e. the T^2, this has been carried out in [5]. We summarize some of the main results of relevance to us. Firstly note that in $n = 2$ the duality group decomposes as $O(2,2:\mathbb{Z}) \cong SL(2;\mathbb{Z})_\tau \times SL(2;\mathbb{Z})_\rho \times \mathbb{Z}_2 \times \mathbb{Z}_2$. The two finite groups correspond to the factorized dualities and will be omitted from our discussion. The two $SL(2;\mathbb{Z})$ factors have simply interpretations acting on the complex structure modulus $\tau = \tau_1 + i\tau_2$ and the complexified Kähler modulus $\rho = \rho_1 + i\rho_2 = \int_{T^2} B + i \text{ vol}(T^2)$. We always assume the B-field to be constant along the torus fibers.

A matrix

$$\begin{pmatrix} a & b \\ c & d \end{pmatrix} \in SL(2;\mathbb{Z})_\tau, \tag{1.33}$$

acts on τ by fractional linear transformations

$$\tau \mapsto \frac{a\tau + b}{c\tau + d}, \tag{1.34}$$

The analogous result holds for elements in $SL(2;\mathbb{Z})_\rho$. The metric, B-field and dilaton solving the supergravity equations of motion for $\mathbb{R}^6 \times \mathcal{X}$ are

$$\begin{aligned} ds^2 &= \eta_{\mu\nu} dx^\mu dx^\nu + e^{2\varphi_1} \tau_2 \rho_2 dz d\bar{z} + G_{ab} dx^a dx^b \\ B &= \rho_1 dx^a \wedge dx^b \\ e^{2\Phi} &= \rho_2. \end{aligned} \tag{1.35}$$

Here $\eta_{\mu\nu}$ is the six-dimensional Minkowski metric and

$$G_{ab} = \frac{1}{\tau_2} \begin{pmatrix} 1 & \tau_1 \\ \tau_1 & \tau_1^2 + \tau_2^2. \end{pmatrix} \tag{1.36}$$

Moreover z are holomorphic coordinates on $D^2 \backslash \{0\}$ and φ_1 is the real part of a holomorphic function with the monodromy as $\theta \to \theta + 2\pi$:

$$e^\varphi \to (c\tau + d) e^\varphi. \tag{1.37}$$

Holomorphicity of τ and ρ implies the supergravity equations of motion.

Observe one more piece of terminology: With the metric and B-fields constant along the torus fibers, such a solution is called *semi-flat*. Often one can complete the fibration by inserting a singular fiber at the origin, at the cost of making metric and B-field depend on the torus coordinates. We will encounter such an example in the following.

The Kaluza-Klein monopole

As a central example, sketched in Fig (1.1), consider the geometric monodromy

$$M = \begin{pmatrix} 1 & 1 \\ 0 & 1 \end{pmatrix} \in SL(2;\mathbb{Z})_\tau. \tag{1.38}$$

The full $O(2,2;\mathbb{Z})$ mondoromy would be $\mathrm{diag}(\varphi, \varphi^{-T})$. We have

$$\exp(\theta M) = \begin{pmatrix} 1 & \theta \\ 0 & 1 \end{pmatrix} \tag{1.39}$$

Solving the Cauhy-Riemann equations one arrives at the well-known result [6]:

$$\tau = \frac{i}{2\pi} \log(\frac{\mu}{z}) = \theta + i \log(\mu / r) \tag{1.40}$$

Here μ is an integration constant. Observe that as $r \to 0$ this function diverges. As it turns out there is a way of completing this construction to a fibration over the full disk D^2. This is done by inserting a singular T^2 over the origin. It is the well-known I_1 Kodaira

fiber, which topologically is a torus with a pinched cycle. Additionally we have $e^{\varphi} = 1$ yielding

$$ds^2 = \eta_{\mu\nu}dx^\mu dx^\nu + \frac{\log(\mu/r)}{2\pi}(dzd\bar{z} + (dx^9)^2) + \frac{2\pi}{\log(\mu/r)}\left(dx^8 + \frac{\theta}{2\pi}dx^9\right)^2. \tag{1.41}$$

This describes the so-called Kaluza-Klein monopole. More precisely this is the *semi-flat* approximation. We are restricted to $r \in (0, \mu)$. In order to extend this metric to $r = 0$ we have add infinitely many corrections[2] to τ_2. Defining $dz = dx + idy$ the so-called Ooguri-Vafa metric [8] reads[3]:

$$ds^2 = dx^2 + dy^2 + V(dx^9)^2 + \frac{1}{V}(dx^8 + A_x dx + A_y dy + A_{x^9}\, dx^9)^2. \tag{1.42}$$

Here $\nabla \times \vec{A} = \nabla V$ with

$$V = \frac{1}{2}\sum_{n\in\mathbb{Z}} \frac{1}{\sqrt{(x^9 - 2\pi n)^2 + x^2 + y^2}} - a_{|n|}. \tag{1.43}$$

The regulator satisfies [9]:

$$a_0 = (-e + \log(4\pi))/\pi, \qquad a_{|n|} = \frac{1}{2\pi|n|}. \tag{1.44}$$

Defining $r^2 = x^2 + y^2$, Poisson resummation of V yields

$$V = \frac{1}{2\pi}\left(\log(1/r) + \sum_{n\neq 0} e^{inx^9} K_0(|n|r)\right), \tag{1.45}$$

that is we indeed have corrections to the KK-monopole.

In fact (1.42) together with (1.40) can be used to construct a Kähler metric on the K3 surface which is very close to being Ricci-flat [9]. To get an idea of how this is done recall that topologically any K3 surface $\mathcal{X}$ is given by

$$\begin{array}{ccc} T^2 & \to & \mathcal{X} \\ & & \downarrow \\ & & \mathbb{CP}^1 \end{array}, \tag{1.46}$$

where the fibration degenerates over 24 points on the base. The singular fibers are all of Kodaira type I_1. Locally around each such point we are in the situation described by the Ooguri-Vafa metric. The crucial observation now is that one can find in the same Kähler class a metric which is semi-flat, i.e. biholomorphic to (1.40). One constructs such a semi-flat metric on the fibration over $\mathbb{CP}^1 \setminus \bigcup_{i=1}^{24} U_i$. Here U_i are small disks encircling the degeneration points. One further glues 24 copies of the Ooguri-Vafa metric in. The resulting metric fails to be Ricci-flat only in the gluing regions. As demonstrated in [9] the metric is exponentially close to being Ricci-flat.

[2]These can be derived from worldsheet instantons, see [7]

[3]We drop the irrelevant 6-dimensional flat part in (1.41)

The NS5-brane

If instead we act on the Kähler modulus ρ with the same monodromy

$$\begin{pmatrix} 1 & 1 \\ 0 & 1 \end{pmatrix} \in SL(2;\mathbb{Z})_\rho \tag{1.47}$$

we again arrive at

$$\rho = \frac{i}{2\pi}\log(\mu/r), \qquad e^{\varphi} = 1. \tag{1.48}$$

Pluggin (1.48) into (1.35) yields

$$\begin{aligned} ds^2 &= \eta_{\mu\nu}dx^\mu dx^\nu + \frac{1}{2\pi}\log(\mu/r)(dr^2 + r^2 d\theta^2 + (dx^8)^2 + (dx^9)^2) \\ B &= \frac{\theta}{2\pi} dx^8 \wedge dx^9, \qquad e^{2\Phi} = \frac{1}{2\pi}\log(\mu/r). \end{aligned} \tag{1.49}$$

This describes an NS5-brane smeared on the T^2. In order to see this one has to consider the full solution. It is described by a harmonic function[4]

$$h(r) = 1 + \sum_{n,m} \frac{1}{r^2 + (x^8 - 2\pi n)^2 + (x^9 - 2\pi m)^2} - \frac{1}{2\pi}\sum_{n\neq 0}\frac{1}{|n|^2}, \tag{1.50}$$

where the last term is a regulator. The metric in terms of this function is given by

$$ds^2 = \eta_{\mu\nu}dx^\mu dx^\nu + h(r)(dr^2 + r^2 d\theta^2 + (dx^8)^2 + (dx^9)^2) \tag{1.51}$$

Poisson resummation of h gives a structure similar to that found in the Ooguri-Vafa metric:

$$h = \frac{1}{2\pi}\left(\log(\mu/r) + \sum_{(k_8,k_9)\in\mathbb{Z}^2\setminus\{(0,0)\}} K_0(\sqrt{k_8^2 + k_9^2}\, r) e^{-i(k_8 x^8 + k_9 x^9)}\right). \tag{1.52}$$

In this case the full T-duality between both corrected metrics is hard to describe. A discussion can be found in [10].

1.2.3 Examples with higher dimensional tori

We now turn to specific examples with $M \in SL(3;\mathbb{Z})$, that is we study geometric monodromies. Again we first consider a space of the form (1.21), i.e. a base manifold S^1. The geometry of $\mathcal{X}$ is determined by the conjugacy class of M. However no explicit classification of the conjugacy classes is known for $SL(n;\mathbb{Z})$, $n \geq 3$. Thus we restrict ourselves to giving a few examples.

[4] We set the radii of both circles in the T^2 equal to 1.

Let us consider the following $SL(3;\mathbb{Z})$ elements, which are all conjugate to each other:

$$M_1 = \begin{pmatrix} 1 & 1 & 0 \\ 0 & 1 & 0 \\ 0 & 0 & 1 \end{pmatrix}, \quad M_2 = \begin{pmatrix} 1 & 1 & 1 \\ 0 & 1 & 0 \\ 0 & 0 & 1 \end{pmatrix}, \quad M_3 = \begin{pmatrix} 1 & 0 & 1 \\ 0 & 1 & 1 \\ 0 & 0 & 1 \end{pmatrix}. \tag{1.53}$$

For M_1 we apply

$$\begin{aligned} G_{T^3}(\theta) &= \left[\exp\left(\theta \log M_1\right)\right]^T G(0) \left[\exp\left(\theta \log M_1\right)\right] = \\ &= \begin{pmatrix} 1 & \theta & 0 \\ \theta & 1+\theta^2 & 0 \\ 0 & 0 & 1 \end{pmatrix}. \end{aligned} \tag{1.54}$$

Thus we equip $\mathcal{X}$ with the metric

$$ds^2 = d\theta^2 + (dx + \theta dy)^2 + dy^2 + dz^2, \tag{1.55}$$

where $(x, y, z) \in T^3$. The topology is given by $\mathcal{X} = S^1 \times \mathcal{M}_3$, where $\mathcal{M}_3$ is a compact quotient of the Heisenberg group. For M_2 and M_3 we obtain

$$\begin{aligned} \mathcal{X}_{M_2}: &\quad ds^2 = d\theta^2 + (dx + \theta dy + \theta dz)^2 + dy^2 + dz^2\,, \\ \mathcal{X}_{M_3}: &\quad ds^2 = d\theta^2 + (dx + \theta dy)^2 + (dy + \theta dz)^2 + dz^2\,. \end{aligned} \tag{1.56}$$

Now it is obvious from the structure of M_1 that this is nothing but the embedding of the examples with T^2 studied previously. We simple have added an extra S^1 to the fiber. Nevertheless this example is interesting as it appears locally in the quintic Calabi-Yau threefold given by

$$\{\sum_{i=0}^{4} z_i^5 + \psi \Pi_{i=0}^4 z_i = 0\} \subset \mathbb{CP}^4. \tag{1.57}$$

Here $\psi \in \mathbb{C} \setminus \{0\}$. We now quote some results from [11, 12] and follow up papers by these authors. A useful review is [13]. Topologically the quintics turn out to be

$$\begin{array}{ccc} T^3 & \to & \mathcal{X} \\ & & \downarrow \\ & & S^3. \end{array} \tag{1.58}$$

However there now is a discriminant locus on the base given by a trivalent graph Γ. Over the edges of this graph the singular fiber is of type $I_1 \times S^1$, i.e. exactly as in the examples above. At the vertices the precise shape is ambiguous [11]. The situation close to a vertex is depicted in Figure 1.2. Note that the base manifold is locally $\mathbb{R}^3$ and the three edges are not contained in any plane. The monodromies around each edge are in fact similar to the ones in (1.53). We have two types of vertices called negative and positive, according to the sign with which the contribute to the Euler characteristic:

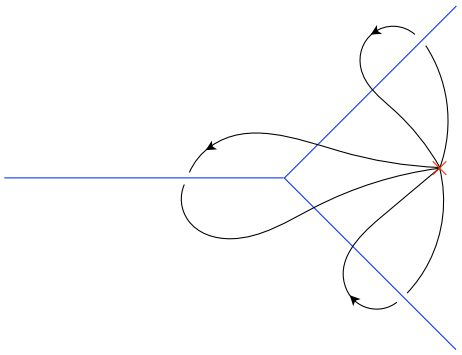

Figure 1.2: Local model of the base of a quintic Calabi-Yau manifold. In blue we have the discriminant locus with generic fiber $S^1 \times I_1$, where I_1 is the singular fishtail fiber from the Kodaira classification. In black we have depicted loops corresponding to the modoromies mentioned in the text. The precise shape of the fiber over the intersection is ambigous. The figure is taken from [1].

- Positive vertex

$$T_{1+} = \begin{pmatrix} 1 & 0 & 1 \\ 0 & 1 & 0 \\ 0 & 0 & 1 \end{pmatrix}, \quad T_{2+} = \begin{pmatrix} 1 & 0 & 0 \\ 0 & 1 & 1 \\ 0 & 0 & 1 \end{pmatrix}, \quad T_{3+} = T_{2+}^{-1} T_{1+}^{-1} = \begin{pmatrix} 1 & 0 & -1 \\ 0 & 1 & -1 \\ 0 & 0 & 1 \end{pmatrix}, \tag{1.59}$$

- Negative vertex

$$T_{1-} = \begin{pmatrix} 1 & 0 & 1 \\ 0 & 1 & 0 \\ 0 & 0 & 1 \end{pmatrix}, \quad T_{2-} = \begin{pmatrix} 1 & 1 & 0 \\ 0 & 1 & 0 \\ 0 & 0 & 1 \end{pmatrix}, \quad T_{3-} = T_{2-}^{-1} T_{1-}^{-1} = \begin{pmatrix} 1 & -1 & -1 \\ 0 & 1 & 0 \\ 0 & 0 & 1 \end{pmatrix}. \tag{1.60}$$

It would be nice to construct a Ricci-flat metric on this local degeneration similarly to the K3 surface. This time the base manifold encircling the degeneration is an open ball in $\mathbb{R}^3$. However as one can imagine this is quite hard. In addition it turns out that the situation above only describes the topology of the manifold. Once we fix additional structures one expects a thickening of the blue edges to two-dimensional strips, see chapter 7 of [14].

An ansatz for $n = 3$

We now describe an ansatz that can be used to construct a semi-flat approximation of the metric on T^3 bundles over $\mathbb{R}^3$ due to [15]. Let $(x_1, x_2, x_3) \in \mathbb{R}^3$ and $(y_1, y_2, y_3) \in T^3$:

$$ds^2 = e^{2\phi_1} dx_1^2 + e^{2\phi_2} dx_2^2 + e^{2\phi_3} dx_3^3 + G_{ij} dy_i dy_j \,, \quad G = V^T V \tag{1.61}$$

where V is given by

$$V = e^{-\frac{2\alpha_1 + \alpha_2}{3}} \begin{pmatrix} 1 & a & b \\ 0 & e^{-\alpha_1} & e^{-\alpha_1} c \\ 0 & 0 & e^{-\alpha_1 - \alpha_2} \end{pmatrix}. \tag{1.62}$$

All of the scalars in (1.61) depend on the coordinates x_i. This is a metric on a real manifold. A complex structure is obtained by pairing coordinates on the base and fiber. The resulting holomorphic one forms are $dz^i = e^{\phi_i} dx^i + i\delta_{ij} V_{jk} dy^k$, explicitly:

$$\begin{aligned} dz^1 &= e^{\phi_1} dx_1 + i e^{\frac{1}{3}(2\alpha_1+\alpha_2)}(dy_1 + a\, dy_2 + b\, dy_3)\,, \\ dz^2 &= e^{\phi_2} dx_2 + i e^{\frac{1}{3}(-\alpha_1+\alpha_2)}(dy_2 + c\, dy_3)\,, \\ dz^3 &= e^{\phi_3} dx_3 + i e^{-\frac{1}{3}(\alpha_1+2\alpha_2)}(dy_3). \end{aligned} \tag{1.63}$$

We thus have

$$J = e^{\phi_i} V_{ij} dx^i \wedge dy^j\,, \quad \Omega = i dz^1 \wedge dz^2 \wedge dz^3\,. \tag{1.64}$$

Ricci-flatness can be inferred from the first order differential equations $d\Omega = dJ = 0$ leading to the following equations:

$$\begin{aligned} &\partial_1 a = e^{-\alpha_1+\phi_1-\phi_2}\partial_2(\alpha_1-\phi_3)\,, \quad \partial_2 a = 2e^{-\alpha_1-\phi_1+\phi_2}\partial_1\phi_2\,, \quad \partial_3 a = 0\,, \\ &\partial_1 b = -2e^{-\alpha_1-\alpha_2+\phi_1-\phi_3}\partial_3\phi_1 + c\partial_1 a\,, \quad \partial_2 b = c\partial_2 a\,, \quad \partial_3 b = 2e^{-\alpha_1-\alpha_2-\phi_1+\phi_3}\partial_1\phi_3\,, \\ &\partial_1 c = 0\,, \quad \partial_2 c = -2e^{-\alpha_2+\phi_2-\phi_3}\partial_3\phi_2\,, \quad \partial_3 c = 2e^{-\alpha_2-\phi_2+\phi_3}\partial_2\phi_3\,, \\ &\partial_2\phi_1 = -\frac{1}{3}\partial_2(2\alpha_1+\alpha_2)\,, \qquad \partial_3\phi_1 = -\frac{1}{3}\partial_3(2\alpha_1+\alpha_2)\,, \\ &\partial_1\phi_2 = \frac{1}{3}\partial_1(-\alpha_1+\alpha_2)\,, \qquad \partial_3\phi_2 = \frac{1}{3}\partial_3(\alpha_1-\alpha_2)\,, \\ &\partial_1\phi_3 = \frac{1}{3}\partial_1(-\alpha_1-2\alpha_2)\,, \qquad \partial_2\phi_3 = -\frac{1}{3}\partial_2(\alpha_1+2\alpha_2)\,. \end{aligned} \tag{1.65}$$

One can easily recover the semi-flat approximation for a T^2 embedded into T^3 by setting $b = c = 0$. With $\tau_1 = a$ and $\tau_2 = e^{-\alpha_1}$ we end up with

$$ds^2 = dx_3^2 + dy_3^2 + \frac{1}{\tau_2}(dx_1^2 + dx_2^2) + G_{ij} dy_i^2 dy_j^2, \tag{1.66}$$

where

$$G = \frac{1}{\tau_2}\begin{pmatrix} 1 & \tau_1 \\ \tau_1 & \tau_1^2 + \tau_2^2. \end{pmatrix} \tag{1.67}$$

The equations (1.65) are solved by $\tau = i\log(\mu/(x_1+ix_2))$ or any other function holomorphic in $x_1 + ix_2$.

Let us return to other examples of T-folds over S^1 with T^3 fibers. An infinite order element not conjugate to any monodromies in (1.53) is given by

$$M_4 = \begin{pmatrix} 1 & 1 & 0 \\ 0 & 1 & 1 \\ 0 & 0 & 1 \end{pmatrix}. \tag{1.68}$$

In this case $\mathcal{X}$ exhibits the structure of a Nil_4-manifold. One computes the metric

$$ds^2 = d\theta^2 + dx^2 + (dy + \theta dx)^2 + \left[\frac{1}{2}(\theta^2 - \theta)dx + \theta dy + dz\right]^2. \tag{1.69}$$

We do not currently know how to extend this to a Ricci-flat manifold over the punctured disk. One ansatz would be to use (1.61). The base should be of the form $\{D^2 \setminus \{0\}\} \times \mathbb{R}$. Solving (1.65) is very hard.

We now turn to non-geometric spaces $\mathcal{X}$. It is now better to think of $\theta \in [0,1]$. In string theory we can glue the to ends together even if say the metric would not be well-defined.

The easiest example is constructed using a β-transformation. The monodromy is given by

$$M_\omega = \begin{pmatrix} \mathbb{E}_3 & 0 \\ -\omega & \mathbb{E}_3 \end{pmatrix}, \quad \omega = \begin{pmatrix} 0 & c & -b \\ -c & 0 & a \\ b & -a & 0 \end{pmatrix}. \tag{1.70}$$

The induced metric and B-field are more complicated than in previous examples:

$$ds^2 = d\theta^2 + \frac{dx^2+dy^2+dz^2}{1+(a^2+b^2+c^2)\theta^2} + \frac{(a\,dx+b\,dy+c\,dz)^2\,\theta^2}{1+(a^2+b^2+c^2)\,\theta^2}, \tag{1.71}$$

$$B = \frac{-c\,dx\wedge dy + b\,x\wedge dz - a\,dy\wedge dz}{1+(a^2+b^2+c^2)\,\theta^2}\theta\,. \tag{1.72}$$

Note that as $\theta \to \theta+1$ we do not obtain a well-defined metric or B-field. There is a very nice trick of how to deal with these non-geometric backgrounds however. We use the so-called accidental isomorphism $SL(4;\mathbb{R}) \cong Spin(3,3;\mathbb{R})$, reviewed in the appendix B. If we restrict the map $\psi : SL(4;\mathbb{R}) \to SO(3,3;\mathbb{R})^+$ to $SL(4;\mathbb{Z})$ we may associate to each element $M \in SO(3,3;\mathbb{Z})$ an element in $SL(4;\mathbb{Z})$:

$$N_\omega := \psi^{-1}(M_\omega) = \begin{pmatrix} 1 & 0 & 0 & 0 \\ 0 & 1 & 0 & 0 \\ 0 & 0 & 1 & 0 \\ a & b & c & 1 \end{pmatrix} \subset SL(4;\mathbb{Z}). \tag{1.73}$$

We interpret N_ω as the monodromy of a T^4-fibration

$$\mathcal{Y} = \frac{T^4 \times [0,1]}{(\theta,0) \sim (N_\omega(\theta),1)}. \tag{1.74}$$

Here $N_\omega(\theta) = \exp(\theta \log(N_\omega))$. It is apparent that $\mathcal{Y}$ is a smooth manifold. It can be endowed with a very simple smooth metric obeying $G_{T^4}(\theta) = N_\omega(\theta)\cdot G_{T^4}(0)$:

$$ds^2 = d\theta^2 + dx^2 + dy^2 + dz^2 + (dw + a\theta dx + b\theta dy + c\theta dz)^2. \tag{1.75}$$

In section [1.4] we will describe a general ansatz for geometric T-folds over the punctured disk with fibers T^4.

1.3 A Global Example of a T-fold with higher rank fibers

In this section we will describe the construction of a collections of T-folds labeled by integers (m, n) of the form

$$\begin{array}{rcl} T^3 & \rightarrow & \mathcal{X}_{mn} \\ & & \downarrow \\ & & D^2. \end{array}$$

This is done by studying Calabi-Yau manifolds $\mathcal{Y}_{mn}$, [16] which are of the form

$$\begin{array}{rcl} T^4 & \rightarrow & \mathcal{Y}_{mn} \\ & & \downarrow \\ & & \mathbb{CP}^1. \end{array}$$

However these manifolds have singular fibers over a certain collection of points on the base, which depends on the integers (m, n). Locally around such a degeneration we have monodromies in $SL(4;\mathbb{Z})$. Applying the map $SL(4;\mathbb{Z}) \rightarrow SO(3,3;\mathbb{Z})$ reviewed in appendix B we construct T-folds by replacing the T^4 fibers with T^3 and the monodromies with the appropriate $SO(3,3;\mathbb{Z})$ elements.

1.3.1 The smooth Calabi-Yau manifolds

The manifolds $\mathcal{Y}_{m,n}$ are more precisely characterized

$$\begin{array}{rcl} T^4 & \rightarrow & \mathcal{Y}_{m,n} \setminus \hat{T}^4_1, ..., \hat{T}^4_M \\ & & \downarrow \\ & & \mathbb{CP}^1 \setminus \{p_1, ..., p_M\}, \end{array} \tag{1.76}$$

with $M = 24 - 4mn > 0$. Each $\hat{T}_i^4$ is topologically the product $T^2 \times I_1$, where I_1 is the fishtail fiber of the Kodaira classification. The monodromies around each p_i are

$$\mathbf{A} = \begin{pmatrix} 1 & 1 & 0 & 0 \\ 0 & 1 & 0 & 0 \\ 0 & 0 & 1 & 0 \\ 0 & 0 & 0 & 1 \end{pmatrix}, \qquad \mathbf{B}_1 = \begin{pmatrix} 2 & 1 & 0 & m \\ -1 & 0 & 0 & -m \\ n & n & 1 & mn \\ 0 & 0 & 0 & 1 \end{pmatrix}, \tag{1.77}$$

$$\mathbf{B}_2 = \begin{pmatrix} 2 & 1 & 0 & 0 \\ -1 & 0 & 0 & 0 \\ 0 & 0 & 1 & 0 \\ 0 & 0 & 0 & 1 \end{pmatrix}, \qquad \mathbf{B}_3 = \begin{pmatrix} 2 & 1 & -m & 0 \\ -1 & 0 & m & 0 \\ 0 & 0 & 1 & 0 \\ n & n & -mn & 1 \end{pmatrix},$$

$$\mathbf{B}_4 = \begin{pmatrix} 2 & 1 & -m & m \\ -1 & 0 & m & -m \\ n & n & 1-mn & mn \\ n & n & -mn & mn+1 \end{pmatrix}, \qquad \mathbf{C}_1 = \begin{pmatrix} 0 & 1 & 0 & -m \\ -1 & 2 & 0 & -m \\ n & -n & 1 & mn \\ 0 & 0 & 0 & 1 \end{pmatrix},$$

$$\mathbf{C}_2 = \begin{pmatrix} 0 & 1 & 0 & 0 \\ -1 & 2 & 0 & 0 \\ 0 & 0 & 1 & 0 \\ 0 & 0 & 0 & 1 \end{pmatrix}, \qquad \mathbf{C}_3 = \begin{pmatrix} 0 & 1 & m & 0 \\ -1 & 2 & m & 0 \\ 0 & 0 & 1 & 0 \\ n & -n & -mn & 1 \end{pmatrix},$$

$$\mathbf{C}_4 = \begin{pmatrix} 0 & 1 & m & -m \\ -1 & 2 & m & -m \\ n & -n & 1-mn & mn \\ n & -n & -mn & mn+1 \end{pmatrix}.$$

Our conventions are such that these are inverse to those found in [16]. In order for the manifold to be well defined no global monodromy must be present, which is equivalent to the constraint

$$\mathbf{A}^{16-4mn}\mathbf{B}_1\mathbf{C}_1\mathbf{B}_2\mathbf{C}_2\mathbf{B}_3\mathbf{C}_3\mathbf{B}_4\mathbf{C}_4 = \mathbb{1}\,. \tag{1.78}$$

Another fact is that all monodromies are conjugate to $\mathbf{A}$. For instance for $\mathbf{B}_4$ and $\mathbf{C}_4$ we have:

$$\mathbf{A} = S_C^{-1}\mathbf{C}_4 S_C\,, \qquad S_C = \begin{pmatrix} -1 & 1 & m & -m \\ -1 & 0 & 0 & 0 \\ n & 0 & 1 & 0 \\ n & 0 & 0 & 1 \end{pmatrix} \in SL(4;\mathbb{Z})\,, \tag{1.79}$$

$$\mathbf{A} = S_B^{-1}\mathbf{B}_4 S_B\,, \qquad S_B = \begin{pmatrix} 1 & 1 & m & -m \\ -1 & 0 & 0 & 0 \\ n & 0 & 1 & 0 \\ n & 0 & 0 & 1 \end{pmatrix} \in SL(4;\mathbb{Z})\,.$$

This implies that locally the geometry is that of $K3 \times T^2$ as a real manifold. However the complex structure does not necessarily respect that factorization.

Indeed only if $m = n = 0$, do we obtain $\mathcal{Y}_{0,0} = K3 \times T^2$. This is easily seen from $\mathbf{B}_2 = \mathbf{B}_i|_{m,n=0} \equiv \mathbf{B}$, $\mathbf{C}_2 = \mathbf{C}_i|_{m,n=0} \equiv \mathbf{C}$. There are now 24 singular fibers and as the notation suggest they are the embeddings of the standard $SL(2;\mathbb{Z})$ $\mathbf{A}$, $\mathbf{B}$, $\mathbf{C}$ monodromies (see appendix D) into $SL(4;\mathbb{Z})$:

$$\mathbf{A}^{16}(\mathbf{BC})^4 = (\mathbf{A}^4\mathbf{BC})^4 \,. \tag{1.80}$$

As is reviewed in appendix D the combination $\mathbf{A}^4\mathbf{BC} = -1$. In IIB compactifications this indicates the presence of an O7 plane with four D7 branes on top.

1.3.2 The T-folds

We are now in a position to map the monodromies A, B_i, C_i from $SL(4;\mathbb{Z})$ into $SO(3,3;\mathbb{Z})$. Explicitly

$$\mathbf{A} \mapsto \mathbf{W} = \begin{pmatrix} 1 & 0 & 0 & 0 & 0 & 0 \\ -1 & 1 & 0 & 0 & 0 & 0 \\ 0 & 0 & 1 & 0 & 0 & 0 \\ 0 & 0 & 0 & 1 & 1 & 0 \\ 0 & 0 & 0 & 0 & 1 & 0 \\ 0 & 0 & 0 & 0 & 0 & 1 \end{pmatrix} , \tag{1.81}$$

$$\mathbf{B}_1 \mapsto \mathbf{X}_1 = \begin{pmatrix} 0 & 1 & -n & 0 & mn & m \\ -1 & 2 & -n & -mn & 0 & m \\ 0 & 0 & 1 & -m & -m & 0 \\ 0 & 0 & 0 & 2 & 1 & 0 \\ 0 & 0 & 0 & -1 & 0 & 0 \\ 0 & 0 & 0 & n & n & 1 \end{pmatrix} ,$$

$$\mathbf{B}_2 \mapsto \mathbf{X}_2 = \begin{pmatrix} 0 & 1 & 0 & 0 & 0 & 0 \\ -1 & 2 & 0 & 0 & 0 & 0 \\ 0 & 0 & 1 & 0 & 0 & 0 \\ 0 & 0 & 0 & 2 & 1 & 0 \\ 0 & 0 & 0 & -1 & 0 & 0 \\ 0 & 0 & 0 & 0 & 0 & 1 \end{pmatrix} ,$$

$$\mathbf{B}_3 \mapsto \mathbf{X}_3 = \begin{pmatrix} 0 & 1 & 0 & 0 & 0 & 0 \\ -1 & 2 & 0 & 0 & 0 & 0 \\ m & -m & 1 & 0 & 0 & 0 \\ 0 & mn & n & 2 & 1 & -m \\ -mn & 0 & -n & -1 & 0 & m \\ -n & n & 0 & 0 & 0 & 1 \end{pmatrix} ,$$

$$\mathbf{B}_4 \mapsto \mathbf{X}_4 = \begin{pmatrix} -mn & 1 & -n & 0 & mn & m \\ -1 & 2-mn & -n & -mn & 0 & m \\ m & -m & 1 & -m & -m & 0 \\ 0 & mn & n & mn+2 & 1 & -m \\ -mn & 0 & -n & -1 & mn & m \\ -n & n & 0 & n & n & 1 \end{pmatrix},$$

$$\mathbf{C}_1 \mapsto \mathbf{Y}_1 = \begin{pmatrix} 2 & 1 & -n & 0 & mn & m \\ -1 & 0 & n & -mn & 0 & -m \\ 0 & 0 & 1 & -m & m & 0 \\ 0 & 0 & 0 & 0 & 1 & 0 \\ 0 & 0 & 0 & -1 & 2 & 0 \\ 0 & 0 & 0 & n & -n & 1 \end{pmatrix},$$

$$\mathbf{C}_2 \mapsto \mathbf{Y}_2 = \begin{pmatrix} 2 & 1 & 0 & 0 & 0 & 0 \\ -1 & 0 & 0 & 0 & 0 & 0 \\ 0 & 0 & 1 & 0 & 0 & 0 \\ 0 & 0 & 0 & 0 & 1 & 0 \\ 0 & 0 & 0 & -1 & 2 & 0 \\ 0 & 0 & 0 & 0 & 0 & 1 \end{pmatrix},$$

$$\mathbf{C}_3 \mapsto \mathbf{Y}_3 = \begin{pmatrix} 2 & 1 & 0 & 0 & 0 & 0 \\ -1 & 0 & 0 & 0 & 0 & 0 \\ -m & -m & 1 & 0 & 0 & 0 \\ 0 & mn & -n & 0 & 1 & m \\ -mn & 0 & -n & -1 & 2 & m \\ n & n & 0 & 0 & 0 & 1 \end{pmatrix},$$

$$\mathbf{C}_4 \mapsto \mathbf{Y}_4 = \begin{pmatrix} 2-mn & 1 & -n & 0 & mn & m \\ -1 & -mn & n & -mn & 0 & -m \\ -m & -m & 1 & -m & m & 0 \\ 0 & mn & -n & mn & 1 & m \\ -mn & 0 & -n & -1 & mn+2 & m \\ n & n & 0 & n & -n & 1 \end{pmatrix}.$$

All these are conjugate to $\mathbf{W}$, because the map we consider is a homomorphism.

By the same token we have

$$\mathbf{W}^{16-4mn}\mathbf{X}_1\mathbf{Y}_1\mathbf{X}_2\mathbf{Y}_2\mathbf{X}_3\mathbf{Y}_3\mathbf{X}_4\mathbf{Y}_4 = \mathbb{1}. \tag{1.82}$$

We now check whether or not the monodromies $(\mathbf{X}_i, \mathbf{Y}_i)$, which are subject to the same interpretation, are geometric or not.

Obviously the pair (X_2, Y_2) in (1.81) are geometric as the correspond to diffeomorphisms.

Both $\mathbf{X}_1$ and $\mathbf{Y}_1$ are a product of a diffeomorphism and a shift and therefore geometric:

$$\mathbf{X}_1 = \begin{pmatrix} 1 & 0 & 0 & 0 & mn & m \\ 0 & 1 & 0 & -mn & 0 & m \\ 0 & 0 & 1 & -m & -m & 0 \\ 0 & 0 & 0 & 1 & 0 & 0 \\ 0 & 0 & 0 & 0 & 1 & 0 \\ 0 & 0 & 0 & 0 & 0 & 1 \end{pmatrix} \begin{pmatrix} 0 & 1 & -n & 0 & 0 & 0 \\ -1 & 2 & -n & 0 & 0 & 0 \\ 0 & 0 & 1 & 0 & 0 & 0 \\ 0 & 0 & 0 & 2 & 1 & 0 \\ 0 & 0 & 0 & -1 & 0 & 0 \\ 0 & 0 & 0 & n & n & 1 \end{pmatrix} . \tag{1.83}$$

Contrarily $(\mathbf{X}_3, \mathbf{Y}_3)$ are non-geometric as they are composed of a β-transformation and a diffeomorphism:

$$\mathbf{X}_3 = \begin{pmatrix} 0 & 1 & 0 & 0 & 0 & 0 \\ -1 & 2 & 0 & 0 & 0 & 0 \\ m & -m & 1 & 0 & 0 & 0 \\ 0 & 0 & 0 & 2 & 1 & -m \\ 0 & 0 & 0 & -1 & 0 & m \\ 0 & 0 & 0 & 0 & 0 & 1 \end{pmatrix} \begin{pmatrix} 1 & 0 & 0 & 0 & 0 & 0 \\ 0 & 1 & 0 & 0 & 0 & 0 \\ 0 & 0 & 1 & 0 & 0 & 0 \\ 0 & mn & n & 1 & 0 & 0 \\ -mn & 0 & -n & 0 & 1 & 0 \\ -n & n & 0 & 0 & 0 & 1 \end{pmatrix} . \tag{1.84}$$

Te pair $(\mathbf{X}_4, \mathbf{Y}_4)$ are also non-geometric. They can be expressed for instance as

$$\mathbf{Y}_4 = \mathrm{T}^{-1} \begin{pmatrix} 1 & 0 & 0 & 0 & mn & m \\ 0 & 1 & 0 & -mn & 0 & -m \\ 0 & 0 & 1 & -m & m & 0 \\ 0 & 0 & 0 & 1 & 0 & 0 \\ 0 & 0 & 0 & 0 & 1 & 0 \\ 0 & 0 & 0 & 0 & 0 & 1 \end{pmatrix} \begin{pmatrix} 2 & 1 & -n & 0 & 0 & 0 \\ -1 & 0 & n & 0 & 0 & 0 \\ 0 & 0 & 1 & 0 & 0 & 0 \\ 0 & 0 & 0 & 0 & 1 & 0 \\ 0 & 0 & 0 & -1 & 2 & 0 \\ 0 & 0 & 0 & n & -n & 1 \end{pmatrix} T , \tag{1.85}$$

$$\mathbf{X}_4 = \tilde{T}^{-1} \begin{pmatrix} 0 & 1 & 0 & 0 & 0 & 0 \\ -1 & 2 & 0 & 0 & 0 & 0 \\ m & -m & 1 & 0 & 0 & 0 \\ 0 & 0 & 0 & 2 & 1 & -m \\ 0 & 0 & 0 & -1 & 0 & m \\ 0 & 0 & 0 & 0 & 0 & 1 \end{pmatrix} \begin{pmatrix} 1 & 0 & 0 & 0 & 0 & 0 \\ 0 & 1 & 0 & 0 & 0 & 0 \\ 0 & 0 & 1 & 0 & 0 & 0 \\ 0 & mn & n & 1 & 0 & 0 \\ -mn & 0 & -n & 0 & 1 & 0 \\ -n & n & 0 & 0 & 0 & 1 \end{pmatrix} \tilde{T}, \tag{1.86}$$

where

$$T = \begin{pmatrix} 1 & 0 & 0 & 0 & 0 & 0 \\ 0 & 1 & 0 & 0 & 0 & 0 \\ 0 & 0 & 1 & 0 & 0 & 0 \\ 0 & 1 & 0 & 1 & 0 & 0 \\ -1 & 0 & 0 & 0 & 1 & 0 \\ 0 & 0 & 0 & 0 & 0 & 1 \end{pmatrix} , \quad \tilde{T} = \begin{pmatrix} 1 & 0 & 0 & 0 & -1 & 0 \\ 0 & 1 & 0 & 1 & 0 & 0 \\ 0 & 0 & 1 & 0 & 0 & 0 \\ 0 & 0 & 0 & 1 & 0 & 0 \\ 0 & 0 & 0 & 0 & 1 & 0 \\ 0 & 0 & 0 & 0 & 0 & 1 \end{pmatrix} . \tag{1.87}$$

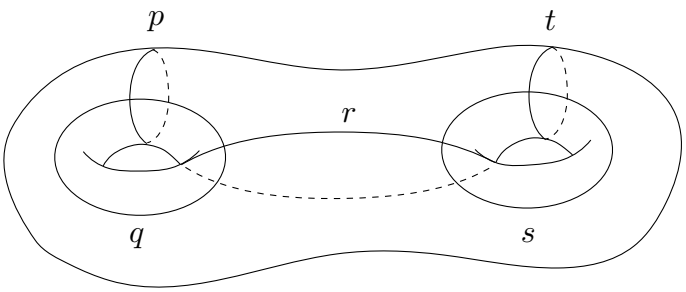

Figure 1.3: The Humphries generators for Σ_2.

1.3.3 The special case of hyperelliptic fibrations

In this section we make some more remarks concerning $\mathcal{Y}_{1,1}$. This manifold corresponds to the monodromies (1.77) with $m = n = 1$. In total there are twenty singular fibers. Notably this manifold can viewed as the Jacobian fibration of a genus two fibration, see [16]. Such a situation has appeared in the context of heterotic/F-theory duality in the literature, [17, 18]. Similarly to the Kodaira classification of singular T^2 fibers there exists a list for genus two surfaces [19]. Colliding such defects on $\mathcal{Y}_{1,1}$ can give interesting T-fects on $\mathcal{X}_{1,1}$ not T-dual to geometric ones, as in [18]. One should keep in mind that constructing Jacbian varieties of singular curves is more involved than in the smooth case.

To be more specific recall that to each curve Σ_g of genus g we can associate the Jacbian variety

$$\mathrm{Jac}(\Sigma_g) := \mathrm{Pic}_0(\Sigma_g), \tag{1.88}$$

i.e. the subgroup of degree zero divisors. If Σ_g is smooth then this variety can be endowed with the topology of a torus T^{2g}. For Σ_2 we thus find a Jacobian T^4. Consider now the fibration

$$\begin{array}{ccc} \Sigma_2 & \to & \mathcal{S} \\ & & \downarrow \\ & & \mathbb{CP}^1 \setminus \{p_1, ..., p_{20}\}, \end{array} \tag{1.89}$$

Over each point p_i the fiber is singular, a looks like a fishtail fiber I_1 with an extra handle attached. It corresponds to a genus two surface with one of the 'outer' cycles pinched. Similarly to elliptic fibrations the total space is still smooth.

To construct $\mathcal{Y}_{1,1}$ we replace each fiber by its Jacobian. For the singular fibers the procedure is more involved [20],[21]) but the end result is topologically $\mathrm{I}_1 \times T^2$. One can actually say more about this genus two fibration. Namely the monodromies (1.77) are in fact in $SP(4;\mathbb{Z})$:

$$\mathbf{A}^t \eta \mathbf{A} = \eta\,, \quad \mathbf{B}_i^t \eta \mathbf{B}_i = \eta\,, \quad \mathbf{C}_i^t \eta \mathbf{C}_i = \eta\,, \tag{1.90}$$

with

$$\eta = \begin{pmatrix} 0 & 1 & 0 & 0 \\ -1 & 0 & 0 & 0 \\ 0 & 0 & 0 & 1 \\ 0 & 0 & -1 & 0 \end{pmatrix} . \tag{1.91}$$

In addition they are all conjugate to $\mathbf{A}$ in $Sp(4,\mathbb{Z})$. As $Sp(4,\mathbb{Z}) = \mathrm{Aut}(H_1(\Sigma_2;\mathbb{Z}))$ and given that the map

$$\Phi \,:\, MCG(\Sigma_2) \to Sp(4,\mathbb{Z})\,, \tag{1.92}$$

is surjective we ifer that each monodromy corresponds to a Dehn twist of Σ_2. A theorem due to Humphries (see for example [22]), states that there are $2g+1 = 5$ generators for $Sp(4;\mathbb{Z})$. Each of these corresponds to a Dehn twist along a cycle see Figure 1.3. Monodromies corresponding to twist along (p,q,t,s) are denoted by capital letters:

$$\mathbf{P} = \mathbf{A} = \begin{pmatrix} 1 & 1 & 0 & 0 \\ 0 & 1 & 0 & 0 \\ 0 & 0 & 1 & 0 \\ 0 & 0 & 0 & 1 \end{pmatrix} , \quad \mathbf{Q} = \begin{pmatrix} 1 & 0 & 0 & 0 \\ -1 & 1 & 0 & 0 \\ 0 & 0 & 1 & 0 \\ 0 & 0 & 0 & 1 \end{pmatrix} , \quad \mathbf{R} = \begin{pmatrix} 1 & 1 & 0 & -1 \\ 0 & 1 & 0 & 0 \\ 0 & -1 & 1 & 1 \\ 0 & 0 & 0 & 1 \end{pmatrix} , \tag{1.93}$$

$$\mathbf{S} = \begin{pmatrix} 1 & 0 & 0 & 0 \\ 0 & 1 & 0 & 0 \\ 0 & 0 & 1 & 0 \\ 0 & 0 & -1 & 1 \end{pmatrix} , \quad \mathbf{T} = \begin{pmatrix} 1 & 0 & 0 & 0 \\ 0 & 1 & 0 & 0 \\ 0 & 0 & 1 & 1 \\ 0 & 0 & 0 & 1 \end{pmatrix} . \tag{1.94}$$

For these generators the well known relation

$$\mathbf{H}^2 = \mathbb{1}\,, \tag{1.95}$$

holds. Here $\mathbf{H}$ is

$$\mathbf{H} = \mathbf{TSRQPPQRST}\,. \tag{1.96}$$

One can express $\mathbf{A}, \mathbf{B}_i, \mathbf{C}_i$ in terms of these generators:

$$\mathbf{B}_i = \mathbf{T}_i\mathbf{QP}(\mathbf{T}_i\mathbf{Q})^{-1}\,, \quad \mathbf{C}_i = \mathbf{T}_i\mathbf{Q}^{-1}\mathbf{P}(\mathbf{T}_i\mathbf{Q}^{-1})^{-1}\,, \tag{1.97}$$

with

$$\mathbf{T}_1 = \begin{pmatrix} 1 & 0 & 0 & -1 \\ 0 & 1 & 0 & 0 \\ 0 & -1 & 1 & 0 \\ 0 & 0 & 0 & 1 \end{pmatrix} , \quad \mathbf{T}_2 = \mathbb{1}\,, \quad \mathbf{T}_3 = \begin{pmatrix} 1 & 0 & 1 & 0 \\ 0 & 1 & 0 & 0 \\ 0 & 0 & 1 & 0 \\ 0 & -1 & 0 & 1 \end{pmatrix} , \quad \mathbf{T}_4 = \begin{pmatrix} 1 & 0 & 1 & -1 \\ 0 & 1 & 0 & 0 \\ 0 & -1 & 1 & 0 \\ 0 & -1 & 0 & 1 \end{pmatrix} . \tag{1.98}$$

1.4 An ansatz for T-folds with T^4 fibers

The following ansatz is described in [23] for a T^4 fibration over the punctured disk in the absence of fluxes:

$$ds^2 = e^{2D}h(z)dzd\bar{z} + e^{-2D}g_{mn}dx^m dx^n, \tag{1.99}$$

where $e^{2D} = \sigma_2\tau_2 - \beta_2^2$ and

$$g_{mn} = \begin{pmatrix} \sigma_2 & \beta_2 & \beta_2\sigma_1 - \beta_1\sigma_2 & -\beta_1\beta_2 + \sigma_2\tau_1 \\ \beta_2 & \tau_2 & \beta_1\beta_2 - \sigma_1\tau_2 & -\beta_2\tau_1 + \beta_1\tau_2 \\ \beta_2\sigma_1 - \beta_1\sigma_2 & \beta_1\beta_2 - \sigma_1\tau_2 & \mathrm{Im}(\bar{\beta}^2\sigma) + |\sigma|^2\tau_2 & |\beta|^2\beta_2 + \mathrm{Im}(\beta\bar{\sigma}\bar{\tau}) \\ -\beta_1\beta_2 + \sigma_2\tau_1 & -\beta_2\tau_1 + \beta_1\tau_2 & |\beta|^2\beta_2 + \mathrm{Im}(\beta\bar{\sigma}\bar{\tau}) & \mathrm{Im}(\bar{\beta}^2\tau) + |\tau|^2\sigma_2 \end{pmatrix}. \tag{1.100}$$

The moduli $\tau = \tau_1 + i\tau_2, \sigma = \sigma_1 + i\sigma_2$ and $\beta = \beta_1 + i\beta_2$ are related to the moduli of a genus two surface whose Jacobian is the T^4. In this sense it is possible to map the $Sp(4;\mathbb{Z})$ monodromies of [18] to $SL(4;\mathbb{Z})$ monodromies and potentially study instanton corrections to the semi-flat construction.

Another application is to embed $T^2_\tau \times T^2_\rho$ solutions of [5], which corresponds to setting $\beta = 1$ and $\sigma = \rho$. We leave this line of research to future work.

Chapter 2

Non-flat points in F-theory compactifications

In this chapter we review results obtained in [24].

We study a phenomenologically interesting F-theory compactification leading to an $SU(5)\times U(1)$ gauge theory [25]. The $U(1)$ factor leads to a Peccei-Quinn type symmetry suppressing the proton decay usually present in $SU(5)$ GUT theories [26, 27].

The concept of F-theory arises when one views the IIB S-duality group $SL(2;\mathbb{Z})$ as the modular group of a T^2. Then IIB is a compactification of a putative twelve dimensional theory. Since there is no twelve dimensional supergravity one should view this more as a computational trick. There is however a duality to M-theory which can be viewed as a Kaluza-Klein reduction of F-theory on a circle. Using these two viewpoints one can make a number of useful statements about IIB compactifications with D7-branes.

2.1 A brief introduction to F-theory

In this section a brief exposition of F-theory [28] is given. Excellent reviews are [29, 30] among others.

In the weak coupling regime IIB string theory reduces to the chiral $\mathcal{N}=2$ supergravity in ten dimensions. The bosonic part of the action in Einstein frame reads as

$$\begin{aligned} S_{\text{IIB}} &= \frac{1}{2\kappa^2}\int d^{10}x\sqrt{-g}\left(R-\frac{\partial_\mu\tau\partial^\mu\tau}{2(\text{Im}\tau)^2}-\frac{1}{2\text{Im}\tau}G_3\wedge *G_3-\frac{1}{4}F_5\wedge *F_5\right)\\ &+\frac{1}{8i\kappa^2}\int d^{10}x\frac{1}{\text{Im}\tau}C_4\wedge G_3\wedge\bar{G}_3. \end{aligned} \tag{2.1}$$

Here $\kappa = \frac{1}{4\pi}(4\pi^2\alpha')^4 = \frac{l_s^8}{4\pi}$, g denotes the determinant of the metric and R its Ricci scalar. Further

$$\begin{aligned} \tau &= C_0 + ie^{-\Phi} \\ G_3 &= dC_2 + \tau dB_2, \end{aligned} \tag{2.2}$$

where Φ is the dilaton, B_2 the Kalb-Ramond field and C_p are the Ramond-Ramond fields. Note that $\mathrm{Im}\tau = g_s$, the string coupling. This action is manifestly invariant under $SL(2;\mathbb{R})$ transformations acting via

$$\begin{aligned} \tau &\mapsto \frac{a\tau + b}{c\tau + d} \\ \begin{pmatrix} C_2 \\ B_2 \end{pmatrix} &\mapsto \begin{pmatrix} a & b \\ c & d \end{pmatrix} \begin{pmatrix} C_2 \\ B_2 \end{pmatrix} \\ (G_4, g_{\mu\nu}) &\mapsto (G_4, g_{\mu\nu}), \end{aligned} \tag{2.3}$$

for $\begin{pmatrix} a & b \\ c & d \end{pmatrix} \in SL(2;\mathbb{R})$. This symmetry reduces to $SL(2;\mathbb{Z})$ at the quantum level. It is called S-duality. For $c \neq 0$ it in inverts the imaginary part of τ and thus relates IIB theory at weak coupling to strong coupling.

τ is called the axio-dilaton, seeing as it combines the axion C_0 and the dilaton Φ. We can study the behavior of τ in the vicinity of a D7-brane. Combining the two transverse spacial coordinates into one complex coordinate, supersymmetry implies holomorphicity for τ. In addition the charge of such a brane is given by

$$\int_{S^1} *F_9 = \int_{S^1} dC_0 = 1, \tag{2.4}$$

where S^1 has unit radius, lies in the complex plane and encircles the location of the brane, which we denote by $z_0 \in \mathbb{C}$. One thus solves for $\tau(z) = \frac{1}{2\pi i}\ln(z - z_0) + \text{regular}$. We see that τ undergoes a monodromy $\tau \to \tau + 1$ when going around the brane. Were we to consider a stack of N coincident branes we would observe a monodromy $\tau \to \tau + N$.

More generally we can associate $SL(2;\mathbb{Z})$ monodromies acting via

$$\tau \mapsto \frac{a\tau + b}{c\tau + d}, \tag{2.5}$$

to detect D7 branes.

This leads to the concept of F-theory: Interpreting τ as the complex structure modulus of an elliptic curve we can encode a IIB compactification on say $B \times \mathbb{R}^{1,3}$ with D7 branes in a completely geometric way by fibering an elliptic curve over $B \times \mathbb{R}^{1,3}$. Degenerations in the fiber are associated to branes. This is like compactifying a putative twelve

dimensional supergravity theory on an elliptic Calabi-Yau manifold X, where

$$\begin{array}{ccc} T^2 & \to & X \\ & & \downarrow \\ & & B. \end{array} \tag{2.6}$$

To understand this it is useful to switch to the M-theory picture. Firstly consider the case where B is a point,i.e. $X = S^1_A \times S^1_B$, where (S^1_A, S^1_B) have radius (R_A, R_B) respectively. If S^1_A denotes the M-theory circle, then the limit $R_A \to 0$ corresponds to IIA compactified on S^1_B. T-duality acting via $R_B \mapsto 1/R_B$ yields IIB compactified on a circle with radius $1/R_B$. Sending $R_B \to 0$ leads to decompactification of the IIB theory.
Thus we end up with the duality

$$\text{IIB} \longleftrightarrow \text{M-theory on } S^1_A \times S^1_B|_{R_A, R_B \to 0}. \tag{2.7}$$

More generally for a given IIB background B containing D7 branes, and X as above we have

$$\text{IIB on } B \longleftrightarrow \text{M-theory on } X|_{T^2 \to 0}. \tag{2.8}$$

Let us explain this in slightly more detail. In the low energy limit M-theory is approximated by the following action:

$$S = \frac{2\pi}{l_M^9} \int \sqrt{-g}R + G_4 \wedge *G_4 - \frac{1}{6} C_3 \wedge G_4 \wedge G_4. \tag{2.9}$$

We consider this on the background $S^1_A \times S^1_B \times M_9$ with metric

$$ds^2 = A \left(\frac{1}{\tau_2}(dx + \tau_1 dy)^2 + \tau_2 dy^2 \right) + ds_9^2, \tag{2.10}$$

where A denotes the overall area of the torus. In general compactifying M-theory to IIA-theory gives a metric of the form

$$ds_M^2 = L^2 e^{4\Phi/3}(dx + C_1)^2 + e^{-2\Phi/3} ds_{IIA}^2, \tag{2.11}$$

where L parametrizes the length of the M-theory circle. Comparison with the previous metric immediately yields

$$C_1 = \tau_1 dy, \quad e^{4\Phi/3} = \frac{A}{L\tau_2}, \quad ds_{IIA}^2 = \frac{\sqrt{A}}{L\sqrt{\tau_2}}(A\tau_2 dy^2 + ds_9^2). \tag{2.12}$$

We now perform T-duality along S^1_B, i.e. the new circle satisfies $\tilde{L}_B = l_s/L_B$ and $C_0 = (C_1)_y = \tau_1$. This also affects the coupling constants

$$g_{IIB} = \tilde{L}_B g_{IIA}. \tag{2.13}$$

To compute $\tilde{L}_B$ and g_{IIB} we dimensionally reduce an M2-brane probe action to a fundamental string and to a D2-brane:

$$T_{F1} = L_B T_{M2} \Rightarrow \frac{1}{l_s^2} = \frac{L_B}{l_s^3}, \qquad T_{D2} = T_{M2} \Rightarrow g_{IIA} l_s^3 = e^{4\Phi/3} l_M^3. \tag{2.14}$$

Taking into account $v = L_B L$ further algebraic manipulations lead to

$$\tau = \tau_1 + i\tau_2 = C_0 + \frac{i}{g_{IIB}}, \tag{2.15}$$

$$ds^2_{IIB} = \frac{\sqrt{A g_{IIB}}}{L}\left(\frac{l_M^6}{A^2} d\tilde{y}^2 + ds_9^2\right). \tag{2.16}$$

This metric is now in string frame. In order to describe the behaviour as $A \to 0$ we switch to Einstein frame

$$ds^2_{IIB,E} = \frac{\sqrt{A}}{L}\left(\frac{L^2 l_s^4}{A^2} d\tilde{y}^2 + ds_9^2\right). \tag{2.17}$$

Rescaling $L = \sqrt{A}$ (which is always possible by shifting the dilaton) we obtain

$$ds^2_{IIB,E} = \frac{l_s^4}{A} d\tilde{y}^2 + ds_9^2. \tag{2.18}$$

Thus the limit $A \to 0$ leads to IIB on $\mathbb{R} \times M_9$. If we choose $M_9 = \mathbb{R}^{1,2} \times B$ with B a Kähler manifold and promote τ to a holomorphic function on B we obtain a torus bundle on the M-theory side. The above discussion holds true fiberwise. The limit $A \to 0$ corresponds to decompatification once again, but now the function τ will encode the brane content of the IIB background.

2.2 The specific model in Weierstrass form

In this section we will describe how the M-theory picture can be used to extract the matter content of a given F-theory compactification on a holomorphic elliptic fibration X with sections.

Assuming that the base manifold B is a toric variety we can embed X into a larger toric variety commonly referred to as the ambient space. A brief review of toric varieties is given in appendix A.

The ambient space is constructed by fibering $\mathbb{P}_{2,3,1}$ over B. We then embed a T^2 into each fiber using the Weierstrass equation. X is the hypersurface defined by

$$y^2 = x^3 + fxz^4 + gz^6. \tag{2.19}$$

Here $f \in \Gamma(B, \bar{K}_B^4)$ and $g \in \Gamma(B, \bar{K}_B^6)$, where $\bar{K}_B$ is the anti-canonical bundle over B. An important example is always $B = \mathbb{P}_3$. Then (f, g) are homogeneous polynomials of degree

$(4, 6)$. An important consequence of choosing (f, g) in this way is that $c_1(X) = 0$, i.e. X is Calabi-Yau. This is obviously desirable for supersymmetric M-theory compactifications.

X need not be a smooth variety in general. In fact singularities of X are crucial for F-theory model building. In this section we wish to describe a model that leads to an $SU(5) \times U(1)$ gauge group in four dimensions.

Singularities of (2.19) are described by the discriminant locus

$$\Delta = 4f^3 + 27g^2 = 0. \tag{2.20}$$

This defines a divisor on B over which the generic fiber T^2 degenerates. If B is complex one dimensional such fibers have been classified by Kodaira [31]. The classification depends on the vanishing order of (f, g, Δ) see Table 2.1.

ord (f,g, Δ)	type	singularity	monodromy
($\geq$0,$\geq$0,0)	I_0	smooth	$\begin{pmatrix} 1 & 0 \\ 0 & 1 \end{pmatrix}$
(0,0,n)	I_n	A_{n-1}	$\begin{pmatrix} 1 & n \\ 0 & 1 \end{pmatrix}$
($\geq$1,1,2)	II	smooth	$\begin{pmatrix} 1 & 0 \\ -1 & 1 \end{pmatrix}$
$(\geq 1, \geq 2, 3)$	III	A_1	$\begin{pmatrix} 0 & 1 \\ -1 & 0 \end{pmatrix}$
$(\geq 2, 2, 4)$	IV	A_2	$\begin{pmatrix} 0 & 1 \\ -1 & -1 \end{pmatrix}$
$(\geq 2, 3, n+6)$ or $(2, \geq 3, n+6)$	I_n^*	D_{n+4}	$\begin{pmatrix} -1 & n \\ 0 & -1 \end{pmatrix}$
$(\geq 3, 4, 8)$	IV^*	E_6	$\begin{pmatrix} -1 & -1 \\ 1 & 0 \end{pmatrix}$
$(3, \geq 5, 9)$	III^*	E_7	$\begin{pmatrix} 0 & -1 \\ 1 & 0 \end{pmatrix}$
$(\geq 4, 5, 10)$	II^*	E_8	$\begin{pmatrix} 0 & -1 \\ 1 & 1 \end{pmatrix}$

Table 2.1: Kodaira list of singularities. Notice that the total space can still be smooth in the cases of an I_1 and II singular fiber. A prime example is the K3 surface sporting 24 I_1 degenerations over distinct points.

Notice that for higher dimensional B the singular fibers may well not be of Kodaira type. However for the model we consider this will only be the case a certain special points, which

we will describe later.

The specific Calabi-Yau manifolds we consider [25], consist of some toric base B together with non-generic homogenenous polynomials f and g:

$$\begin{aligned} y^2 = x^3 + \quad & (C_1C_3 - B^2C_0 - \frac{1}{3}C_2^2)xz^4 + \\ & (C_0C_3^2 - \frac{1}{3}C_1C_2C_3 + \frac{2}{27}C_2^3 - \frac{2}{3}B^2C_0C_2 + \frac{1}{4}B^2C_1^2)z^6, \end{aligned} \tag{2.21}$$

where (B, C_1, C_2, C_3) are sections of line bundles of appropriate degree. A useful example is furnished by $B = \mathbb{CP}^3$, for which we include a Sage Math code in the appendix A.

In addition to the zero section $(x, y, z) = (1, 1, 0)$ one has the non-trivial section

$$(x, y, z) = (C_3^2 - \frac{2}{3}B^2C_2^2, -C_3^3 + B^2C_2C_3 - \frac{1}{2}B^4C_1, B). \tag{2.22}$$

The existence of this extra section, leads to an additional global $U(1)$ factor in the F-theory compactification. This can be deduced by carefully tracing F/M-theory duality. We postpone this discussion towards the end of this section 2.2.1.

As it turns out if one specifies (2.21) further one can generate a gauge group $SU(5) \times U(1)$. To see this let ω be a section of $\mathcal{O}_B(1)$, or simply a holomorphic coordinate on the base and consider

$$\begin{aligned} B &= \delta \\ C_0 &= \frac{1}{4}\omega^2(d_3^2\alpha^2 + 4\omega\alpha\gamma) \\ C_1 &= \frac{1}{2}\omega(c_2d_3^2\alpha + 2\omega(d_2\alpha + c_2\gamma)) \\ C_2 &= \frac{1}{4}(d_3^2c_2^2 + 2\omega(2d_2c_2 - d_3\alpha\delta)) \\ C_3 &= \omega\beta - \frac{1}{2}c_2d_3\delta. \end{aligned} \tag{2.23}$$

Here $\alpha, \beta, \gamma, \delta, c_2, d_2, d_3$ are section of line bundles on B, which should be thought of as homogeneous polynomials of appropriate degree. This is possible as B is (embedded in) a toric variety.

Thus the discriminant becomes

$$\Delta = \frac{1}{16}\omega^5 P, \tag{2.24}$$

where P is a product of polynomials in the sections given above. The term ω^5 implies that the fiber over $\Sigma = \{\omega = 0\} \subset B$ is of type I_5, as can be read off from Table 2.1. This leads

to a gauge group $SU(5)$ upon compactification as will be explained in the sequel. For this reason Σ is called the GUT divisor.

In order to make sense of the M-theory compactification one resolves the model (2.23). To do this one rewrites (2.21) in terms of a $Bl_{[0,1,0]}\mathbb{P}_{1,1,2}$ fibration [32] via the birational map

$$\begin{aligned} x &= b_2^2 v^2 + b_2(w - \frac{1}{2}(b_0 u^2 + b_1 uv)) + (c_3 - \frac{1}{2}b_1 b_2)uv \\ y &= b_2^2 v(w - \frac{1}{2}(b_0 u^2 + b_1 uv)) + b_2^3 v^3 + b_2(c_3 - \frac{1}{2}b_1 b_2)uv^2 \\ &\quad + (b_2(c_2 + \frac{1}{2}(b_1^2 - b_2 b_0)) - (c_3 - \frac{1}{2}b_1 b_2)^2/b_2)u^2 v \\ z &= u \end{aligned} \tag{2.25}$$

Here $(u, v, w) \in Bl_{[0,1,0]}\mathbb{P}_{1,1,2}$. We also have the identification

$$\begin{aligned} B &= b_2 \\ C_0 &= c_0 - \frac{1}{4}b_0 \\ C_1 &= c_1 - \frac{1}{2}b_0 b_1 \\ C_2 &= c_2 - \frac{1}{4}b_1^2 - \frac{1}{2}b_0 b_2 \\ C_3 &= c_2 - \frac{1}{2}b_1 b_2 \end{aligned} \tag{2.26}$$

Let s parametrize the exceptional $\mathbb{P}^1$ in $Bl_{[0,1,0]}\mathbb{P}_{1,1,2}$. Then our manifold can be described by the hypersurface equation

$$\begin{aligned} b_2 v^2 w + s w^2 + b_1 s w v u \quad & + b_0 s^2 w u^2 = c_3 v^3 u + \\ & + c_2 s v^2 u^2 + c_1 s^2 v u^3 + c_0 s^3 u^4, \end{aligned} \tag{2.27}$$

with:

$$\begin{aligned} b_0 &= \omega d_3 \alpha, \\ b_1 &= c_2 d_3 \\ b_2 &= \delta \\ c_0 &= \omega^3 \alpha\gamma \\ c_1 &= \omega^2(d_2\alpha + c_2\gamma) \\ c_2 &= \omega c_2 d_2 \\ c_3 &= \omega\beta. \end{aligned} \tag{2.28}$$

The resolution procedure described in [25] leads to a complete intersection Calabi-Yau:

$$\mathrm{HSE}_1 \; : \quad \lambda_1 e - \lambda_2 s P_2 = 0\,, \tag{2.29}$$

$$\text{HSE}_2 \; : \quad \lambda_2\, Q - \lambda_1\, u\, P_1 = 0\,, \tag{2.30}$$

with the polynomials

$$Q = e_1\, s\, w^2 - e_4^2\, e_0\, \beta\, v^3\, u + e_4\, \delta\, v^2\, w\,, \tag{2.31}$$

$$P_1 = e_4\, e_0\, d_2\, u\, v + d_3\, w + e_1\, e_4\, e_0^2\, \gamma\, s\, u^2\,, \tag{2.32}$$

$$P_2 = c_2\, v + e_0\, e_1\, \alpha\, s\, u\,. \tag{2.33}$$

The toric ambient space is given by the following toric data, see appendix A for a brief introduction:

u	v	w	s	e_0	e_1	e	e_4	λ_1	λ_2	HSE_1	HSE_2
1	1	2	0	0	0	0	0	1	0	1	4
0	1	1	1	0	0	0	0	2	0	2	3
$-c_B$	0	0	$[\delta]$	$[\omega]$	0	0	0	$2[\delta]+[\omega]+[\alpha]-c_B$	0	$2[\delta]+[\omega]+[\alpha]-c_B$	$[\delta]$
0	0	-1	0	-1	1	0	0	0	0	0	-1
0	-1	-2	0	-1	0	1	0	-2	0	-1	-4
0	-1	-1	0	-1	0	0	1	-1	0	-1	-2
0	0	0	0	0	0	0	0	1	1	1	1

Here $[x]$ denotes the degree of section x and the homogeneous Stanley-Reisner ideal is given by

$$\text{SR-I} = \{u\,w,\, u\,e,\, u\,e_4,\, v\,s,\, v\,e_1,\, w\,e_0,\, s\,e_0,\, e_0\,e,\, \lambda_1\,\lambda_2,\, s\,e,\, s\,e_4,\, w\,e_4\}\,. \tag{2.34}$$

As it turns out (2.29) and (2.30) still contain singularities, which cannot be resolved without violating the Calabi-Yau condition. They are located at

$$\alpha = \gamma = 0, \tag{2.35}$$

and thus generically lie away from the GUT-divisor. The correct technical description of these is as $\mathbb{Q}$-factorial terminal singularities. If the base B is complex two dimensional they give rise to hypermultiplets uncharged under any continous massless gauge group, as was explained in [33, 34]. We explain how to deal with them in section 2.6. Since the physics we are about to study revolves around the GUT-divisor we can safely ignore these singularities and assume our manifold to be smooth.

There is however another interesting feature of (2.29) and (2.30) and that is the presence of a non-flat point. To this end recall that a fibration is called flat if the dimension of the fiber is constant over the base. This is the case for our singular fourfold, but when we resolve we find that over the locus

$$\omega = \alpha = c_2 = 0, \tag{2.36}$$

the fiber dimension is of complex dimension two. Before delving into the details of this locus we explain the generic features of these backgrounds. In particular how the gauge group $SU(5) \times U(1)$ arises.

2.2.1 Gauge group from F/M-theory duality

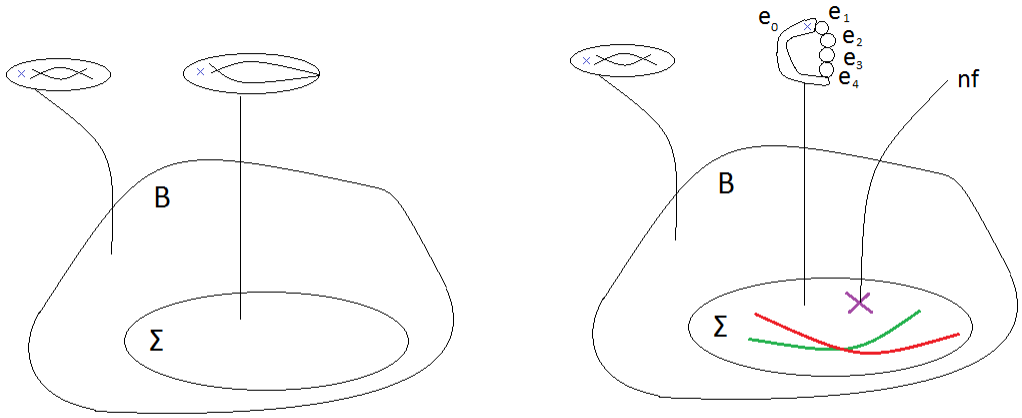

Figure 2.1: Sketch of the resolution. e_0 corresponds to this original singular fiber. The zero section intersects the fiber in the marked spots. The second section S_1 is not shown, but intersects the fiber similarly. On the right we schematically display curves inside Σ over which some of the e_i split further. Notice that Σ has codimension one on the base B. We also indicate the points over which the fiber becomes non-flat. These actually lie at the intersection of matter curves which not depicted here.

In order to infer the gauge group of the low-dimensional theory one exploits F/M-theory duality. This is very subtle and we only summarize the results. In general X is singular. We consider its crepant (i.e. Calabi-Yau) resolution Y. In general after resolution of the I_5 singularity the fiber will topologically look like 5 spheres or $\mathbb{CP}^1$s intersecting according to the extended Dynking diagram A_5, see Figure 2.1. We label each of their homology classes them $e_0, ..., e_4 \in H_2(Y)$. We consider the fibration

$$\begin{array}{rl} e_i \rightarrow & E_i \\ & \downarrow \\ & \Sigma \end{array} \tag{2.37}$$

and denote its homology class by $[E_i]$. These are very important divisors. By Poincare duality $[E_i]$ is mapped to a two form which we denote by the same symbol.

In order to infer the gauge group of the M-theory compactification we expand the M-theory three-form C_3

$$C_3 = A_0^S \wedge ([S_0] - \frac{1}{2}[\bar{K}_B]) + \sum_{\alpha=1}^{h^{1,1}(B)} A_\alpha \wedge [\pi^* D_\alpha] + \\ + A_1^S \wedge [\sigma(S_1)] + \sum_{i=0}^{4} A_i \wedge [E_i]. \tag{2.38}$$

Here $[S_0], [S_1], [\bar{K}_B], [\pi^* D_\alpha]$ denote the Poincare duals of the zero section, the image under the Shioda map σ [35, 36] of the additional section [1], the anticanonical class and the pullbacks of divisors on B. The resulting gauge group in M-theory is $U(1)^{1+h^{1,1}(B)+1+5}$. However the gauge fields A_0^S, A_α do not uplift to gauge fields in the F-theory compactification. This is very subtle but can broadly be explained as follows:

- A_α are in fact obtained by reducing two-forms b_α on the circle $\tilde{S}_B^1$ mentioned above. These two-forms arise from expanding $C_4 = ... + \sum_{\alpha=1}^{h^{1,1}(B)} b_\alpha \wedge [\pi^* D_\alpha]$ and are parts of tensor multiplets in the F-theory compactification.
- The field A_0 is a Kaluza-Klein field and is part of the metric of the F-theory compactification. An M2-brane wrapping the generic T^2 fiber n times will have $U(1)$-charge $q_0 = ([S_0] - \frac{1}{2}\bar{K}_B) \cdot n[T^2] = n$. In the F-theory limit $T^2 \to 0$ these states become massless. Negative n are achieved by flipping the orientation of $[T^2]$.

We now trace the F-theory origins of A_1^S, A_i. These do uplift to $U(1)$ gauge fields in F-theory because the divisors $[\sigma(S_1)], [E_i]$ satisfy

$$[D] \cdot \pi^*(D_\alpha) = 0, \qquad [D] \cdot [S_0] \cdot \pi^*(D_\alpha) = 0, \quad \forall D_\alpha \in H_{2n-4}(B). \tag{2.39}$$

The first condition guarantees the absence of massive $U(1)$ fields arising from divisors in the base. The second condition implies zero intersection number with the generic T^2 fiber.This implies that all M2-branes wrapping the generic fiber carry equal charge under the field A_0[2].

To summarize A_1^S, A_i do indeed uplift to $U(1)$ gauge fields in F-theory. Moreover the A_i form the Cartan subgroup of $SU(5)$ as can be seen from studying the M-theory Coulomb branch.
To do this remember that M2-branes are electrically charged under C_3. If we have an M2-brane wrapping any curve C, its charge under A_i is

$$q_i = \int_C [E_i] = [C] \cdot [E_i]. \tag{2.40}$$

[1] Essentially this is to guarantee the conditions (2.39). Observe that for the zero section: $\sigma([S_0]) = [S_0] - \frac{1}{2}\bar{K}_B$ on a smooth space.

[2] As explained in [29] these M2-branes correspond to KK states in the S^1 compactification of F- to M-theory.

If $[C] = e_i$ then the vector $\vec{q}$ will correspond to the simple roots of $SU(5)$. Thus we obtain particles in the adjoint representation.
Over certain codimension one loci on Σ the fiber structure changes, because certain e_is split into two $\mathbb{P}^1$s. M2 branes wrapping (formal sums of) such curves furnish other representations of $SU(5)$ such as the fundamental **5** and antisymmetric **10**[3].
Moreover these $[C]$ also have non-trivial intersection with $\sigma(S_1)$. This number gives us the $U(1)$ charge under A_1^S.

In general such states carry mass

$$m = |\int_C J|, \tag{2.41}$$

with J the Kähler form of Y. Since $[C]$ are curves in the fiber they become massless in the F-theory limit of vanishing fiber size. This corresponds to moving to the origin of the M-theory Coulomb branch. As we have seen the gauge group $U(1)^5$ enhances to $SU(5)$ in this limit.

We close this section by remarking that when two curves intersect, often (but not always) the fiber structure will be enhanced in such a way that all states in both representations are present leading to Yukawa interactions. In our case all Yukawa points except for one have already been analysed in [25].

2.2.2 The structure of the matter curves

All in all we end up with an F-theory compactification, which exhibits a gauge group of $SU(5) \times U(1)$. The curves on $\Sigma = \{\omega = 0\}$ with the additional specification

$$\mathbf{10}_{-2}: \quad d_3 = 0\,, \qquad \mathbf{10}_3: \quad c_2 = 0\,, \tag{2.42}$$

are responsible for states in the **10** representation of $SU(5)$. The $U(1)$ charge is given by the subscripts.

In turn the fundamental representation of $SU(5)$ appears at the loci

$$\begin{aligned} \mathbf{5}_{-6}: &\quad \delta = 0\,, \\ \mathbf{5}_{-1}: &\quad \alpha^2\, c_2\, d_2^2 + \alpha^3\, \beta\, d_3^2 + \alpha^3\, d_2\, d_3\, \delta - 2\,\alpha\, c_2^2\, d_2\, \gamma - \alpha^2\, c_2\, d_3\, \delta\, \gamma + c_2^3\, \gamma^2 = 0\,, \\ \mathbf{5}_{4}: &\quad \beta\, d_3 + d_2\, \delta = 0\,. \end{aligned} \tag{2.43}$$

Furthermore we have singlets under $SU(5)$ with $U(1)$ charge ± 5 and ± 10 at the loci

$$\begin{aligned} \mathbf{1}_{\pm 10}: &\quad \beta = \delta = 0\,, \\ \mathbf{1}_{+5}: &\quad 12\omega(2\omega^2\beta^3 + c_2^2 d_3 \delta^2(d_3\beta + d_2\delta) + \omega\delta(\alpha\delta^2(d_3\beta + d_2\delta) + \\ &\quad + c_2(\gamma\delta^3 3 d_3 \beta^2 2 d_2 \beta\delta))) = 0 \end{aligned} \tag{2.44}$$

[3] In our specific model these splitting $\mathbb{P}^1$s have been identified in [25]

$$\begin{aligned}\mathbf{1}_{-5}: \quad & \omega^2(\omega^2\beta^4 + c_2\delta^2(d_3\beta + d_2\delta)(c_2 d_3\beta + c_2 d_2\delta d_3\alpha\delta^2) + \\ & \omega\delta(\alpha\gamma\delta^5 d_3\alpha\beta^2\delta^2 + 2c_2\beta^2(d_3\beta + d_2\delta))) = 0.\end{aligned}$$

These curves intersect in various places on Σ. This leads to Yukawa couplings of the form

$$\begin{aligned}\mathbf{10}_{-2}\,\bar{\mathbf{5}}_6\,\bar{\mathbf{5}}_{-4}: \quad & \omega = d_3 = \delta = 0\,, \\ \mathbf{10}_{-2}\,\bar{\mathbf{5}}_1\,\bar{\mathbf{5}}_1: \quad & \omega = d_3 = \alpha\, d_2 - c_2\,\gamma\,, \\ \mathbf{10}_3\,\bar{\mathbf{5}}_{-4}\,\bar{\mathbf{5}}_1: \quad & \omega = c_2 = \beta\, d_3 + d_2\,\delta\,, \\ \mathbf{10}_{-2}\,\mathbf{10}_{-2}\,\mathbf{5}_4: \quad & \omega = d_3 = d_2 = 0\,, \\ \mathbf{10}_{-2}\,\mathbf{10}_3\,\mathbf{5}_{-1}: \quad & \omega = d_3 = c_2 = 0\,, \\ \mathbf{10}_3\,\mathbf{10}_3\,\mathbf{5}_{-6}: \quad & \omega = c_2 = \delta = 0\,,\end{aligned} \tag{2.45}$$

and

$$\begin{aligned}\bar{\mathbf{10}}_{-3}\,\mathbf{10}_{-2}\,\mathbf{1}_5: \quad & \omega = d_3 = c_2 = 0\,, \\ \bar{\mathbf{5}}_{-4}\,\mathbf{5}_{-6}\,\mathbf{1}_{10}: \quad & \omega = \delta = \beta = 0\,, \\ \bar{\mathbf{5}}_1\,\mathbf{5}_{-6}\,\mathbf{1}_5: \quad & \omega = \delta = \alpha^2\, c_2\, d_2^2 + \alpha^3\,\beta\, d_3^2 - 2\,\alpha\, c_2^2\, d_2\,\gamma + c_2^3\,\gamma^2 = 0\,, \\ \bar{\mathbf{5}}_{-4}\,\mathbf{5}_{-1}\,\mathbf{1}_5: \quad & \omega = \beta\, d_3 + d_2\,\delta = \alpha^2\, c_2\, d_2^2 - 2\,\alpha\, c_2^2\, d_2\,\gamma - \alpha^2\, c_2\, d_3\,\delta\,\gamma + c_2^3\,\gamma^2 = 0.\end{aligned} \tag{2.46}$$

Finally there is the more mysterious intersection

$$\omega = \alpha = c_2 = 0, \tag{2.47}$$

where the $\mathbf{10}_3$ intersects the triple self-intersection of $\mathbf{5}_{-1}$. There is no gauge invariant coupling made out of these representations containing only three fields. In fact we will show that in the weak coupling regime the coupling $\mathbf{10}_3\mathbf{5}_{-1}\mathbf{5}_{-1}\mathbf{5}_{-1}$ is present. In contrast to the usual analyses the fiber over the locus (2.47) is of complex dimension two. There are many ways to wrap M2-branes over cycles in the fiber, and one also has to consider the effect of an M5-brane wrapping the entire cycle. Such a state would correspond to a string, or one brane in four dimensions and therefore must be ruled out. We will adress this problem next.

2.3 The Freed-Witten anomaly for an M5-brane

So far we only considered the M-theory three form C_3. However we need to take its flux G_4 into consideration as well. Firstly, in order to cancel the Freed-Witten anomaly we require in accordance with [37, 38]:

$$G_4 + \tfrac{1}{2}c_2(Y_4) \in H^4(Y_4, \mathbb{Z}). \tag{2.48}$$

Here Y_4 is the resolved Calabi-Yau four-fold. If the restriction of G_4 to the non-flat fiber is non-zero this implies a violation of the Freed-Witten anomaly for M5-branes wrapping this cycle [38]. This is necessary in order for strings arising by such a wrapping to be forbidden

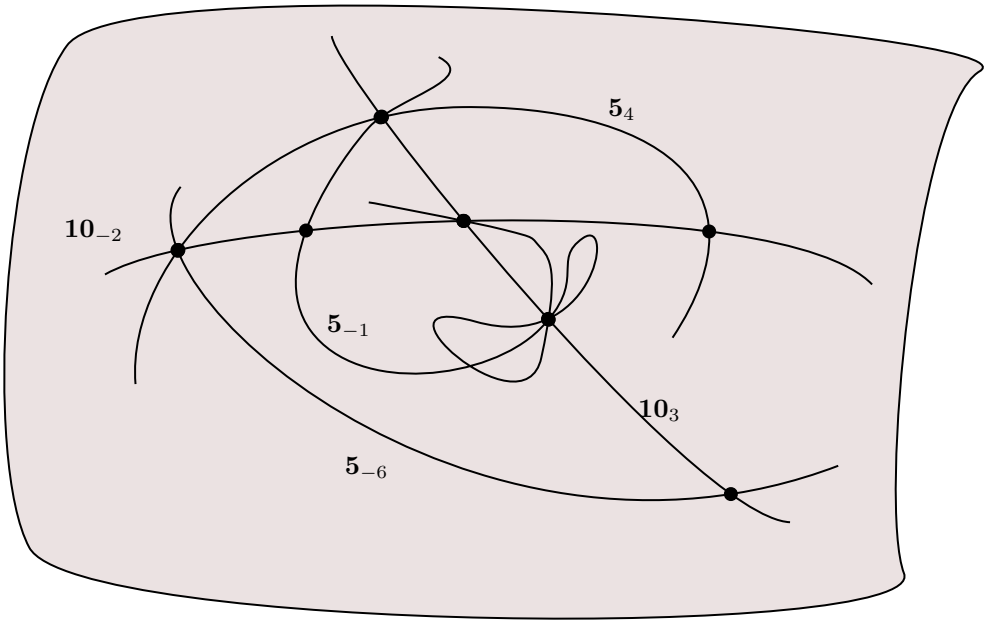

Figure 2.2: The GUT-divisor with the matter curves. The dots denote the Yukawa points (2.45) and the non-flat point at the intersection of the $\mathbf{10}_3$-curve with the $\mathbf{5}_{-1}$-curve. Picture taken from [24].

in four dimensions. Such strings could obtain a mass from C_3 even if $G_4|_{\text{NF}}= 0$ as was mentioned in a similar context in [39].

The restriction of G_4 to the non-flat fiber has to be non vanishing if

$$\int_{NF} c_2(Y_4) = 2k + 1, \tag{2.49}$$

as (2.48) can only be satisfied if G_4 is non-zero.

The computation of $c_2(Y_4)$ for the model (2.19) yields [40]:

$$\begin{aligned} c_2(Y_4) = \; & \left(c_2(B_3) - c_1(B_3)^2\right) + \\ & +6\, c_1(B_3)\,(S + U + c_1(B_3) - [\delta]) - \\ & -[\delta]\,(S - U - c_1(B_3) - [\delta])\,. \end{aligned} \tag{2.50}$$

Here we adopt the convention $U = \text{divisor}\,(\{u = 0\})$ and similarly for all other coordinates.

The four form flux in F-theory compactifications on Y_4 is a sum of several fluxes with

different origins. Schematically

$$G_4 = G_4(U(1)) + \sum_{\text{matter}} G_4^i. \tag{2.51}$$

Each of these summands is subject to the conditions

$$\begin{aligned} \int G_4^i [S_0][\pi^* D_a] &= 0 \\ \int G_4^i [\pi^* D_a][\pi^* D_b] &= 0 \\ \int G_4^i [E_i][\pi^* D_a] &= 0, \end{aligned} \tag{2.52}$$

for all divisors D_a on B. The first two conditions can be derived by matching the M-theory Chern-Simons terms with the one loop terms in the F-theory reduction on S^1. Physically they secure that the tower of KK-states is not affected by the flux. The third condition guarantees that all matter arising from a matter curve has the same chiral index.

We now explain the various pieces in (2.51). On the one hand we have the part associated with the extra section. Via the Shioda map [35, 36, 41] we can turn the section S_1 into a $(1,1)$-form. Wedged with another such form we obtain a $(2,2)$-form known as the $U(1)$-flux given by:

$$G_4^{U(1)}(\mathcal{F}) = \mathcal{F}\left(5\left(S - U - [\delta] - c_1(B_3)\right) + 4\,E_1 + 3\,\Lambda_2 + 2\left(E - \Lambda_2\right) + E_4\right) \tag{2.53}$$

with $\mathcal{F} \in \pi^* H^{1,1}(B_3, \mathbb{Z})$. The Shioda homomorphim guarantees that (2.52) is satisfied.

On the other hand we have fluxes arising from the so-called matter surfaces. A matter surface is obtained by considering a fibration over a matter curve, where in the fiber we can take any combination of the $\mathbb{P}^1$s. Such a combination is associated to a weight vector β_a and the corresponding surface is denoted by S_a. Unfortunately (2.52) is not satisfied by the Poincare dual $[S_a]$, and we need to add corrections:

$$G_4(S_a, \kappa) = \kappa([S_a] + [I]\beta_a C_{i,j}^{-1} E_i) \tag{2.54}$$

Here κ is a normalization constant to make G_4 integral. In the case of $SU(5)$ we have $\kappa + 5$. $C_{i,j}^{-1}$ is the inverse of the $SU(5)$ Cartan matrix. The polynomial I describes the location of the matter curve in the ambient space.

Consider for instance the curve $\mathbf{10}_{-2}$ located at $d_3 = 0$. In the fiber we consider a $\mathbb{P}^1$ with weight vector

$$\beta_a = (1, -1, 0, 1). \tag{2.55}$$

Thus the structure of $G_4(\mathbf{10}_{-2})$ is

$$G_4(\mathbf{10}_{-2}) = \quad \kappa \left(S_{\beta_a} + [I](1,-1,0,1) C_{i,j}^{-1} \begin{pmatrix} E_1 \\ \Lambda_2 \\ E - \Lambda_2 \\ E_4 \end{pmatrix} \right)$$

$$= 5S_{\beta_a} + [I](2E_1 - \Lambda_2 + (E - \Lambda_2) + 3E_4). \tag{2.56}$$

Now we could simply say $[I] = [d_3]$ since the curve is located at $d_3 = 0$. However considering (2.58) we would like to express things in terms of $[\delta]$. Using cohomological relations we can substitute $[d_3] = 2c_1(B_3) - [\alpha] - [\omega] - [\delta]$ to obtain:

$$\begin{aligned}
G_4(\mathbf{10}_{-2}) &= 5\,(E_1 - \Lambda_1)\,E_4 - (2\,c_1(B_3) - ([\delta] + [\alpha] + [\omega]))\times \\
&\qquad \times (2\,E_1 - \Lambda_2 + (E - \Lambda_2) + 3\,E_4)\,, \\
G_4(\mathbf{10}_3) &= 5\,\Lambda_1\,E_4 - ([\delta] + [\alpha] + [\omega] - c_1(B_3))(3\,E_1 + \Lambda_2 - (E - \Lambda_2) + 2\,E_4)\,, \\
G_4(\mathbf{5}_{-6}) &= 5\,E_1\,U - [\delta]\,(4\,E_1 + 3\,\Lambda_2 + 2\,(E - \Lambda_2) + E_4)\,, \\
G_4(\mathbf{5}_{-1}) &= ([P_1] - \Lambda_2)([P_2] - \Lambda_1) + S\,[P_1] - (4\,c_1(B_3) - 2\,[\delta] - 3\,[\omega] - [\alpha])\times \\
&\qquad \times (-E_1 - 2\,\Lambda_2 + 2\,(E - \Lambda_2) + E_4)\,, \\
G_4(\mathbf{5}_4) &= 5\,(E_1\,([P_1] - \Lambda_2 - E_4) + \Lambda_1\,E_4) - (3\,c_1(B_3) - ([\alpha] + 2\,[\omega]))\times \\
&\qquad \times (E_1 - 3\,\Lambda_2 - 2\,(E - \Lambda_2) - E_4)\,.
\end{aligned} \tag{2.57}$$

A calculation with Sage reveals that

$$\begin{aligned}
c_2(Y_4) &= \left(c_2(B_3) - c_1(B_3)^2\right) + 6\,c_1(B_3)\,(S + U + c_1(B_3) - [\delta]) + \\
&\qquad - G_4^{U(1)}(\omega) - G_4(\mathbf{10}_{-2}) - G_4(\mathbf{5}_4) - G_4^{\mathrm{nf}} + \text{even terms} = \\
&= G_4^{U(1)}(\omega) + G_4(\mathbf{10}_{-2}) + G_4(\mathbf{5}_4) + G_4^{\mathrm{nf}} + \text{even terms}\,,
\end{aligned} \tag{2.58}$$

where G_4^{nf} is the flux corresponding to the four cycle $\mathcal{FS}$:

$$G_4^{\mathrm{nf}} = [c_2]\,(E - \Lambda_2 - E_1) + E_1\,(\Lambda_1 - S)\,. \tag{2.59}$$

Because none of the other fluxes in (2.58) localize to the non-flat fiber and because G_4^{nf} is odd we conclude that M5-branes wrapping the non-flat point are forbidden.

2.4 The IIB compactification at weak coupling

We review the weak coupling limit of F-theory in appendix D. In short one considers a IIB orientifold compacitfication on a Calabi-Yau threefold, which is a branched double cover of the base B_3. This is a hypersurface in a toric variety of the form

$$\xi^2 = F, \tag{2.60}$$

where the geometric part of the orientifold involution is $\xi \leftrightarrow -\xi$. The orientifold seven plane is located at $F = 0$.

As we will see the non-flat point in this limit is transformed into a conifold singularity. We compute the desired **10555** coupling mediated by D(-1)-brane instantons. Since this is holomorphic we expect this term survives throughout moduli space.

2.4.1 Taking the weak coupling limit

In this section we will work entirely on the singular space (2.21). To take the weak coupling limit we have to pass from the Weierstrass equation (2.19) to Tate form [42] by completing the square in y and the cubic equation in x:

$$y^2 + a_1 xyz + a_3 yz^3 = x^3 + a_2 x^2 z^2 + a_4 xz^4 + a_6 z^6. \tag{2.61}$$

The $a_i \in \Gamma(\bar{K}_B^i)$, more specifically up to irrelevant numerical factors:

$$\begin{aligned} a_1 &= b_1 \\ a_2 &= -(b_0\, b_2 + c_2) \\ a_3 &= -(b_2\, c_1 + b_0\, c_3) \\ a_4 &= (b_2^2\, c_0 + b_0\, b_2\, c_2 + c_1\, c_3) \\ a_6 &= -(b_2^2\, c_0\, c_2 - b_1\, b_2\, c_0\, c_3 + b_0\, b_2\, c_1\, c_3 + c_0\, c_3^2). \end{aligned} \tag{2.62}$$

Following [42], we set

$$\begin{aligned} \mathbf{b}_2 &= a_1^2 + 4\, a_2 \\ \mathbf{b}_4 &= a_1\, a_3 + 2\, a_2^2 \\ \mathbf{b}_6 &= a_3^2 + 4\, a_6. \end{aligned} \tag{2.63}$$

These are the same sections as those appearing in (2.28). In terms of these sections the original Weierstrass model corresponds to

$$f = -\frac{1}{48}(\mathbf{b}_2^2 - 24\mathbf{b}_4),\ g = \frac{1}{864}(\mathbf{b}_2^3 + 36\mathbf{b}_2\mathbf{b}_4 - 216\mathbf{b}_6). \tag{2.64}$$

This allows us to express the discriminant $\Delta = 4f^3 + 27g^2$ in terms of the a_i.

The weak coupling limit is obtained by expanding the $\mathbf{b}_i$ in terms of a parameter ϵ [43] with the condition that $\mathbf{b}_2$, $\mathbf{b}_4$, and $\mathbf{b}_6$ scale (at leading oder) as ϵ^0, ϵ^1, and ϵ^2, respectively. This can be achieved in several ways. We simply take

$$c_i \to \epsilon\, c_i, \tag{2.65}$$

in (2.63). Defining the expansion

$$\begin{aligned} \mathbf{b}_2 &= R + O(\epsilon) \\ \mathbf{b}_4 &= S\epsilon + O(\epsilon^2) \\ \mathbf{b}_6 &= T\epsilon^2 + O(\epsilon^3) \end{aligned} \tag{2.66}$$

the discriminant at weak coupling becomes

$$\Delta = \frac{1}{4}R^2\,(-RT + S^2)\epsilon^2 + O(\epsilon^3) =: \epsilon^2\, R^2\, \Delta_{w.c.} + O(\epsilon^3), \tag{2.67}$$

Expressing $\Delta_{w.c.}$ in terms of (2.62) yields

$$\begin{aligned}\Delta_{w.c} \;&\sim b_2\,(b_2^3\,c_0^2 - b_1\,b_2^2\,c_0\,c_1 + b_0\,b_2^2\,c_1^2 - 2\,b_0\,b_2^2\,c_0\,c_2 + b_1^2\,b_2\,c_0\,c_2 + \\ &-b_0\,b_1\,b_2\,c_1\,c_2 + b_0^2\,b_2\,c_2^2 + 3\,b_0\,b_1\,b_2\,c_0\,c_3 - 2\,b_0^2\,b_2\,c_1\,c_3 - b_1^3\,c_0\,c_3 + \\ &+b_0\,b_1^2\,c_1\,c_3 - b_0^2\,b_1\,c_2\,c_3 + b_0^3\,c_3^2)\,.\end{aligned} \tag{2.68}$$

The D-branes are located at $\Delta_{w.c} = 0$ in this limit. The IIB background is the Calabi-Yau threefold

$$\xi^2 - R = 0\,, \tag{2.69}$$

where $\{R = 0\}$ is the orientifold plane. The action

$$\xi \longleftrightarrow -\xi\,. \tag{2.70}$$

is the orientifold projection.

We now consider our specific model by setting b_i and c_i to:

$$\begin{aligned} &b_0 = -\omega\,d_3\,\alpha + b_{0,2}\,\omega^2\,, && b_1 = -c_2\,d_3 + b_{1,1}\,\omega\,, && b_2 = \delta\,, \\ &c_0 = -\omega^3\,\alpha\,\gamma\,, && c_1 = -\omega^2\,(d_2\,\alpha + c_2\,\gamma)\,, && c_2 = -\omega\,c_2\,d_2\,, \\ & && c_3 = -\omega\,\beta\,. \end{aligned} \tag{2.71}$$

Comparison with the expansion (2.28) we have extra terms in b_0 and b_1 of higher order in ω. This corresponds to deforming the complex structure and does not spoil the physical properties of our background. The defining equation (2.69) becomes

$$\xi^2 + c_2^2\,d_3^2 + \omega\,(b_{1,1}^2\,\omega - 4\,b_{0,2}\,\omega\,\delta + 4\,\alpha\,\delta\,d_3 - 2\,b_{1,1}\,c_2\,d_3) = 0. \tag{2.72}$$

We restrict to the vicinity of the singular point

$$\xi = \omega = c_2 = \alpha = 0, \tag{2.73}$$

where the higher order coupling **10555** should stem from. This means that $\delta, d_3, b_{1,1}, b_{0,2}$ are now effectively constants and the prescription

$$(u,\,w,\,\sigma) := (c_2\,d_3,\,b_{1,1}^2\,\omega - 4\,b_{0,2}\,\omega\,\delta + 4\,\alpha\,\delta\,d_3 - 2\,b_{1,1}\,c_2\,d_3,\,\omega), \tag{2.74}$$

transforms our equation into the well-known form:

$$\xi^2 = u^2 + \sigma w\,. \tag{2.75}$$

The conifold can alternatively be written in terms of homogeneous coordinates α_i, β_i which are related to our coordinates via

$$(\xi,\,u,\,\sigma,\,w) = (\tfrac{1}{2}(\alpha_1\beta_2 - \alpha_2\beta_1),\,\tfrac{1}{2}(\alpha_1\beta_2 + \alpha_2\beta_1),\,-\alpha_1\beta_1,\,\alpha_2\beta_2). \tag{2.76}$$

Here

$$\alpha_i \longleftrightarrow \beta_i \,. \tag{2.77}$$

yields the orientifold involution.

In terms of these coordinates the D-brane locus becomes

$$\begin{aligned}\Delta_{w.c.} \sim \alpha_1^5\,\beta_1^5\,\Big((-2\,b_{1,1}^2\,\delta^2\,\gamma + 8\,b_{0,2}\,\delta^3\,\gamma + b_{1,1}^3\,\delta\,d_2 - 4\,b_{0,2}\,b_{1,1}\,\delta^2\,d_2 - b_{1,1}^3\,\beta\,d_3)\,\alpha_1^3 + \\ + (-2\,b_{1,1}^2\,\delta\,d_2 + 8\,b_{0,2}\,\delta^2\,d_2 + 6\,b_{1,1}^2\,\beta\,d_3)\,\alpha_1^2\,\alpha_2 + (8\,\delta^2\,\gamma - 4\,b_{1,1}\,\delta\,d_2 - 12\,b_{1,1}\,\beta\,d_3)\,\alpha_1\,\alpha_2^2 + \\ + (8\,\delta\,d_2 + 8\,\beta\,d_3)\,\alpha_2^3\Big)\,\Big((-2\,b_{1,1}^2\,\delta^2\,\gamma + 8\,b_{0,2}\,\delta^3\,\gamma + b_{1,1}^3\,\delta\,d_2 - 4\,b_{0,2}\,b_{1,1}\,\delta^2\,d_2 - b_{1,1}^3\,\beta\,d_3)\,\beta_1^3 + \\ + (-2\,b_{1,1}^2\,\delta\,d_2 + 8\,b_{0,2}\,\delta^2\,d_2 + 6\,b_{1,1}^2\,\beta\,d_3)\,\beta_1^2\,\beta_2 + \\ + (8\,\delta^2\,\gamma - 4\,b_{1,1}\,\delta\,d_2 - 12\,b_{1,1}\,\beta\,d_3)\,\beta_1\,\beta_2^2 + (8\,\delta\,d_2 + 8\,\beta\,d_3)\,\beta_2^3\Big)\,.\end{aligned} \tag{2.78}$$

From this expression we read off the flavor brane/image brane loci as

$$P_1 = \eta_0\,\alpha_1^3 + \eta_1\,\alpha_1^2\alpha_2 + \eta_2\,\alpha_1\alpha_2^2 + \eta_3\,\alpha_2^3 \;\; = 0 \tag{2.79}$$

$$P_2 = \eta_0\,\beta_1^3 + \eta_1\,\beta_1^2\beta_2 + \eta_2\,\beta_1\beta_2^2 + \eta_3\,\beta_2^3 \;\; = 0. \tag{2.80}$$

The GUT brane/image brane are at $\alpha_1 = 0$ and $\beta_1 = 0$, respectively. Close to (2.73) the η_i's are invertible and thus we obtain the factorization

$$P_1 = \Pi_{i=1}^3 (A^i\alpha_1 + B^i\alpha_2)\,, \tag{2.81}$$

$$P_2 = \Pi_{i=1}^3 (A^i\beta_1 + B^i\beta_2)\,. \tag{2.82}$$

2.4.2 The derived category approach

As it turns out the physics of singular compactification backgrounds can be described by their derived categories of coherent sheaves. In general this analyses is extremely involved, but for the conifold it has already been carried out [39] and all that remains is to study the non-flat point from this perspective. If we were to have only one factor in each of the P_i in (2.81) we would be exactly in the situation studied there. The presence of three factors only requires minor adjustments.

D-branes on the conifold

We start with the conifold

$$\text{Spec}\;\left(\mathbb{C}[\xi,u,w,\sigma]/\langle\xi^2 - u^2 - \sigma w\rangle\right). \tag{2.83}$$

This is a toric variety with homogeneous coordinates

α_1	α_2	β_1	β_2
1	1	-1	-1

. (2.84)

The moment map becomes

$$|\alpha_1|^2+|\alpha_2|^2-|\beta_1|^2-|\beta_2|^2= 0. \tag{2.85}$$

We can apply a small resolution yielding

$$|\alpha_1|^2+|\alpha_2|^2-|\beta_1|^2-|\beta_2|^2= t. \tag{2.86}$$

Depending on the sign of t we have different Kähler structures. We call these varieties $Y_\pm$respectively.
The orientifold involution acts as $t \leftrightarrow -t$ and thus interchanges the two resolutions with each other.

As explained the appendix C D-branes on $Y_\pm$ are objects of $D^b(\mathrm{QCoh}(Y_\pm))$ and open string states between them correspond to (derived) morphisms which are given by the so-called Ext-groups.

The strategy from here on is to describe the D-brane setup corresponding to the intersection of the three $\mathbf{5}^i_{-1}$ curves with the $\mathbf{10}_3$ curve using the derived category. As it turns we need to include a D(-1)-instanton by wrapping a D1-brane on the resolution $\mathbb{P}^1$. The limit $\mathrm{vol}(\mathbb{P}^1) \to 0$ is taken by integrating over the instanton zero modes. Considering (a part of) the superpotential of this setup we observe that this leads to the desired coupling.

The non-flat point at weak coupling

As explained around (2.81) the locations of various branes are vanishing loci of polynomials. Such branes are easily described in the derived category:

$$\begin{aligned} F_0^i &= \mathcal{O} \xrightarrow{A_i\alpha_1+B_i\alpha_2} \mathcal{O}(1) \\ F_1^i &= \mathcal{O} \xrightarrow{A_i\beta_1+B_i\beta_2} \mathcal{O}(-1) \\ G_0 &= \mathcal{O} \xrightarrow{\alpha_1} \mathcal{O}(1) \\ G_1 &= \mathcal{O} \xrightarrow{\beta_1} \mathcal{O}(-1) \end{aligned} \tag{2.87}$$

The index i runs over $1, 2, 3$. The maps are simply multiplication by the coordinates. The locations of the branes are given by the kernels, e.g. $A^i\alpha_1 + B^i\alpha_2 = 0$.

Branes wrapping the resolution $\mathbb{P}^1$ are given by

$$\begin{aligned} S_0 &\cong \mathcal{O}(2) \xrightarrow{(\beta_2,-\beta_1)^T} \mathcal{O}(1)^{\oplus 2} \xrightarrow{(\beta_1,\beta_2)} \mathcal{O} \\ S_1 &\cong \mathcal{O}(1) \xrightarrow{(-\beta_2,\beta_1)^T} \mathcal{O}^{\oplus 2} \xrightarrow{(\beta_1,\beta_2)} \mathcal{O}(-1) \to 0. \end{aligned} \tag{2.88}$$

As mentioned before open string states correspond to Ext-groups. These have already been computed in [39]:

$$\mathrm{Ext}^i(G_0, I_0) = (0, \mathbb{C}, 0, 0), \quad \mathrm{Ext}^i(G_0, I_1) = (0, 0, \mathbb{C}, 0) \tag{2.89}$$

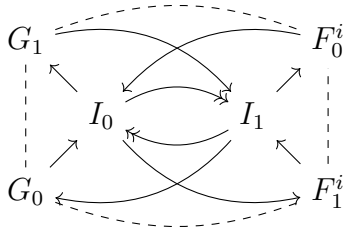

Figure 2.3: The quiver theory corresponding to the Ext groups computed in the text. For simplicity only one pair of flavour branes is shown. Figure taken from [24].

$$\mathrm{Ext}^i(G_1, I_0) = (0, 0, \mathbb{C}, 0), \quad \mathrm{Ext}^i(G_1, I_1) = (0, \mathbb{C}, 0, 0) \tag{2.90}$$
$$\mathrm{Ext}^i(F_0, I_0) = (0, \mathbb{C}, 0, 0), \quad \mathrm{Ext}^i(F_0, I_1) = (0, 0, \mathbb{C}, 0) \tag{2.91}$$
$$\mathrm{Ext}^i(F_1, I_0) = (0, 0, \mathbb{C}, 0), \quad \mathrm{Ext}^i(F_1, I_1) = (0, \mathbb{C}, 0, 0), \tag{2.92}$$

together with

$$\mathrm{Ext}^i(G_0, G_1) \cong (0, \mathbb{C}[\alpha_2\beta_2], 0, 0), \quad \mathrm{Ext}^i(G_0, F_1) \cong (0, \mathbb{C}[\alpha_1\beta_2], 0, 0) \tag{2.93}$$
$$\mathrm{Ext}^i(G_1, G_0) \cong (0, \mathbb{C}[\beta_2\alpha_2], 0, 0), \quad \mathrm{Ext}^i(G_1, F_0) \cong (0, \mathbb{C}[\beta_1\alpha_2], 0, 0) \tag{2.94}$$
$$\mathrm{Ext}^i(F_0, F_1) \cong (0, \mathbb{C}[\alpha_1\beta_1], 0, 0), \quad \mathrm{Ext}^i(F_0, G_1) \cong (0, \mathbb{C}[\alpha_2\beta_1], 0, 0) \tag{2.95}$$
$$\mathrm{Ext}^i(F_1, F_0) \cong (0, \mathbb{C}[\beta_1\alpha_1], 0, 0), \quad \mathrm{Ext}^i(F_1, G_0) \cong (0, \mathbb{C}[\beta_2\alpha_1], 0, 0). \tag{2.96}$$

In addition a simple argument using the non-commutative crepant resolution [39] yields

$$\mathrm{Ext}^1(I_1, I_0) \cong \mathrm{Ext}^1(I_0, I_1) \cong \mathbb{C}^2. \tag{2.97}$$

Note that we are not interested in their precise structure here. We only need to convince ourselves that open string states actually do exist. One summarizes in a simple quiver diagram Figure 2.3. We now occupy the G_i nodes with multiplicity five and the F_i nodes with mulitplicity one. Further we occupy only the I_1 node with a single instanton. Orientifolding leads to the quiver shown in Figure 2.4.

Now the superpotential is given by

$$W_{\text{inst}} = \lambda_1^i \mathbf{10}^{[ij]} \lambda_1^j + \lambda_1^i \left((\mathbf{5}^1)^i \nu_{11} + (\mathbf{5}^2)^i \nu_{12} + (\mathbf{5}^3)^i \nu_{13} \right). \tag{2.98}$$

Integration leads to

$$\int d\lambda_1^i d\nu_{11} d\nu_{12} d\nu_{13} \exp(W_{\text{inst}}) = \mathbf{10}\ \mathbf{5}^1\mathbf{5}^2\mathbf{5}^3, \tag{2.99}$$

as desired.

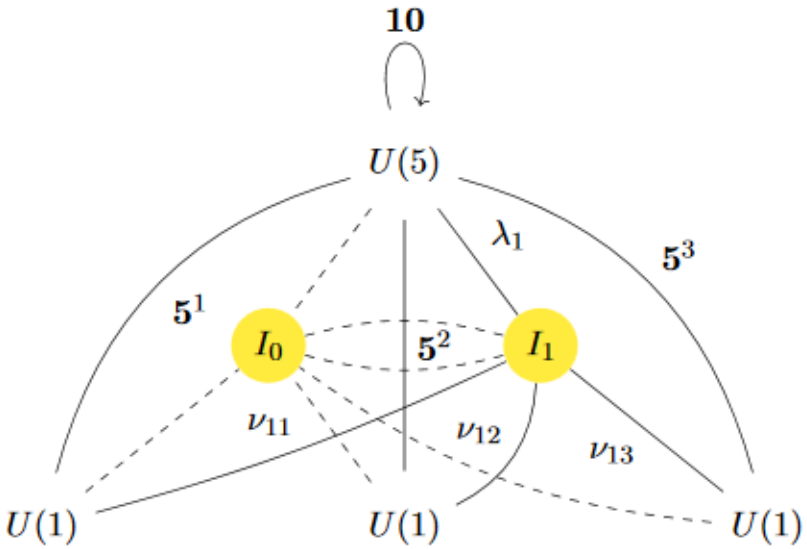

Figure 2.4: Zero modes of open string states between the various branes upon orientifolding. Dashed lines correspond to empty states as the node I_0 is left unoccupied. Figure taken from [24].

2.5 The mirror picture

Similarly to [39] we will consider the given setup from the mirror symmetry perspective. As is well-established D3-branes probing the conifold singularity are mapped to D6-branes wrapping certain three-cycles in the mirror manifold [44].

When considering BPS states the mirror is a (singular) fibration over the complex plane with fiber $\mathbb{C}^* \times \Sigma$ [44, 45], defined by the equations by

$$\begin{aligned} uv &= W\,, \\ P(x,y) &= W. \end{aligned} \tag{2.100}$$

The potential $W \in \mathbb{C}$ is in fact a product of the variables $u, v \in \mathbb{C}$. These lie in the the $\mathbb{C}^*$ fiber for non-banishing W. The coordinates $x, y \in \mathbb{C}^*$ define a punctured Riemann surface of genus zero, which we denote by Σ.

Normally

$$P(x,y) = 1 + x + y + rxy^{-1}, \quad r \in \mathbb{C}. \tag{2.101}$$

Choosing a framing $x = xy^2$ [46] and rescaling appropriately we arrive at

$$P(x,y) = q + x + y + xy - xy^2\,. \tag{2.102}$$

The parameter q parameterizes the complex structure.

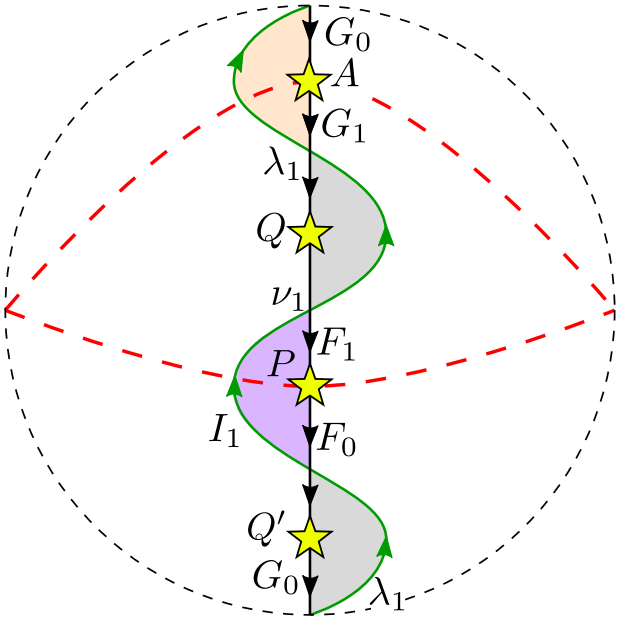

Figure 2.5: The location of the $U(5)$ and $U(3)$ stacks. The green line is the image of the D-branes instanton. The shaded region show worldsheet instantons mediating the coupling. The stars denote the puntucres. The orientifold involution corresponds to a reflection along the red line. The outer dashed line is identified into a single point. Figure taken from [24] and adapted in turn from [39].

The three-cycles wrapped by the D6-branes are identified as follows: Notice that $W = q$ and $W = q + 1$ make $P(x, y)$ singular, and in fact there is a collapsing one-cycle at both of those points. Denote this one-cycle by S^1_P and consider an $S^1_{uv} \in \{uv = W \neq 0\}$. At the point $W = 0$ this S^1_{uv} collapses as well. Choose line segments connecting 0 with q and $q + 1$ respectively. The total space of the fibration $S^1_P \times S^1_{uv}$ has the topology S^3. It is precisely those cycles that are wrapped by the D6-branes.

It is not at all straightforward to map the brane stacks of the previous section to this setup, as the precise action of the mirror map on these cycles is unknown. However the images for one $U(5)$ and one $U(1)$ stack have already been identified in [39]. We employ this result by considering the three $\mathbf{5}^i$ branes to be coincident. We then have a $U(3)$ stack. Once we compute the relevant coupling, we will employ a Higgs mechanism to arrive at the desired result.

In order to infer the desired superpotential term it suffices to consider the restriction to Σ over $W = 0$ [47, 48, 49]. This results in Figure 2.5.

Let us explain some of the features of Figure 2.5. Obviously the $G_0 \sim G_1$ and $F_0 \sim F_1$ stacks correspond to $U(5)$ and $U(3)$ respectively. In green we have the image of the I_1 instanton, which after orientifolding carries gauge group $O(1) = \mathbb{Z}_2$. In shaded regions we

have world sheet instantons. We read off the following open string states charged under various groups:

	$U(5)$	$U(3)$	$O(1)$
A	$\mathbf{10}$	$\mathbf{1}$	0
Q	$\mathbf{5}$	$\overline{\mathbf{3}}$	0
P	$\mathbf{1}$	$\mathbf{3}$	0
λ	$\overline{\mathbf{5}}$	$\mathbf{1}$	1
ν	$\mathbf{1}$	$\mathbf{3}$	1

. (2.103)

Thus we obtain the effective action:

$$S_{\text{inst}} = \lambda^i Q_i^a \nu_a + \lambda^i A_{[ij]} \lambda^j + \nu_a P^{[ab]} \nu_b \tag{2.104}$$

here a raised index means that we are going to the complex conjugate representation. Integrating out the zero modes gives

$$W_{\text{nf}} = \varepsilon_{abc} \varepsilon^{ijklm} A_{[ij]} Q_k^a Q_l^b Q_m^c + \varepsilon_{abc} \varepsilon^{ijklm} A_{[ij]} A_{[kl]} Q_m^a P^{[bc]} \cong AQ^3 + A^2 PQ. \tag{2.105}$$

Generally there are (unknown) coefficients related to the area of the instantons in front of each term. We are only interested in the general structure however.

As mentioned previously this correspondss to all $\mathbf{5}$ branes aligning. If we wish consider them as distinct, we have to break $U(3)$ down to $U(1)^3$ by making the P fields massive, with equal mass for convenience. Then we obtain

$$W_{\text{nf}} \to AQ^3 + A^2 PQ + mP^2. \tag{2.106}$$

We now integrate our the P and arrive at

$$W'_{\text{nf}} = AQ^3 - \frac{1}{4m}(QA^2)^2. \tag{2.107}$$

In the limit $m \to \infty$ we obtain the result of the previous section.

2.6 Anomaly cancellation in 6D

In this section we deal with the $\mathbb{Q}$-factorial terminal singularities $\alpha = \gamma = 0$ mentioned above. This is done by verifying the anomaly cancellation in six dimensions and assigning uncharged hypermultiplets to these singular points.

We now consider the same setup but with the base $B_2 = \mathbb{CP}^2$. As it turns out this variety does not admit a smooth crepant resolution, i.e. the resolution is not Calabi-Yau. In general if there is a resolution

$$\rho : \hat{X}_3 \longrightarrow X, \tag{2.108}$$

we have

$$K_{\hat{X}_3} = \rho^* K_X + \sum a_i E_i, \tag{2.109}$$

where E_i are resolution divisors and a_i some numbers. Since X is Calabi-Yau its canonical class is trivial. Thus if it turns out that $a_i > 0$ for at least one i the resolution is not Calabi-Yau any longer. The singularities of X that obstruct this are referred to as *terminal*.

If moreover a small resolution is not possible the singularities are dubbed $\mathbb{Q}$-*factorial*[4]. As it turns out the singularities $\alpha = \gamma = 0$ are terminal and $\mathbb{Q}$-factorial. Since X is Calabi-Yau, a smooth deformation is guaranteed to exist [50]. This means a family $\{X_t\}_t$ parametrized by a complex variable t, such that X_t is smooth for $t \neq 0$ and $X_0 = X$. This fact will serve us when verifying the anomaly cancellation.

The physical interpretation of these singularities is derived from M-theory: As these singularities are codimension 2, we can locally resolve these by inserting $\mathbb{P}^1$s in the fiber. This violates the Calabi-Yau condition and thus breaks supersymmetry. Wrapping M2-branes gives particles, which become massless in the F-theory limit. We thus associate hypermultiplets, uncharged under any massless continuous gauge group to such singularities. They could still be charged under either massive or discrete groups [33, 34].

Such multiplets are necessary to cancel the gravitational anomaly in 6D as we now compute for this example.

Given the number of tensor- (excluding the gravitational), vector- and hypermultiplets, n_T, n_V, n_H, the anomaly cancellation condition is:

$$29n_T - n_V + n_H = 273. \tag{2.110}$$

In general

$$n_T = h^{1,1}(B_2) - 1, \quad n_V = \dim G, \tag{2.111}$$

for gauge group G. Thus we obtain for $B_2 = \mathbb{CP}^2$:

$$n_T = 0, \qquad n_V = 24 + 1 = 25. \tag{2.112}$$

According to our previous discussion the number of hypermultiplets splits up into uncharged and charged respectively:

$$n_H = n_H^0 + n_H^c. \tag{2.113}$$

n_H^c is easily computed using Bezouts theorem, whereas the computation of n_H^0 makes use of the complex deformation $\{X_t\}_t$ mentioned above.

[4]This is related to the fact that every Weil divisor W is $\mathbb{Q}$-Cartier, i.e. $\exists q \in \mathbb{Q}$ s.t. qW is Cartier.

2.6.1 The number of charged hypermultiplets

The charge hypermultiplets are now located in codimension 2 on the base, i.e. they are isolated points. There is a variety charged under $SU(5)$ by $\mathbf{10}, \mathbf{5}$ and $\mathbf{1}$.

$$\deg(\delta) = 2, \qquad \deg(\alpha) = 1, \tag{2.114}$$

implying

$$\begin{aligned}
[\alpha] &\Rightarrow \deg(\alpha) = 1 \\
[\beta] = c_1(B_2) + [\delta] - [\omega] &\Rightarrow \deg(\beta) = 4 \\
[\gamma] = 4c_1(B_2) - 2[\delta] - 3[\omega] - [\alpha] &\Rightarrow \deg(\gamma) = 4 \\
[\delta] &\Rightarrow \deg(\delta) = 2 \\
[c_2] = [\delta] + [\alpha] + [\omega] - c_1(B_2) &\Rightarrow \deg(c_2) = 1 \\
[d_2] = 3c_1(B_2) - [\delta] - 2[\omega] - [\alpha] &\Rightarrow \deg(d_2) = 4 \\
[d_3] = 2c_1(B_2) - [\delta] - [\alpha] - [\omega] &\Rightarrow \deg(d_3) = 2.
\end{aligned}$$

The states charged as **10** are

$$\{\omega = 0\} \cap \{c_2 = 0\}, \quad \{\omega = 0\} \cap \{d_3 = 0\}. \tag{2.115}$$

By Bezouts theorem there are $\deg(\omega) \cdot (\deg(d_3) + \deg(c_2)) = 3$ such points. Because there are 10 $\mathbb{P}^1$s in the fiber there are $3 \cdot 10 = 30$ multiplets charged under **10**.

The **5** loci are at the intersection of $\omega = 0$ and any of the following loci:

$$\begin{aligned}
\mathbf{5}_{-6}: &\quad \delta = 0\,, \\
\mathbf{5}_{-1}: &\quad \alpha^2\, c_2\, d_2^2 + \alpha^3\, \beta\, d_3^2 + \alpha^3\, d_2\, d_3\, \delta - 2\,\alpha\, c_2^2\, d_2\, \gamma - \alpha^2\, c_2\, d_3\, \delta\, \gamma + c_2^3\, \gamma^2 = 0\,, \\
\mathbf{5}_{4}: &\quad \beta\, d_3 + d_2\, \delta = 0\,.
\end{aligned} \tag{2.116}$$

There are $2 + 6 + 11 = 19$ such points giving us $5 \cdot 19 = 95$ multiplets.

The $\mathbf{1}_{\pm 10}$ states are located at

$$\delta = \omega\beta - \tfrac{1}{2} c_2 d_3 \delta = 0, \tag{2.117}$$

or equivalently

$$\delta = \beta = 0. \tag{2.118}$$

Counting degrees we get

$$\deg(\delta) \cdot \deg(\beta) = 2 \cdot 4 = 8, \tag{2.119}$$

multiplets with such charge.

$\mathbf{1}_{\pm 5}$ states localize at

$$F_1 := \quad \beta \mathrm{c}_2^2 d_3^2 \delta^2 + \mathrm{c}_2^2 d_2 d_3 \delta^3 - 3\beta^2 \mathrm{c}_2 d_3 \delta\omega - 2\beta \mathrm{c}_2 d_2 \delta^2 \omega$$

$$+\gamma \mathrm{c}_2\delta^4\omega + \alpha\beta d_3\delta^3\omega + \alpha d_2\delta^4\omega + 2\beta^3\omega^2 = 0, \tag{2.120}$$

$$\begin{aligned} F_2 := \quad & -\alpha\beta \mathrm{c}_2 d_3^2\delta^4 - \alpha \mathrm{c}_2 d_2 d_3\delta^5 + \beta^2 \mathrm{c}_2^2 d_3^2\delta^2 + \\ & 2\beta \mathrm{c}_2^2 d_2 d_3\delta^3 + \mathrm{c}_2^2 d_2^2\delta^4 - 2\beta^3 \mathrm{c}_2 d_3\delta\omega \\ & -2\beta^2 \mathrm{c}_2 d_2\delta^2\omega + \alpha\beta^2 d_3\delta^3\omega + \beta^4\omega^2 - \alpha\gamma\delta^6\omega = 0. \end{aligned} \tag{2.121}$$

One must also exclude points satisfying the following conditions as they have already been accounted for previously:

$$\begin{aligned} \delta = \beta = 0 \\ \delta d_2 + \beta d_3 = 0 \\ c_2 = \omega = 0 \\ \delta = \omega = 0. \end{aligned} \tag{2.122}$$

Counting the number of points $F_1 = F_2 = 0$ we obtain $14 \cdot 18$. One must now remove (2.122) taking into account proper intersection multiplicities:

$$14 \cdot 18 - 16 \cdot 2 \cdot 4 - 2 \cdot 6 - 1 \cdot 1 \cdot 1 - 10 \cdot 2 \cdot 1 = 91. \tag{2.123}$$

Collecting all these we get

$$n_H^c = 30 + 95 + 8 + 91 = 224, \tag{2.124}$$

charged hypermultiplets.

2.6.2 The number of uncharged hypermultiplets

To compute n_H^0 we need the topological Euler characteristic and $h^{1,1}(X)$. By constructing the deformations explicitly we can compute

$$h^{1,1}(X_t) = 6. \tag{2.125}$$

Now we employ [51]

$$\chi(X_{\mathrm{Sing}}) - \chi(X_t) = \sum_P m_P, \tag{2.126}$$

P are singular points and m_P their Milnor numbers defined as

$$m_P := \dim_{\mathrm{Krull}} \mathcal{O}_P / \langle \partial_i f \rangle, \tag{2.127}$$

where we assume that P is given locally as the vanishing of one function f. For our specific case of $B = \mathbb{CP}^2$ we locally can express the points P on our variety as

$$A_1\alpha\gamma + A_2\alpha + A_3\gamma + A_4 = 0. \tag{2.128}$$

This leads to

$$m_P = \dim\mathbb{C}[x_0, x_1]/\langle A_1\gamma(x_0, x_1) + A_2, A_1\alpha(x_0, x_1) + A_3\rangle = 2, \tag{2.129}$$

considering that $[\alpha] = 1$ and $[\gamma] = 4$. This also implies that there are 4 such points on B.

$\chi(X_t)$ can be computed using Sage[5]

$$\chi(X_t) = -132. \tag{2.130}$$

Thus

$$\chi(X_{\text{Sing}}) = \chi(X_t) + \sum_P m_P = -124. \tag{2.131}$$

Therefore as in [33, 34]

$$n_H^0 = 1 + h^{1,1} - \frac{1}{2}\chi(X_{\text{sing}}) + \frac{1}{2}\sum_P m_P = 7 + 62 + 4 = 73. \tag{2.132}$$

Taking into account the universal hypermultiplet we arrive at

$$1 + n_H^0 + n_H^c - n_V = 1 + 73 + 224 - 25 = 273. \tag{2.133}$$

[5]It is interesting to note that for singular varieties there are generalized Chern classes called Chern-Schwarz-MacPherson classes [51].

Chapter 3

Ricci-flat metrics on total spaces of vector bundles over flag manifolds

3.1 Introduction

In this chapter we summarize results obtained in [52].

Compact Calabi-Yau manifolds do not posses isometries, making the construction of explicit Ricci-flat Kähler metrics extremely hard. However non-compact Calabi-Yau spaces can have symmetries and provide local models of compact spaces, like the Ooguri-Vafa metric. In this chapter we consider total spaces of certain vector bundles over flag manifolds. We use an ansatz due to Calabi to construct such metrics in all Kähler classes.

A application to string theory is the following: Consider the total space of the canonical line bundle over the flag manifold. Introducing a radial and an angular coordinate in the fiber we can take the limit $r \to \infty$. It is a general result that the remaining S^1 bundle over the flag is a Sasaki-Einstein manifold. Such manifolds appear in string theory in the context of Klebanov-Witten theory, i.e. when considering compactifications on products of AdS and $X_{\text{Sasaki}-\text{Einstein}}$. It would be interesting to analyse the physical effect of different choice of Kähler classes for the explicit metrics we find.

3.1.1 The flag manifold

Flag manifolds can be seen as generalizations of Grassmannians. A point in (the complex) $Gr(m,n)$ is a sequence of complex linear spaces

$$0 \subset L_m \subset L_n = \mathbb{C}^n, \tag{3.1}$$

where $\dim_{\mathbb{C}} L_m = m$.

A point in a flag manifold $\mathscr{F}_{n_1,...,n_s}$ is called a flag. This is a sequence of nested complex vector spaces of dimensions $m_1, ..., m_s = n$:

$$0 \subset L_1 \subset \ldots \subset L_s = \mathbb{C}^n \,, \tag{3.2}$$

where $\dim_{\mathbb{C}} L_k = m_k$. A flag with $s = 2$ corresponds to a point in the Grassmannian.

Another important set of integers is given by

$$m_k = \sum_{i=1}^{k} n_i \,. \tag{3.3}$$

The set of all flags of the form (3.2) is a manifold and in fact:

$$\mathscr{F}_{n_1,...,n_s} = \frac{GL(n,\mathbb{C})}{P_{n_1,...,n_s}} \simeq \frac{U(n)}{U(n_1) \times ... \times U(n_s)} \,. \tag{3.4}$$

Here $P_{n_1,...,n_s}$ is formed by matrices of the form

$$\begin{pmatrix} A_{n_1} & * & ... & * \\ 0 & A_{n_2} & ... & * \\ ... & ... & ... & ... \\ 0 & ... & 0 & A_{n_s} \end{pmatrix}, \tag{3.5}$$

with $A_i \in GL(i;\mathbb{C})$. We sometimes refer to (3.4) simply as $\mathscr{F}$ for brevity. These manifolds carry complex structures and were extensively studied in the classical work[53].

If we view $\mathscr{F}$ as a quotient of $GL(n;\mathbb{C})$ we have already fixed a complex structure. If we view it as a unitary quotient there are many complex structure in correspondence with the ordering of the n_i in the quotient. We always use the ordering in (3.4).

Note that for an s-step flag we have forgetful projections to flags with fewer steps by forgetting about one of the subspaces in (3.2). In particular we have the maps

$$\pi_k : \mathscr{F} \to Gr(m_k; n). \tag{3.6}$$

The first Chern class of a flag manifold can be expressed as

$$c_1(\mathscr{F}_{n_1,...,n_s}) = -\sum_{k=1}^{s-1}(n_k + n_{k+1})c_1(U_k), \tag{3.7}$$

where U_k are pullbacks of tautological bundles over $Gr(m_k, n)$. More details on this are given in section 3.3.1.

3.1.2 Kähler potentials on flag manifolds

We will be interested in Kähler metrics and thus Kähler potentials. The most general potential is a sum of so-called quasi-potentials[54, 55, 56]. These are pullbacks of Kähler potentials on the Grassmannians via the forgetful projections π_k.

To be more explicit let

$$W = (w_1, .., w_n) \in Gl(n; \mathbb{C}), \tag{3.8}$$

with column vectors w_i. Consider also an $n \times m_k$-matrix Z_k of rank m_k

$$Z_k = (w_1, ..., w_{m_k}), \quad \text{where} \;\; m_k = \sum_{l=1}^{k} n_l. \tag{3.9}$$

Oviously Z_k corresponds to point in $Gr(m_k, n)$ under the projcetion π_k. We can then introduce the function

$$t_k = \det\left(Z_k^\dagger Z_k\right) . \tag{3.10}$$

$\log(t_k)$ is a Kähler potential on the Grassmannian $Gr(m_k, n)$. Then the most general $SU(n)$ invariant potential on $\mathscr{F}$ [54, 55] is given by

$$\mathscr{K}_{\mathscr{F}} = \sum_{k=1}^{s-1} \gamma_k \, \log(t_k) \, , \qquad \gamma_k > 0 \, . \tag{3.11}$$

Later we will also consider the manifolds $\left(\mathscr{F} \times \mathbb{CP}^{q-1}\right)$[1]. A potential on these manifolds is obtained by adding a Fubini-Study term

$$\mathscr{K}_{\mathscr{F}\times\mathbb{CP}^{q-1}} = \gamma_0 \, \log\left(t_0\right) + \sum_{k=1}^{s-1} \gamma_k \, \log(t_k), \tag{3.12}$$

where $\log(t_0) = q \log\left(\sum_{i=1}^{q} |z_i|^2\right)$. The Kähler cone is $\gamma_k > 0$ and is exhausted by the arising metrics.

Let us now turn to the problem of constructing Ricci-flat metrics on the total spaces of certain bundles over both $\mathscr{F}$ and $\mathscr{F} \times \mathbb{CP}^{q-1}$. It is a fact that the total space of the canonical bundle over (a product) of flag manifolds has trivial Chern class. This can be deduced from the fact that the first Chern class of the bundle 'cancles' the first Chern class of the manifold. Define

$$X_K := \text{the total space of} \;\; K_{\mathscr{F}\times\mathbb{CP}^{q-1}} \, . \tag{3.13}$$

This is a non-compact Calabi-Yau manifold. The Calabi-Yau theorem[57, 58, 59], guarantees the existence of a Ricci-flat metric in *every* Kähler class for a compact space. In the

[1] We will explain the role of q shortly.

non-compact case the theorem is unproven in full generality, however for the manifolds we consider a proof is given in [60, 61].

Calabi's ansatz [62] gives a Ricci-flat Kähler metric on X_K provided one chooses γ_i in such a manner that $\mathscr{K}_{\mathscr{F}\times\mathbb{CP}^{q-1}}$ yields a Kähler-Einstein metric. This obviously means that the Kähler class is *fixed*. The Kähler potential on X_K is given by the ansatz

$$\mathscr{K}_{X_K} = \mathscr{K}_0(|u|^2\exp(\mathscr{K}^{\mathrm{KE}}_{\mathscr{F}\times\mathbb{CP}^{q-1}})), \tag{3.14}$$

where the superscript 'KE' indicates the choice of γ_i and u is a holomorphic coordinate on the fiber. Note that $\mathscr{K}_0$ depends only one one real variable. The condition

$$R_{i\bar{j}} = -\partial_i\partial_{\bar{j}}\log\det g = 0, \tag{3.15}$$

can be seen to lead to an ODE for $\mathscr{K}_0$ which is easily solved. We will give more details below.

To summarize: Calabi's Ansatz gives a Ricci-flat Kähler metric on X_K in a *fixed* Kähler class. It is in fact not hard to generalize (3.14) to give metrics in all Kähler classes and this has been carried out in [63]. The ansatz is simply

$$\mathscr{K}_{X_K} = \mathscr{K}_{\mathscr{F}\times\mathbb{CP}^{q-1}}(\gamma_k) + \mathscr{K}_0(|u|^2\exp(\mathscr{K}^{\mathrm{KE}}_{\mathscr{F}\times\mathbb{CP}^{q-1}})). \tag{3.16}$$

This ansatz gives metrics in all classes $\gamma_k > 0$ and can be shown to be Ricci-flat by the same method as indicated above.

We now describe the central idea of [52], which is motivated by the following low-dimensional example found in the physics literature: In [64] the metrics of [63] had been constructed on $K_{\mathbb{CP}^1\times\mathbb{CP}^1}$. The two Kähler moduli can be geometrically related to the volumes of the two spheres at the zero section.

The crucial observation is now the following: If one allows one of the spheres to approach zero volume[2], one obtains a Ricci-flat metric on the orbifold bundle $\mathbb{C}^2/\mathbb{Z}_2$ with base $\mathbb{CP}^1$. Resolving yields the metric on $\mathcal{O}(-1)\oplus\mathcal{O}(-1)$ over $\mathbb{CP}^1$[65]. Note also that we have only one Kähler parameter left, as the base has only one modulus.

The generalization is as follows: Consider the total space X_K of the canonical bundle $K_{\mathscr{F}\times\mathbb{CP}^{q-1}}$. We have $\gamma_k, k = 1,..,s-1$ as the Kähler parameters from $\mathscr{F}$ and γ_0 from $\mathbb{CP}^{q-1}$. Allowing the volume of $\mathbb{CP}^{q-1}$ to approach zero, which means that $\gamma_0 = 0$ is allowed in the metric, is equivalent to 'moving $\mathbb{CP}^{q-1}$ to the fiber'. The fiber then 'becomes the total space of a line bundle over $\mathbb{CP}^{q-1}$' which is nothing but $\mathbb{C}^q$. We will be more precise in later sections.

[2]We will explain this precisely in the following section.

It turns out that in this situation (3.16) still describes a Ricci-flat Kähler metric in all Kähler classes however on a different manifold, called X_V. It can only be constructed if q divides the first Chern class $c_1(\mathscr{F}_{n_1,\dots,n_s})$. Then we can form the line bundle $K_{\mathscr{F}}^{1/q}$ and define

$$X_V := \text{the total space of } \underbrace{K_{\mathscr{F}}^{1/q} \oplus \ldots \oplus K_{\mathscr{F}}^{1/q}}_{q \text{ times}} \tag{3.17}$$

We summarize the idea in the following figure:

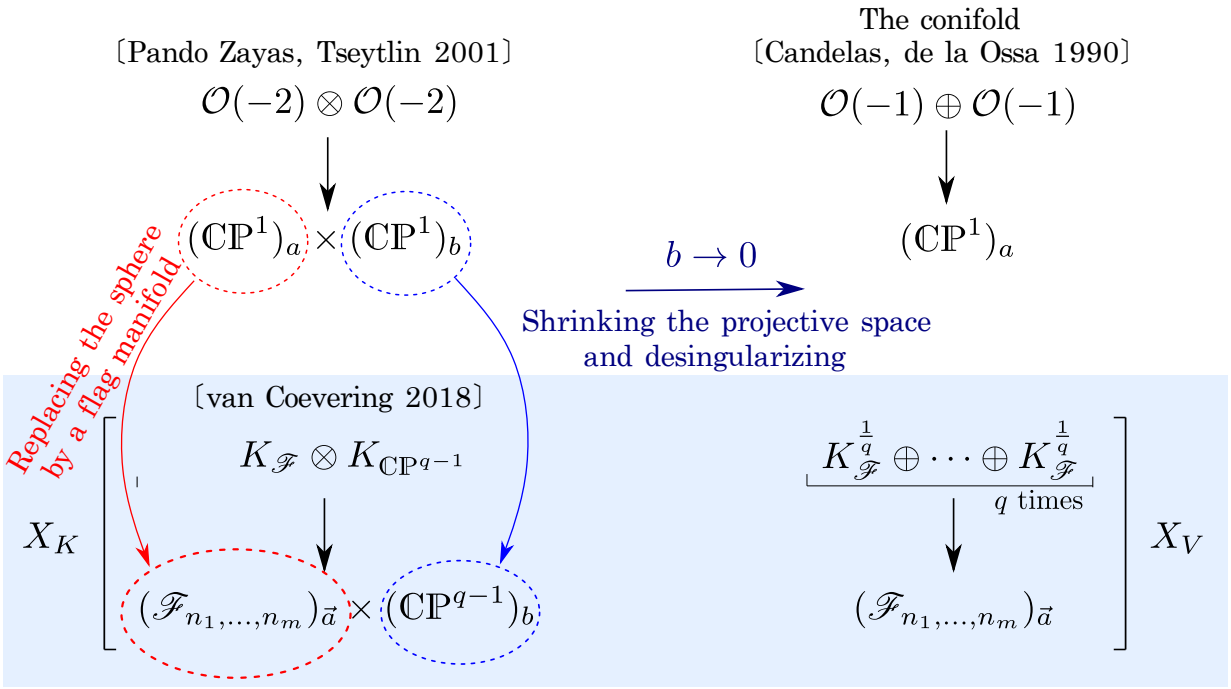

Figure 3.1: Taken from [52]. In the upper part we depict the process of shrinking one of the spheres in the Pando Zayas-Tseytlin metric. As mentioned in the text this yields an orbifold bundle which is resolved to the Candelas-de la Ossa metric on the resolved conifold. In the lower part we present the generalization.

The main result

In the following we will prove:

Proposition. *In each Kähler class on X_K there exists a complete Ricci-flat metric. If in addition a positive integer q satisfying $q|(n_k + n_{k+1})$ $(k = 1 \dots s-1)$ is given, then X_V admits a complete Ricci-flat metric in every Kähler class. The line elements for metrics*

on both spaces are

$$ds^2 = \sum_{k=0}^{s-1} \gamma_k(\mu)\partial\bar{\partial}\log t_k + \frac{Q(\mu)}{4}\,d\mu^2 + \frac{1}{Q(\mu)}\left(d\phi + \mathrm{Im}(A)\right)^2, \tag{3.18}$$

where $(c_k := n_k + n_{k+1})$

$$\gamma_0(\mu) = q(\alpha+\mu), \quad \gamma_k(\mu) = c_k(a_k+\mu) \quad (k \geq 1),$$

$$Q(\mu) = \frac{F'(\mu)}{F(\mu)}, \quad F(\mu) = \int_C^{\mu} d\mu'(\alpha+\mu')^{q-1} \prod_{1\leq i<j\leq s}\left(\sum_{k=i}^{j-1} c_k(a_k+\mu')\right)^{n_i n_j} \tag{3.19}$$

Moreover

$$A := \partial\left(q\log t_0 + \sum_{k=1}^{s-1} c_k \log t_k\right), \tag{3.20}$$

and is the holomorphic connection of $K_{\mathscr{F}\times\mathbb{CP}^{q-1}}$*. The complex structure acts as* $\mathscr{J}\left(\frac{1}{2}Q(\mu)d\mu\right) = d\phi + \mathrm{Im}(A)$*.*

We have the following two cases:

If $\alpha + C > 0$*,* $a_k + C > 0$ *for all* k*, and* $\phi \in [0, 2\pi]$ *we obtain metrics on* X_K *in all Kähler classes.*

If $a_k - \alpha > 0$ *for all* k*,* $C = -\alpha$*, and* $\phi \in [0, 2\pi q]$ *(3.18)-(3.19) give metricss on* X_V *in all Kähler classes. The fiber with origin removed is* $\mathbb{C}^q \setminus \{0\}$ *and can be seen as the total space of a* $\mathbb{C}^*$ *bundle over* $\mathbb{CP}^{q-1}$*. If we parametrize* $\mathbb{C}^*$ *by* x_0 *we have* $\frac{\phi}{q} = \arg(x_0)$*.*

3.2 A review of the simplest case $\mathscr{F} = \mathbb{CP}^1$

In this section we describe the upper part of Figure 3.1, that is we consider the canonical bundle over $\mathbb{CP}^1 \times \mathbb{CP}^1$.

Let us define homogenous coordinates $(z_1, z_2) \in \mathbb{CP}^1$ and $(w_1, w_2) \in \mathbb{CP}^1$ we have the following potential X_K:

$$\mathscr{K} = a_1\,K_1 + a_2\,K_2 + \mathscr{K}_0\left(\underbrace{|u|^2 e^{K_1+K_2}}_{:=e^t}\right), \tag{3.21}$$

$$K_1 = 2\log\left(|z_1|^2+|z_2|^2\right), \qquad K_2 = 2\log\left(|w_1|+|w_2|^2\right) \tag{3.22}$$

K_i are the Fubini-Study potentials on the respective $\mathbb{CP}^1$s. Their sum is the potential for the Einstein metric on $\mathbb{CP}^1 \times \mathbb{CP}^1$. The a_i are the Kähler parameters related to the sizes of the two spheres.

An important point now is to not that $\mathscr{K}_0$ only depends on a single real variable t. For computational convenience one applies the Legendre transform

$$\mathscr{K}_0 = \mu t - H. \tag{3.23}$$

The line element then takes the form (z and w are local holomorphic coordinates on the spheres)

$$\begin{aligned} ds^2 &= (\mu + a_1)\,(ds^2)_{\mathbb{CP}^1_z} + (\mu + a_2)\;(ds^2)_{\mathbb{CP}^1_w} + \frac{H_{\mu\mu}}{4} d\mu^2 + \frac{1}{H_{\mu\mu}}\,(d\phi + \mathrm{Im}(A))^2, \\ (ds^2)_{\mathbb{CP}^1_z} &= \frac{2\,dz d\bar{z}}{(1+|z|^2)^2}, \quad (ds^2)_{\mathbb{CP}^1_w} = \frac{2\,dw d\bar{w}}{(1+|w|^2)^2}\,, \\ A &= 2\left(\frac{\bar{z}dz}{1+|z|^2} + \frac{\bar{w}dw}{1+|w|^2}\right). \end{aligned} \tag{3.24}$$

We see that $\mu + a_i$ measures the volume of the respective spheres. In order to calculate the Ricci tensor we employ the identity $R_{i\bar{j}} = -\partial_i \partial_{\bar{j}} \log\det g$. Ricci-flatness can then be seen to follow from

$$2(\mu + a_1)(\mu + a_2) = \frac{d}{d\mu}\left(e^{H_\mu}\right). \tag{3.25}$$

This allows us to solve for $H_{\mu\mu}$:

$$Q(\mu) = H_{\mu\mu} = \frac{F_0'(\mu)}{F_0(\mu)}, \qquad F_0(\mu) = \int_{\mu_0}^{\mu} d\mu'\;\; 3(\mu' + a_1)(\mu' + a_2) \tag{3.26}$$

The claim is that (3.24) describe metrics on both X_K and X_V in this case the canonical bundle of $\mathbb{CP}^1 \times \mathbb{CP}^1$ and the resolved conifold. This can in fact be deduced from the different choices of μ_0 in the above equations.

There are two choices

- $\mu_0 > \max(-a_1, -a_2)$. This leads to the canonical bundle as both the spheres have non-zero volume[64].
- $\mu_0 = \max(-a_1, -a_2)$. This leads to the conifold as one of the spheres is allow to shrink to zero size[65].

One easily verifies that the metric is positive definite in both cases.

The only problematic limit is $\mu \to \mu_0$ where the metric may develop a singularity. In the first case the limit is $H_{\mu\mu} = \frac{1}{\mu - \mu_0} + \ldots$ as $\mu \to \mu_0$. Substituting $r = (\mu - \mu_0)^{1/2}$ transforms the metric into

$$(ds^2)_{\mu\to\mu_0} = (\mu_0 + a_1)\,(ds^2)_{\mathbb{CP}^1_z} + (\mu_0 + a_2)\;(ds^2)_{\mathbb{CP}^1_w} + dr^2 + r^2\,(d\phi + \mathrm{Im}(A))^2\,. \tag{3.27}$$

If ϕ ranges $\phi \in [0, 2\pi]$ we only have a coordinate singularity at $r = 0$, i.e. the metric is smooth.

For the second case assume $\max(-a_1, -a_2) = -a_1$. Then since $F_0(\mu)$ vanishes at $\mu = -a_1$ to second order we have $H_{\mu\mu} = \frac{2}{\mu+a_1} + \ldots$. Substituting $r = (2(\mu + a_1))^{1/2}$ transforms the metric

$$(ds^2)_{\mu\to\mu_0} = (a_2 - a_1)\,(ds^2)_{\mathbb{CP}^1_w} + dr^2 + r^2\left(\frac{dzd\bar{z}}{(1+|z|^2)^2} + \left(\frac{1}{2}d\phi + \frac{1}{2}\mathrm{Im}(A)\right)^2\right). \quad (3.28)$$

If were to impose $\phi \in [0, 2\pi]$ we would obtain a $\mathbb{C}^2/\mathbb{Z}_2$ orbifold singularity at $r = 0$. Thus we require $\phi \in [0, 4\pi]$ which is the smoothing alluded to above.

3.3 General flag manifolds

3.3.1 The first Chern class

We start by deriving (3.7). To this end define vector bundles ξ_j and U_j $(j = 1, ..., s)$. Over the point

$$0 \subset L_1 \subset ... \subset L_{s-1} \subset L_s = \mathbb{C}^n \quad (3.29)$$

the fiber of ξ_j is L_j/L_{j-1}, and the fiber of U_j is L_j. Thus U_j are the pullbacks of the tautological bundles and $x_j = U_j/U_{j-1}$. It is known [66] that the tangent bundle decomposes as

$$T\mathscr{F}_{n_1,...,n_s} = \bigoplus_{1\le i<j\le s} \xi_i^* \otimes \xi_j. \quad (3.30)$$

Thus we can already calculate

$$c_1(\mathscr{F}_{n_1,...,n_s}) = \sum_{i<j}(-n_j c_1(\xi_i) + n_i c_1(\xi_j)). \quad (3.31)$$

Then since $x_j = U_j/U_{j-1}$ we arrive at the desired result

$$c_1(\mathscr{F}_{n_1,...,n_s}) = -\sum_{k=1}^{s-1}(n_k + n_{k+1})c_1(U_k). \quad (3.32)$$

We have moreover $\mathrm{Pic}(\mathscr{F}) \simeq H^2(\mathscr{F}, \mathbb{Z})$[67, Prop. 2.1.2][68]. Thus if there is an integer q such that $q|(n_k + n_{k+1})$ $\forall k$ we can form the line bundle $K_{\mathscr{F}}^{1/q}$.

The Ricci-form on a Kähler manifold represents the first Chern class. Defining $(u_1, ..., u_n) \in U(n)$ we can write

$$c_1(U_k) = \left[\frac{1}{2\pi i}\sum_{i=1}^{m_k}\sum_{j=m_k+1}^{n} J_{ij} \wedge J_{ji}\right], \quad (3.33)$$

with $J_{ij} = \sum_m \bar{u}_{jm} du_{im}$. The Kähler-Einstein metric on $\mathscr{F}$ with proportionality factor one is then given by

$$ds^2 = \sum_{k=1}^{s-1}(n_k + n_{k+1}) \sum_{i=1}^{m_k} \sum_{j=m_k+1}^{n} |J_{ij}|^2. \tag{3.34}$$

This corresponds to a potential of the form (3.11) with $\gamma_k = n_k + n_{k+1}$.

3.3.2 Details of the generalized Calabi-Ansatz

We now assume the existence of a q dividing $c_k := n_k + n_{k+1}$ for all $k = 1, \ldots, s-1$. Also we take $\vec{z} = (z_1, ..., z_{q-1}) \in \mathbb{C}^{q-1}$.

Following Calabi's ansatz on X_K we define

$$\mathscr{K} = \alpha q \log(1 + |\vec{z}|^2) + \sum_{k=1}^{s-1} a_k c_k \log t_k + \mathscr{K}_0(\underbrace{|u|^2(1 + |\vec{z}|^2)^q \Pi_k t_k^{c_k}}_{=:e^t}). \tag{3.35}$$

The constants (α, a_k) are the Kähler moduli and we will determine their range later. To reiterate u is a holomorphic coordinate on the fiber and the z_i of $\vec{z}$ are local holomorphic coordinates on $\mathbb{CP}^{q-1}$ and . This same potential can be defined on X_V the only difference being that (u, z_i) are local coordinates on the $\mathbb{C}^q$-fiber.

$\mathscr{K}_0$ only depends on t and $\mathscr{K}_0'$ and $\mathscr{K}_0''$ denote its first and second derivatives. It is convenient to perform a Legendre transform

$$H = \mu t - \mathscr{K}_0, \tag{3.36}$$

whence

$$\mathscr{K}_0' = \mu, \quad \mathscr{K}_0'' = \frac{1}{H_{\mu\mu}}, \quad t = H_\mu. \tag{3.37}$$

μ is interpreted as the moment map for the $U(1)$-action $u \to e^{i\alpha}u$.

The metric arising from (3.35) is

$$ds^2 = q(\alpha + \mu) ds^2_{FS} + \sum_{k=1}^{s-1} c_k(a_k + \mu)\pi_k^*(ds_k^2) + \frac{1}{|u|^2 H_{\mu\mu}} |du + uA|^2, \tag{3.38}$$

with ds^2_{FS} the Fubini-Study metric on $\mathbb{CP}^{q-1}$ and

$$\pi_k^*(ds_k^2) = (\partial_i \bar{\partial}_j \log t_k) dy^i d\bar{y}^j \tag{3.39}$$

$$A = \sum_{i,k} c_k \partial_i \log t_k dy^i + q\partial_i \log(1 + |\vec{z}|^2) dz^i. \tag{3.40}$$

We have denoted by y^i the complex coordinates on $\mathscr{F}$.

In order to bring this in the form (3.18) on can simply introduces the angular variable $\phi = \arg(u)$. Using the definition of t in (3.35) we get

$$\log u = \frac{t}{2} + i\phi - \frac{q}{2}\log(1+|\vec{z}|^2) - \frac{c_k}{2}\sum_k \log t_k. \tag{3.41}$$

As $t = H_\mu$ one can decompose

$$\frac{du}{u} + A = d\log u + A = \frac{H_{\mu\mu}d\mu}{2} + iD\phi, \tag{3.42}$$

where $D\phi = d\phi + \mathrm{Im}(A)$. The complex structure $\mathscr{J}$ acts on holomorphic one-forms by multiplication with $-i$ and so:

$$\mathscr{J}\left(\frac{H_{\mu\mu}d\mu}{2}\right) = D\phi\,. \tag{3.43}$$

In the metric (3.38) we can substitute

$$\frac{1}{H_{\mu\mu}}|\frac{du}{u} + A|^2 = H_{\mu\mu}\frac{d\mu^2}{4} + \frac{(D\phi)^2}{H_{\mu\mu}}. \tag{3.44}$$

We have shown that $Q(\mu)$ from the proposition is $Q(\mu) = H_{\mu\mu}$. Denote the metric eqrefLineElement by g. Its Ricci-tensor is $R_{i\bar{j}} = -\partial_i\bar{\partial}_j \log\det g$,. Ricci-flatness follows from

$$\det g \sim \kappa\bar{\kappa} \tag{3.45}$$

where κ is a holomorphic functions. We show in appendix E that

$$\det g = |\kappa|^2 \frac{1}{|u|^2 H_{\mu\mu}} \frac{q^{q-1}(\alpha+\mu)^{q-1}}{(1+|\vec{z}|^2)^q} \frac{1}{\prod_k t_k^{c_k}} f(\mu), \tag{3.46}$$

with a holomorphic κ and

$$f(\mu) = \prod_{1\le i<j\le s}\left(\sum_{k=i}^{j-1} c_k(a_k+\mu)\right)^{n_i n_j}. \tag{3.47}$$

Again

$$e^t = |u|^2(1+|\vec{z}|^2)^q \prod_k t_k^{c_k} \tag{3.48}$$

from (3.35), and $H_\mu = t$, imply that (3.45) is solved by the ordinary differential equation

$$(\alpha+\mu)^{q-1} f(\mu) = H_{\mu\mu}\exp(H_\mu) = \partial_\mu \exp(H_\mu). \tag{3.49}$$

3.3.3 Solving the Ricci-flatness condition

Ricci-flatness (3.49) implies

$$H_\mu = \log\left(\int_C^\mu d\mu'(\alpha+\mu')^{q-1}f(\mu')\right). \tag{3.50}$$

Thus

$$H_{\mu\mu} = \frac{(\alpha+\mu)^{q-1}f(\mu)}{\int_C^\mu d\mu'(\alpha+\mu')^{q-1}f(\mu')}. \tag{3.51}$$

The choices of integration constant C will correspond to metrics on X_K and X_V as we will describe below.

Behavior at ∞

Before analysing the behaviour near $\mu \to C$ we take the limit

$$H_{\mu\mu} \to \frac{N}{\mu} \qquad \text{as} \qquad \mu \to \infty, \tag{3.52}$$

with $N = q + \dim_{\mathbb{C}}(M)$. Substituting $\mu = \frac{1}{N}r^2$, we find

$$ds^2|_{\mu\to\infty} = dr^2 + r^2\left(\frac{1}{N}ds^2_{KE} + \frac{1}{N^2}(D\phi)^2\right), \tag{3.53}$$

with $ds^2_{KE} = qds^2_{FS} + \sum_{k=1}^{s-1} c_k\pi_k^*(ds^2_k)$.

This line element has the form of a cone $(dr^2 + r^2(...))$. The term in brackets describes Sasakian manifold, i.e. a $U(1)$-bundle over $\mathscr{F}_{n_1,...,n_s} \times \mathbb{CP}^{q-1}$. We will now demonstrate that ϕ takes values in $[0, 2\pi]$ on X_K and in $[0, 2\pi q]$ on X_V.

The metric on X_K

We now turn to the limit $\mu \to C$. Let C satisfy

$$a_k + C > 0, \qquad \alpha + C > 0. \tag{3.54}$$

This makes C larger than the largest root of $(\alpha+\mu)^{q-1}f(\mu)$. This implies that $H_{\mu\mu}$ is strictly positive and the metric is positive-definite. Then we take the limit

$$H_{\mu\mu} = \frac{1}{\mu - C} + O(1), \qquad \text{as} \qquad \mu \to C, \tag{3.55}$$

Substituting $r^2 = \mu - C$ yields

$$\frac{1}{H_{\mu\mu}}\left|\frac{du}{u} + A\right|^2 = dr^2 + r^2(D\phi)^2 + ..., \tag{3.56}$$

i.e. a smooth metric. We can indentify the $\mathbb{C}$ fiber as $K_{\mathscr{F}\times\mathbb{CP}^{q-1}}$ via the connection A. Thus we indeed have a smooth metric on X_K.

On the base we have in the $\mu \to C$ limit

$$ds^2 = \gamma_0\, ds^2_{FS} + \sum \gamma_k\, \pi_k^*(ds_k^2), \tag{3.57}$$

with $\gamma_0 = q(\alpha + C), \gamma_k = c_k(a_k + C)$. Comparison with the most general Kähler potential (3.11) implies that all Kähler classes are reached in (3.54).

The metric on X_V

Note that the term $\mu + \alpha$ measure the volume of $\mathbb{CP}^{q-1}$ in (3.38). Thus allowing $C = -\alpha$ should correspond to its volume going to zero. In order for the metric to be positive-definite we now require

$$a_k - \alpha > 0. \tag{3.58}$$

Combining (3.47), (3.51) we see that $H_{\mu\mu}$ is positive for $\mu > -\alpha$.

We now have to show that the metric is smooth in the vicinity of the zero section, i.e. in the limit $\mu \to -\alpha$. To this end observe that

$$\int_{-\alpha}^{\mu} d\mu'(\alpha + \mu')^{q-1} f(\mu') = \delta(\alpha + \mu)^q \left(1 + O(\alpha + \mu)\right), \qquad \delta = \frac{f(-\alpha)}{q} > 0.$$

Again using $t = H_\mu$, (3.50) implies

$$e^t = \delta(\alpha + \mu)^q \left(1 + O(\alpha + \mu)\right). \tag{3.59}$$

We expand part of the Kähler potential in terms of $\alpha + \mu$

$$\begin{aligned} &\mathscr{K}_0 = \mu H_\mu - H = \\ &= \mu \log\left(\delta(\alpha+\mu)^q\right) - \log(\delta)\ (\mu+\alpha) - q(\mu+\alpha)(\log(\mu+\alpha) - 1) + \text{const.} = \\ &= -q\alpha \log(\mu+\alpha) + q(\mu+\alpha) + \text{const.} \end{aligned} \tag{3.60}$$

Plugging into (3.35) taking (3.59) into account we obtain up to an additive constant:

$$\mathscr{K} = \sum_{k=1}^{s-1} (a_k - \alpha) c_k \log t_k + B \left(\sum_{m=0}^{q-1} |x_m|^2\right) \prod_k t_k^{\frac{c_k}{q}} + \ldots, \qquad B = \frac{q}{\delta^{\frac{1}{q}}}. \tag{3.61}$$

An important point is that the appearance of the the coordinates $(x_0, \cdots, x_{q-1})$ in the $\mathbb{C}^q$ fiber. They are can be expressed in terms of $(u, \vec{z})$ as

$$x_0 = u^{\frac{1}{q}}, \quad x_i = u^{\frac{1}{q}} z_i \quad i > 0. \tag{3.62}$$

This changes the periodicity of $\arg(u)$ to $[0, 2\pi q]$ and corresponds to the desingularization of the orbifold singularity alluded to in figure 3.1.

We now have to check that the metric is smooth and that the topology of the bundle is indeed $K_{\mathscr{F}}^{1/q} \oplus ... \oplus K_{\mathscr{F}}^{1/q}$. The latter statement is checked by identifying the holomorphic connection of $K_{\mathscr{F}}^{1/q}$ as $\widehat{A} = \sum_k \frac{c_k}{q}\, \partial \log(t_k)$. The line element of (3.61) is

$$ds^2 = \sum_{k=1}^{s-1} c_k(a_k - \alpha) ds_k^2 + \prod_k t_k^{\frac{c_k}{q}} \sum_{m=0}^{q-1} \left| dx_m + \widehat{A} x_m \right|^2 + \dots \tag{3.63}$$

We now can identify V in the second term.

To check smoothness we introduce a non-holomorphic complex coordinate $\tau_m = \left(\prod_k t_k^{\frac{c_k}{q}} \right)^{1/2} x_m = \rho_m e^{i\phi_m}$ and transform (3.63) into:

$$\begin{aligned} ds^2 &= \sum_{k=1}^{s-1} c_k(a_k - \alpha) ds_k^2 + \sum_{m=0}^{q-1} \left| d\tau_m + i \,\mathrm{Im}(\widehat{A}) \tau_m \right|^2 + \dots = \\ &= \sum_{k=1}^{s-1} c_k(a_k - \alpha) ds_k^2 + \sum_{m=0}^{q-1} \left(d\rho_m^2 + \rho_m^2 (d\phi_m + \mathrm{Im}(\widehat{A}))^2 \right) + \dots \end{aligned} \tag{3.64}$$

This is smooth if ϕ_m take values in $[0, 2\pi]$.

Appendix A

A review of toric varieties

In this section we review necessary facts about toric varieties for F-theory compactifications. A readable introduction for string theorists has been given in [69]. The standard reference is [70].

A.1 The moment map construction

The term torus refers to the algebraic group $\mathbb{C}^* \times .... \times \mathbb{C}^*$ acting on our variety. A toric variety is a complex algebraic variety, which contains an algebraic torus as a Zariski-dense subset, whose action on itself extends to the whole space. For instance for projective space we have

$$\{z_0 \cdot z_n \neq 0\} \subset \mathbb{P}^n. \tag{A.1}$$

Another example is the conifold

$$\{xy - zw = 0\} \subset \mathbb{C}^4. \tag{A.2}$$

It contains the torus $(\mathbb{C}^*)^3$ embedded via

$$(t_1, t_2, t_3) \mapsto (t_1, t_2, t_3, t_1 t_2 t_3^{-1}). \tag{A.3}$$

Obviously zero is not in the image, but the action extends.

There are different ways to construct toric varieties. In general a toric variety corresponds to a fan Σ a collection of rational, strongly convex, polyhedral cones $\sigma \in N \cong \mathbb{Z}^n$. They encode the action of the torus T_N on X. Each one dimensional cone is generated by a single lattice vector u_i, and we associate a homogenous coordinate x_i to it. We then define the toric variety X as

$$X = \left(\mathbb{C}^k \setminus Z_\Sigma\right) / (\mathbb{C}^*)^{k-3}. \tag{A.4}$$

Here $x_1, ..., x_k$ are coordinates on $\mathbb{C}^k$. Moreover $Z_\Sigma = \bigcup_I \{x_i = 0 \ \forall i \in I\}$, where the index sets I correspond to collections of vectors $(u_i)_{i \in I}$ not generating cones in Σ. The $(\mathbb{C}^*)^{k-3}$

action is given by $k-3$ charge vectors $\vec{Q}_a$ satisfying

$$\sum_i Q_a^i u_i = 0. \tag{A.5}$$

Usually one summarizes the charges in a table called toric data. The action on the coordinates is given by

$$(x_1, ..., x_n) \sim (\lambda^{Q_a^1} x_1, ..., \lambda^{Q_a^n} x_n), \tag{A.6}$$

where $\lambda \in \mathbb{C}^*$. This is not the action of the torus T_N.

Moreover we have the moment maps

$$\mu_a : \sum_i Q_a^i |x_i|^2 = t_a. \tag{A.7}$$

It turns out that

$$X = \frac{\bigcap \mu_a^{-1}(t_a)}{U(1)^{k-3}}, \tag{A.8}$$

with the obvious $U(1)$ actions $x_i \to e^{iQ_a^i \alpha_a} x_i$.

Examples:
1) Consider the fan with one dimensional cones $u_1 = (1,0), u_2 = (0,1), u_3 = (-1,-1)$. The collection (u_1, u_2, u_3) does not define a cone satisfying all conditions we stated above. Thus the set $Z_\Sigma = \{x_1 = x_2 = x_3 = 0\}$. We thus have

$$X = \frac{\mathbb{C}^3 \setminus \{x_1 = x_2 = x_3 = 0\}}{\mathbb{C}^*}. \tag{A.9}$$

Since $1 \cdot u_1 + 1 \cdot u_2 + 1 \cdot u_3 = 0$ we have the action of an element $\lambda \in \mathbb{C}^*$:

$$\lambda \cdot (x_1, x_2, x_3) = (\lambda x_1, \lambda x_2, \lambda x_3), \tag{A.10}$$

whence $X = \mathbb{CP}^2$.

2) The conifold corresponds to a single cone $\sigma \subset \mathbb{R}^3$, spanned by $u_1 = (1,0,0), u_2 = (0,1,0), u_3 = (1,0,1), u_4 = (0,1,1)$. The subset Z_Σ is empty. There is a single charge vector $(1,1,-1,-1)$ due to the relation $u_1 + u_2 - u_3 - u_4 = 0$. The moment map is

$$|x_1|^2 + |x_2|^2 - |x_3|^2 - |x_4|^2 = 0. \tag{A.11}$$

The small resolution is obtained, see page 523 of [70] by taking $\Sigma = \sigma_1 \cup \sigma_2$, with $\sigma_1 = \text{Cone}(u_1, u_3, u_4)$ and $\sigma_2 = \text{Cone}(u_1, u_2, u_4)$. We have $Z_\Sigma = \{x_i = 0, \ \forall i\}$, avoiding the singular point $x_i = 0$. Thus the moment map is now

$$|x_1|^2 + |x_2|^2 - |x_3|^2 - |x_4|^2 = t, \tag{A.12}$$

for $t \neq 0$.

A.2 Verifying the Calabi-Yau condition

Let us make some more remarks about hypersurfaces and complete intersections in toric varieties. In general each vector u_i corresponds to a homogeneous coordinate x_i and thus to a Weil divisor $D_i = \{x_i = 0\}$. The first Chern class of the variety is given by

$$c_1(X) = \sum D_i. \tag{A.13}$$

A (possible singular) hypersurface $Y \subset X$ will satisfy

$$TY \oplus NY = TX, \tag{A.14}$$

and thus

$$c_1(Y) = c_1(X) - c_1(NY) = \sum D_i - c_1(NY). \tag{A.15}$$

If $Y = \{P = 0\}$ then $c_1(NY) = [P]$, where $[P]$ is the first Chern class of the line bundle associated to the divisor P. Since P is homogenous in the x_i we can take any monomial to compute $c_1(NY)$.

It is best to illustrate this in an example. Consider $\mathbb{P}^4$ given by the toric data

x_0	x_1	x_2	x_3	x_4
1	1	1	1	1

(A.16)

The charge vector $(1, 1, 1, 1, 1)$ implies that $[x_i] \sim [x_j]$ in the Class group. Now we consider $Y = \{P = 0\}$, where

$$P = x_0^5 + x_1^5 + x_2^5 + x_3^5 + x_4^5 + \psi \Pi x_i, \tag{A.17}$$

with $\psi \in \mathbb{C}$. We then have

$$[P] \sim 5[x_i] \sim \sum [x_i], \tag{A.18}$$

and thus

$$c_1(P = 0) = 0, \tag{A.19}$$

i.e. the quintic Calabi-Yau.

Another important example in F-theory is $T^2 \subset \mathbb{P}_{1,2,3}$:

u	v	w
1	1	2

(A.20)

Again we have $[u] \sim [v]$ and $[w] \sim 2[u]$. Thus the equation

$$w^2 + b_0 u^2 w + b_1 uvw + b_2 v^2 w - c_0 u^4 - c_1 u^3 v - c_2 u^2 v^2 - c_3 u v^3, \tag{A.21}$$

defines a compact Calabi-Yau one-fold or a T^2. There several ways to embed T^2 into toric varieties and they are classified by so-called tops. The one at hand is called F6 [71, 72].

For a complete intersection we require that $[P_1] + [P_2] \sim \sum D_i$. One verifies this easily by comparing the charges of a monomial with the sum of the charges of the coordinates.

Constructing the ambient space

In [1]:
```
n=3 # degree of delta
```

In [2]:
```
Npoints=matrix([[ 0, 0, 0,-1, 1],
                [ 0, 0, 0,-1,-1],
                [ 0, 0, 0, 1, 0],
                [ 0, 0, 0, 0, 1],
                [ 0, 0, 1, 0, 0],
                [ 0, 0, 1, 1, 0],
                [ 0, 0, 1, 1,-1],
                [ 0, 0, 1, 0,-1],
                [ 0, 1, 0, 0, 0],
                [ 1, 0, 0, 0, 0],
                [-1,-1,-1,-4, 4-n]])
```

In [3]:
```
LatticePolytope(Npoints).is_reflexive()
```

Out[3]: True

In [4]:
```
print LatticePolytope(Npoints).poly_x('Dg33P')
```

```
M:535 22 N:13 11 H:6,0,479 [2958]
5 13  points of P-dual and IP-simplices
    0    0    0    0    0    0    0    0    0    1   -1    0    0
    0    0    0    0    0    0    0    0    1    0   -1    0    0
    0    0    0    0    1    1    1    1    0    0   -1    0    0
   -1   -1    1    0    0    1    1    0    0    0   -4   -1    0
    1   -1    0    1    0    0   -1   -1    0    0    1    0    0
------------------------------------------------------------    #IP-simp=7
    1    1    2    0    0    0    0    0    0    0    0    0   4=d  codim=3
    0    1    1    1    0    0    0    0    0    0    0    0   3=d  codim=3
    0    1    5    0    1    0    0    0    1    1    1    0  10=d  codim=0
    0    1    4    0    0    1    0    0    1    1    1    0   9=d  codim=0
    0    0    3    0    0    0    1    0    1    1    1    0   7=d  codim=1
    0    0    4    0    0    0    0    1    1    1    1    0   8=d  codim=1
    0    0    1    0    0    0    0    0    0    0    0    1   2=d  codim=4
5 12  m:8 4 n:6 4  M:535 22 N:13 11  p=0123b456789a
   1   -1    0    1    0    0    0   -1   -1    0    0    1
   0    2   -1   -1    1    0   -1    0    1    0    0    3
   0    0    0    0    0    1    1    1    1    0    0   -1
   0    0    0    0    0    0    0    0    0    1    0   -1
   0    0    0    0    0    0    0    0    0    0    1   -1
```

In [5]:
```
print Npoints.transpose()

p_tri = PointConfiguration(Npoints.transpose().augment(vector([0,0,0,0,0])).tra
nspose())

p_tri=p_tri.restrict_to_star_triangulations((0,0,0,0,0))

p_tri=p_tri.restrict_to_fine_triangulations()

tria=p_tri.triangulate()

tria=p_tri.triangulations_list()

#The following is a trick, to save computational power. We first construct the
ambient space before
#the small resolution. Then we add the vectors corresponding to the P1 by hand,
see below.
triangl=[[i[:-1] for i in j] for j in tria]

print len(tria)
```

```
[ 0  0  0  0  0  0  0  0  0  1 -1]
[ 0  0  0  0  0  0  0  0  1  0 -1]
[ 0  0  0  0  1  1  1  1  0  0 -1]
[-1 -1  1  0  0  1  1  0  0  0 -4]
[ 1 -1  0  1  0  0 -1 -1  0  0  1]
20
```

In [6]:
```
R.<u,v,w,s,z1,z2,z3,e0,e1,e,e4> = PolynomialRing(QQ,11)
```

In [7]:
```
j=0
for i in triangl:
    j+=1
    faecher=Fan(i,Npoints)
    tor=ToricVariety(faecher,coordinate_names='u,v,w,s,e0,e1,e,e4,z1,z2,z3,lam
1,lam2')
    sri=tor.Stanley_Reisner_ideal()
    if v*s in sri and v*e1 in sri and w*u in sri and w*e0 in sri and w*e4 in sr
i and u*e in sri\
                and s*e in sri and e0*e in sri and u*e4 in sri and s*e0 in sri
and s*e4 in sri\
                and e0*z1*z2*z3 in sri and e1*z1*z2*z3 in sri and e*z1*z2*z3 i
n sri and e4*z1*z2*z3 in sri:
        print j,sri
        basis_triangulierung=i
    else:
        print str(j)+": no"
```

```
1: no
2: no
3: no
4: no
5: no
6: no
7: no
8: no
9: no
10: no
11: no
12: no
13: no
14: no
15: no
16 Ideal (u*w, u*e, u*e4, v*s, v*e1, w*e0, s*e0, e0*e, s*e, s*e4, w*e4, e0*z1*z
2*z3, e1*z1*z2*z3, e*z1*z2*z3, e4*z1*z2*z3) of Multivariate Polynomial Ring in
u, v, w, s, e0, e1, e, e4, z1, z2, z3 over Rational Field
17: no
18: no
19: no
20: no
```

In [8]:
```
uplift_triangulation=[]

for i in basis_triangulierung:
    uplift_triangulation.append(i+[11])
    uplift_triangulation.append(i+[12])
```

In [9]:
```
ALPHA=1 #the degree of alpha is chosen to be one.
```

In [10]:
```
#This is the set of vectors satisfying the charges given in chapter 2: The last
two vectors correspond to the
# small resolution P1:

Npoints=matrix([[ 0, 0, 0,-1, 1, 0],
                [ 0, 0, 0,-1,-1, 1],
                [ 0, 0, 0, 1, 0, 0],
                [ 0, 0, 0, 0, 1, 1],
                [ 0, 0, 1, 0, 0, 0],
                [ 0, 0, 1, 1, 0, 0],
                [ 0, 0, 1, 1,-1,-1],
                [ 0, 0, 1, 0,-1, 0],
                [ 0, 1, 0, 0, 0, -3+n+ALPHA],
                [ 1, 0, 0, 0, 0, 0],
                [-1,-1,-1,-4,4-n, 0],
                [ 0, 0, 0, 0, 0,-1],
                [ 0, 0, 0, 0, 0, 1]])

print Npoints.transpose()
```

```
[ 0  0  0  0  0  0  0  0  0  1 -1  0  0]
[ 0  0  0  0  0  0  0  0  1  0 -1  0  0]
[ 0  0  0  0  1  1  1  1  0  0 -1  0  0]
[-1 -1  1  0  0  1  1  0  0  0 -4  0  0]
[ 1 -1  0  1  0  0 -1 -1  0  0  1  0  0]
[ 0  1  0  1  0  0 -1  0  1  0  0 -1  1]
```

In [11]:
```
faecher=Fan(uplift_triangulation,Npoints)
tor=ToricVariety(faecher,coordinate_names='u,v,w,s,e0,e1,e,e4,z1,z2,z3,lam1,lam
2')
sri=tor.Stanley_Reisner_ideal()
print sri
ring=tor.coordinate_ring()
# ring.inject_variables()
```

```
Ideal (u*w, u*e, u*e4, v*s, v*e1, w*e0, s*e0, e0*e, lam1*lam2, s*e, s*e4, w*e4,
e0*z1*z2*z3, e1*z1*z2*z3, e*z1*z2*z3, e4*z1*z2*z3) of Multivariate Polynomial R
ing in u, v, w, s, e0, e1, e, e4, z1, z2, z3, lam1, lam2 over Rational Field
```

In [12]:
```
tor.is_complete()
```

Out[12]: True

In [13]:
```
tor.is_smooth()
```

Out[13]: False

In [14]:
```
tor.is_orbifold()
```

Out[14]: True

Some (co)homological definitions

In [15]:
```
U, V, W, S, E0, E1, E, E4, Z1, Z2, Z3, L1, L2=[tor.divisor(i).cohomology_class
()
                                               for i in range(len(tor.gens()))]
```

In [16]:
```
HS = -tor.K().cohomology_class(); HS
```

Out[16]:
```
[-5*s - e1 + 5*e + 2*e4 + 2*z3 + 5*lam1 - 3*lam2]
```

In [17]:
```
Kb = 4 #The canonical class of P3 is 4 times the generic hypersurface of degree
one.
```

In [18]:
```
#The degrees of the defining eqution of our complete intersection:

P1 = (2*Kb - n - 1 - ALPHA)*Z3 + W;
P2 = (Kb - (2*Kb - n - 1 - ALPHA))*Z3 + V;
Q = E1 + S + 2*W;
```

In [19]:
```
HS1=(L1+E);
HS2=(L2+Q);
```

In [20]:
```
tor.c(1) - HS1 - HS2 #Our CS is Calabi-Yau
```

Out[20]:
```
[0]
```

The intersection structure of the resolutions P1s in the fiber

In [21]:
```
[[tor.integrate(Z1*Z2*tor.divisor(i).cohomology_class()*tor.divisor(j).cohomolo
gy_class()*HS1*HS2)\
  for i in [4,5,6,7]] for j in [4,5,6,7]]
```

Out[21]:
```
[[-2, 1, 0, 1], [1, -2, 1, 0], [0, 1, -2, 1], [1, 0, 1, -2]]
```

In [22]:
```
ExcDiv = [E0, E1, L2, E - L2, E4]
```

In [23]:
```
[[tor.integrate(Z1*Z2*Ei*Ej*HS1*HS2)\
  for Ei in ExcDiv] for Ej in ExcDiv]
```

Out[23]:
```
[[-2, 1, 0, 0, 1],
 [1, -2, 1, 0, 0],
 [0, 1, -2, 1, 0],
 [0, 0, 1, -2, 1],
 [1, 0, 0, 1, -2]]
```

P1 intersection structure over matter curves

In [24]:
```
#We treat the sections over the base as variables

poly_ring.<u, v, w, s, z1, z2, z3, e0, e1, e, e4, lam1, lam2, alpha, beta, delt
a, gamma, c2, d2, d3, B0,\
            B1, B2, C0, C1, C2, C3> = QQ[]
poly_ring
```

Out[24]:
```
Multivariate Polynomial Ring in u, v, w, s, z1, z2, z3, e0, e1, e, e4, lam1, la
m2, alpha, beta, delta, gamma, c2, d2, d3, B0, B1, B2, C0, C1, C2, C3 over Rati
onal Field
```

In [25]:
```
poly_Q  = e1*s*w^2 - e4^2*e0*beta*v^3*u + e4*delta*v^2*w;
poly_P1 = e4*e0*d2*u*v + d3*w + e1*e4*e0^2*gamma*s*u^2;
poly_P2 = c2*v + e1*e0*alpha*s*u;
```

In [26]:
```
hse1 = lam1*e - lam2*s*poly_P2;
hse2 = lam2*poly_Q - lam1*u*poly_P1;
```

In [27]:
```
SR_ideal=ideal(u*w, u*e, u*e4, v*s, v*e1, w*e0, s*e0, e0*e, lam1*lam2,\
               s*e, s*e4, w*e4, e0*z1*z2*z3, e1*z1*z2*z3, e*z1*z2*z3,\
               e4*z1*z2*z3)
SR_ideal
```

Out[27]:
```
Ideal (u*w, u*e, u*e4, v*s, v*e1, w*e0, s*e0, e0*e, lam1*lam2, s*e, s*e4, w*e4,
z1*z2*z3*e0, z1*z2*z3*e1, z1*z2*z3*e, z1*z2*z3*e4) of Multivariate Polynomial R
ing in u, v, w, s, z1, z2, z3, e0, e1, e, e4, lam1, lam2, alpha, beta, delta, g
amma, c2, d2, d3, B0, B1, B2, C0, C1, C2, C3 over Rational Field
```

In [28]:
```
#This function checks if a set of monomials is in an ideal. Later this function
is used to remove
# generators of ideals that violate the chosen SRI.

def SRI_check(gens,ideal):
    monome=1
    for i in gens:
        if i.is_monomial():
            monome*=i
    if monome in ideal:
        return True
    else:
        return False
```

In [29]:
```
#We exploit the relations in the SRI to write the generators of certain ideals
simpler

for i in [e0,e1,e,e4]:
    subs_string=str(i)+'=0'
    for j in poly_ring.gens():
        if i*j in SR_ideal:
            subs_string+=', '+str(j)+'=1'
    print subs_string
```

```
e0=0, w=1, s=1, e=1
e1=0, v=1
e=0, u=1, s=1, e0=1
e4=0, u=1, w=1, s=1
```

In [30]:
```
E_0=[e0, hse1.subs(e0=0, w=1, s=1, e=1), hse2.subs(e0=0, w=1, s=1, e=1)];
E_1=[e1, hse1.subs(e1=0, v=1), hse2.subs(e1=0, v=1)];
E_2=[e, poly_P1.subs(e=0, u=1, s=1, e0=1), lam2];
E_3=[e, poly_P2.subs(e=0, u=1, s=1, e0=1), hse2.subs(e=0, u=1, s=1, e0=1)];
E_4=[e4, hse1.subs(e4=0, u=1, w=1, s=1), hse2.subs(e4=0, u=1, w=1, s=1)];
```

In [31]:
```
for i in [E_0,E_1,E_2,E_3,E_4]:
    for j in ideal(i).complete_primary_decomposition():
        if not SRI_check(j[1].gens(),SR_ideal):
            print j[1].gens()
```

```
[e0, v*lam2*c2 - lam1, v*e4*lam1*delta - u*lam1*c2*d3 + e1*lam2*c2, v^2*e4*delt
a - u*v*c2*d3 + e1, u*lam1*lam2*c2^2*d3 - e1*lam2^2*c2^2 - e4*lam1^2*delta]
[e1, s*lam2*c2 - e*lam1, u*e0*e4^2*lam2*beta + u^2*e0*e4*lam1*d2 - w*e4*lam2*de
lta + u*w*lam1*d3, u^2*s*e0*e4*c2*d2 + u*e0*e*e4^2*beta + u*w*s*c2*d3 - w*e*e4*
delta]
[lam2, e, e1*e4*gamma + v*e4*d2 + w*d3]
[e, e1*alpha + v*c2, v^3*e4^2*lam2*beta - v^2*w*e4*lam2*delta - w^2*e1*lam2 + e
1*e4*lam1*gamma + v*e4*lam1*d2 + w*lam1*d3]
[e4, e1*lam2 - lam1*d3, e0*lam1*alpha*d3 + v*lam2*c2 - e*lam1, e0*e1*alpha*d3 +
v*c2*d3 - e1*e]
```

10_3 curve (c2=0)

In [32]:
```
for i in [E_0,E_1,E_2,E_3,E_4]:
    print "Naive substitution:"
    print [j.subs(c2=0) for j in i]
    print "Ideal decomposition:"
    for j in ideal(i+[c2]).complete_primary_decomposition():
        if not SRI_check(j[1].gens(),SR_ideal):
            print j[1].gens()
```

```
Naive substitution:
[e0, lam1, v^2*e4*lam2*delta - u*lam1*d3 + e1*lam2]
Ideal decomposition:
[c2, lam1, e0, v^2*e4*delta + e1]
Naive substitution:
[e1, e*lam1, -u*e0*e4^2*lam2*beta - u^2*e0*e4*lam1*d2 + w*e4*lam2*delta - u*w*l
am1*d3]
Ideal decomposition:
[c2, lam1, e4, e1]
[c2, lam1, e1, u*e0*e4*beta - w*delta]
[c2, e, e1, u*e0*e4^2*lam2*beta + u^2*e0*e4*lam1*d2 - w*e4*lam2*delta + u*w*lam
1*d3]
Naive substitution:
[e, e1*e4*gamma + v*e4*d2 + w*d3, lam2]
Ideal decomposition:
[c2, lam2, e, e1*e4*gamma + v*e4*d2 + w*d3]
Naive substitution:
[e, e1*alpha, -v^3*e4^2*lam2*beta + v^2*w*e4*lam2*delta + w^2*e1*lam2 - e1*e4*l
am1*gamma - v*e4*lam1*d2 - w*lam1*d3]
Ideal decomposition:
[c2, alpha, e, v^3*e4^2*lam2*beta - v^2*w*e4*lam2*delta - w^2*e1*lam2 + e1*e4*l
am1*gamma + v*e4*lam1*d2 + w*lam1*d3]
[c2, e, e1, v^3*e4^2*lam2*beta - v^2*w*e4*lam2*delta + v*e4*lam1*d2 + w*lam1*d
3]
Naive substitution:
[e4, -e0*e1*lam2*alpha + e*lam1, e1*lam2 - lam1*d3]
Ideal decomposition:
[c2, lam1, e4, e1]
[c2, e4, e1*lam2 - lam1*d3, e0*alpha*d3 - e]
```

In [33]:
```
poly_P2.subs(e4=0,e1=0),poly_Q.subs(e4=0,e1=0)
```

Out[33]: (v*c2, 0)

In [34]:
```
[tor.integrate(Z2*L1*E4*E1*Z3*exc_i) for exc_i in ExcDiv[1:]]
```

Out[34]: [-1, 0, 1, -1]

In [35]:
```
poly_P2.subs(c2=0,e1=0),poly_Q.subs(c2=0,e1=0)
```

Out[35]: (0, -u*v^3*e0*e4^2*beta + v^2*w*e4*delta)

In [36]:
```
[tor.integrate(Z2*L1*E1*(W+3*Z1)*Z3*exc_i) for exc_i in ExcDiv[1:]]
```

Out[36]: [-1, 0, 1, 0]

In [37]:
```
poly_P2.subs(c2=0,e1=0,e=0),poly_Q.subs(c2=0,e1=0,e=0),poly_P1.subs(c2=0,e1=0,e=0)
```

Out[37]: (0, -u*v^3*e0*e4^2*beta + v^2*w*e4*delta, u*v*e0*e4*d2 + w*d3)

In [38]:
```
[tor.integrate(Z2*E*E1*(W+E4+L2+3*Z1)*Z3*exc_i) for exc_i in ExcDiv[1:]]
```

Out[38]: [0, 1, -2, 1]

the sum of the previously shown weight vectors is the highest weight vector for the 10 representation of SU(5) allowing

us to identify the combination of curves in the fiber leading to this state

5_-6 curve

In [39]:
```
curve_5_m6 = delta
```

In [40]:
```
for i in [E_0,E_1,E_2,E_3,E_4]:
    print "Ideal decomposition:"
    for j in ideal(i+[curve_5_m6]).complete_primary_decomposition():
        if not SRI_check(j[1].gens(),SR_ideal):
            print j[1].gens()
            print 'co-dim: '+str(j[1].ring().ngens()-j[1].dimension())
    print "######################"
```

```
Ideal decomposition:
[delta, e0, u*lam1*d3 - e1*lam2, v*lam2*c2 - lam1, u*v*c2*d3 - e1]
co-dim: 4
######################
Ideal decomposition:
[delta, e1, u, s*lam2*c2 - e*lam1]
co-dim: 4
[delta, e1, s*lam2*c2 - e*lam1, e0*e4^2*lam2*beta + u*e0*e4*lam1*d2 + w*lam1*d
3, u*s*e0*e4*c2*d2 + e0*e*e4^2*beta + w*s*c2*d3]
co-dim: 4
######################
Ideal decomposition:
[delta, lam2, e, e1*e4*gamma + v*e4*d2 + w*d3]
co-dim: 4
######################
Ideal decomposition:
[delta, e, e1*alpha + v*c2, v^3*e4^2*lam2*beta - w^2*e1*lam2 + e1*e4*lam1*gamma
+ v*e4*lam1*d2 + w*lam1*d3]
co-dim: 4
######################
Ideal decomposition:
[delta, e4, e1*lam2 - lam1*d3, e0*lam1*alpha*d3 + v*lam2*c2 - e*lam1, e0*e1*alp
ha*d3 + v*c2*d3 - e1*e]
co-dim: 4
######################
```

In [41]:
```
[tor.integrate(Z2*E1*U*HS1*Z3*exc_i) for exc_i in ExcDiv[1:]]
```

Out[41]:
```
[-1, 0, 0, 0]
```

In [42]:
```
for j in ideal([hse1, hse2, e1, u]).complete_primary_decomposition():
    if not SRI_check(j[1].gens(),SR_ideal):
        print j[1].gens()
```

```
[delta, e1, u, v*s*lam2*c2 - e*lam1]
```

Non-flat fiber

In [43]:
```
non_flat_point=[c2,alpha]
```

In [44]:
```
for i in [E_0,E_1,E_2,E_3,E_4]:
    print "Naive substitution:"
    print [j.subs(c2=0,alpha=0) for j in i]
    print "Ideal decomposition:"
    for j in ideal(i+non_flat_point).complete_primary_decomposition():
        if not SRI_check(j[1].gens(),SR_ideal):
            print j[1].gens()
            print 'co-dim: '+str(j[1].ring().ngens()-j[1].dimension())
```

```
Naive substitution:
[e0, lam1, v^2*e4*lam2*delta - u*lam1*d3 + e1*lam2]
Ideal decomposition:
[c2, alpha, lam1, e0, v^2*e4*delta + e1]
co-dim: 5
Naive substitution:
[e1, e*lam1, -u*e0*e4^2*lam2*beta - u^2*e0*e4*lam1*d2 + w*e4*lam2*delta - u*w*l
am1*d3]
Ideal decomposition:
[c2, alpha, lam1, e4, e1]
co-dim: 5
[c2, alpha, lam1, e1, u*e0*e4*beta - w*delta]
co-dim: 5
[c2, alpha, e, e1, u*e0*e4^2*lam2*beta + u^2*e0*e4*lam1*d2 - w*e4*lam2*delta +
u*w*lam1*d3]
co-dim: 5
Naive substitution:
[e, e1*e4*gamma + v*e4*d2 + w*d3, lam2]
Ideal decomposition:
[c2, alpha, lam2, e, e1*e4*gamma + v*e4*d2 + w*d3]
co-dim: 5
Naive substitution:
[e, 0, -v^3*e4^2*lam2*beta + v^2*w*e4*lam2*delta + w^2*e1*lam2 - e1*e4*lam1*gam
ma - v*e4*lam1*d2 - w*lam1*d3]
Ideal decomposition:
[c2, alpha, e, v^3*e4^2*lam2*beta - v^2*w*e4*lam2*delta - w^2*e1*lam2 + e1*e4*l
am1*gamma + v*e4*lam1*d2 + w*lam1*d3]
co-dim: 4
Naive substitution:
[e4, e*lam1, e1*lam2 - lam1*d3]
Ideal decomposition:
[c2, alpha, lam1, e4, e1]
co-dim: 5
[c2, alpha, e4, e, e1*lam2 - lam1*d3]
co-dim: 5
```

In [45]:
```
#We indeed have a complex two dimensional subvariety

for j in ideal([hse1, hse2, e, c2]).complete_primary_decomposition():
    if not SRI_check(j[1].gens(),SR_ideal):
        print j[1].gens()
        print 'co-dim: '+str(j[1].ring().ngens()-j[1].dimension())
```

```
[c2, lam2, e, u^2*s*e0^2*e1*e4*gamma + u*v*e0*e4*d2 + w*d3]
co-dim: 4
[c2, alpha, e, u^3*s*e0^2*e1*e4*lam1*gamma + u*v^3*e0*e4^2*lam2*beta + u^2*v*e0
*e4*lam1*d2 - v^2*w*e4*lam2*delta - w^2*s*e1*lam2 + u*w*lam1*d3]
co-dim: 4
[c2, e, e1, u*v^3*e0*e4^2*lam2*beta + u^2*v*e0*e4*lam1*d2 - v^2*w*e4*lam2*delta
+ u*w*lam1*d3]
co-dim: 4
```

In [46]:
```
for j in ideal([hse1, hse2, lam2, c2]).complete_primary_decomposition():
    if not SRI_check(j[1].gens(),SR_ideal):
        print j[1].gens()
        print 'co-dim: '+str(j[1].ring().ngens()-j[1].dimension())
```

```
[c2, lam2, e, u^2*s*e0^2*e1*e4*gamma + u*v*e0*e4*d2 + w*d3]
co-dim: 4
```

In [47]:
```
for j in ideal([hse1, hse2, c2, e1]).complete_primary_decomposition():
    if not SRI_check(j[1].gens(),SR_ideal):
        print j[1].gens()
        print 'co-dim: '+str(j[1].ring().ngens()-j[1].dimension())
```

```
[c2, lam1, e4, e1]
co-dim: 4
[c2, lam1, e1, u*v*e0*e4*beta - w*delta]
co-dim: 4
[c2, e, e1, u*v^3*e0*e4^2*lam2*beta + u^2*v*e0*e4*lam1*d2 - v^2*w*e4*lam2*delta
+ u*w*lam1*d3]
co-dim: 4
```

In [48]:
```
for j in ideal([hse1, hse2, lam1, e1]).complete_primary_decomposition():
    if not SRI_check(j[1].gens(),SR_ideal):
        print j[1].gens()
        print 'co-dim: '+str(j[1].ring().ngens()-j[1].dimension())
```

```
[lam1, e1, s, u*v*e0*e4*beta - w*delta]
co-dim: 4
[c2, lam1, e4, e1]
co-dim: 4
[c2, lam1, e1, u*v*e0*e4*beta - w*delta]
co-dim: 4
```

In [49]:
```
for j in ideal([hse1, hse2, e1, s]).complete_primary_decomposition():
    if not SRI_check(j[1].gens(),SR_ideal):
        print j[1].gens()
        print 'co-dim: '+str(j[1].ring().ngens()-j[1].dimension())
```

```
[lam1, e1, s, u*v*e0*e4*beta - w*delta]
co-dim: 4
```

We compute the charge vectors of those P1s in the non-flat fiber that mediate the desired Yukawa coupling

In [50]:
```
[tor.integrate(Z1*Z2*E*E1*W*E0),\
 tor.integrate(Z1*Z2*E*E1*W*E1),\
 tor.integrate(Z1*Z2*E*E1*W*L2),\
 tor.integrate(Z1*Z2*E1*E*W*(E-L2)),\
 tor.integrate(Z1*Z2*E*E1*W*E4)]
```

Out[50]: [0, 0, 1, -1, 0]

In [51]:
```
[tor.integrate(Z1*Z2*E1*E*L1*E0),\
 tor.integrate(Z1*Z2*E1*E*L1*E1),\
 0,\
 tor.integrate(Z1*Z2*V*E*L1*(E-L2)),\
 tor.integrate(Z1*Z2*E1*E*L1*E4)]
```

Out[51]: [0, 0, 0, -1, 1]

In [52]:
```
[tor.integrate(Z1*Z2*E1*E*HS2*E0),\
 tor.integrate(Z1*Z2*V*E*HS2*E1),\
 tor.integrate(Z1*Z2*E1*E*P1*L2),\
 tor.integrate(Z1*Z2*V*E*HS2*(E-L2)),\
 tor.integrate(Z1*Z2*E1*E*HS2*E4)]
```

Out[52]:
```
[0, 0, 1, -2, 1]
```

In [53]:
```
[tor.integrate(Z1*Z2*E4*E*HS2*E0),\
 tor.integrate(Z1*Z2*E4*E*HS2*E1),\
 tor.integrate(Z1*Z2*E4*E*W*L2),\
 tor.integrate(Z1*Z2*E4*E*HS2*(E-L2)),\
 tor.integrate(Z1*Z2*E4*E*HS2*E4)]
```

Out[53]:
```
[0, 1, 0, 0, -1]
```

In [54]:
```
[tor.integrate(Z1*Z2*W*E*HS2*E0),\
 tor.integrate(Z1*Z2*W*E*HS2*E1),\
 tor.integrate(Z1*Z2*W*E*P1*L2),\
 tor.integrate(Z1*Z2*W*E*HS2*(E-L2)),\
 tor.integrate(Z1*Z2*W*E*HS2*E4)]
```

Out[54]:
```
[0, 1, 1, -2, 0]
```

In [55]:
```
[tor.integrate(Z1*Z2*E*W*W*E0),\
 tor.integrate(Z1*Z2*E*W*W*E1),\
 tor.integrate(Z1*Z2*E*W*W*L2),\
 tor.integrate(Z1*Z2*E*W*W*(E-L2)),\
 tor.integrate(Z1*Z2*E*W*W*E4)]
```

Out[55]:
```
[0, 0, 1, -1, 0]
```

Second Chern class and fluxes

In [56]:
```
# Second Chern class of our variety by adjunction:
Ch2 = (tor.c()/(1+HS1)/(1+HS2)).part_of_degree(2)
Ch2
```

Out[56]:
```
[-9*e1*z3 - 8*e*z3 + 20*e4*z3 + 20*z3^2 + 5*s*lam1 - 8*e1*lam1 - 35*e*lam1 - 9*
e4*lam1 + 44*z3*lam1 - 17*lam1^2 - 10*s*lam2 + 7*e1*lam2 + 40*e*lam2 + 11*e4*la
m2 - 42*z3*lam2 - 21*lam2^2]
```

In [57]:
```
Cartan = matrix([[-2,1,0,0],[1,-2,1,0],[0,1,-2,1],[0,0,1,-2]]);
Cartan
```

Out[57]:
```
[-2  1  0  0]
[ 1 -2  1  0]
[ 0  1 -2  1]
[ 0  0  1 -2]
```

In [58]:
```
# Due to the structure of the fluxes we want to express everything only in term
s of the following Cohomology classes
mybase1 = [[z3, Z3], [u, U], [s, S], [e1, E1], [lam2, L2], [e, E], [e4, E4]]
```

In [59]:
```
#Construct a basis of H^4
longbase = []
for i, ele1 in enumerate(mybase1):
    for ele2 in mybase1[i:]:
        if (ele1[1]*ele2[1]*HS1*HS2) != (S*E):
            longbase.append([ele1[0]*ele2[0], ele1[1]*ele2[1]])
```

In [60]:
```
[[j, [i[0] for i in longbase][j]] for j in range(22)] # v
```

Out[60]:
```
[[0, z3^2],
 [1, u*z3],
 [2, s*z3],
 [3, z3*e1],
 [4, z3*lam2],
 [5, z3*e],
 [6, z3*e4],
 [7, u^2],
 [8, u*s],
 [9, u*e1],
 [10, s^2],
 [11, s*e1],
 [12, e1^2],
 [13, e1*lam2],
 [14, e1*e],
 [15, e1*e4],
 [16, lam2^2],
 [17, e*lam2],
 [18, e4*lam2],
 [19, e^2],
 [20, e*e4],
 [21, e4^2]]
```

In [61]:
```
#Again we only choose terms consisting of only (z3,s,u,e1,e,e4,lam1,lam2)

mybase2 = [longbase[i] for i in [0, 1, 2, 3, 4, 5, 6, 18, 13, 9, 15]]
print [i[0] for i in mybase2]
print len(mybase2)
matrix([[tor.integrate(i[1]*j[1]*HS1*HS2) for j in mybase2] for i in mybase2]).
right_kernel_matrix()
```

```
[z3^2, u*z3, s*z3, z3*e1, z3*lam2, z3*e, z3*e4, e4*lam2, e1*lam2, u*e1, e1*e4]
11
```

Out[61]:
```
[]
```

In [62]:
```
intersection_matrix = matrix([[tor.integrate(i[1]*j[1]*HS1*HS2) for j in mybase
2] for i in mybase2])
```

In [63]:
```
E_vec = vector(ExcDiv[1:]);
mybase2_vec = vector([bas_i[1] for bas_i in mybase2]);
```

Image under the Shioda homomorphism of the additional section

In [64]:
```
wX = 5*((S - U - (Kb + n)*Z3)) + (4*E1 + 3*L2 + 2*(E - L2) + E4)
```

In [65]:
```
G4_U1 = Z3*wX;
G4_U1
```

Out[65]:
```
[4*e1*z3 + 7*e*z3 - 19*e4*z3 - 40*z3^2 - 15/2*s*lam1 + 15/2*e1*lam1 + 30*e*lam1
+ 15/2*e4*lam1 - 55/2*z3*lam1 + 15*lam1^2 + 15/2*s*lam2 - 15/2*e1*lam2 - 30*e*l
am2 - 15/2*e4*lam2 + 57/2*z3*lam2 + 15*lam2^2]
```

In [66]:
```
gen_10_m2 = (intersection_matrix.inverse()*vector(\
    [tor.integrate(HS1*(2*Kb - (n + ALPHA +1))*Z3*E1*E4*bas_i[1]) for bas_i in
mybase2])).dot_product(mybase2_vec);

G4_10_m2 = 5*(gen_10_m2 - \
           Z3*(Cartan.inverse()*vector([tor.integrate(HS1*HS2*gen_10_m2*Z3*i) f
or i in E_vec])).dot_product(E_vec));
G4_10_m2
```

Out[66]:
```
[-6*e1*z3 - 3*e*z3 + 6*e4*z3 - 5*e4*lam2 + 6*z3*lam2]
```

Chosen Charge vector

In [67]:
```
5*Cartan.inverse()*vector([tor.integrate(HS1*HS2*gen_10_m2*Z3*i) for i in E_ve
c])/(2*Kb - (n + ALPHA +1))
```

Out[67]:
```
(2, -1, 1, 3)
```

In [68]:
```
gen_10_m2 = (intersection_matrix.inverse()*vector(\
    [tor.integrate(HS1*HS2*(E1 - L1)*E4*bas_i[1]) for bas_i in mybase2])).dot_p
roduct(mybase2_vec);

G4_10_m2 = 5*(gen_10_m2 - \
           Z3*(Cartan.inverse()*vector([tor.integrate(HS1*HS2*gen_10_m2*Z3*i) f
or i in E_vec])).dot_product(E_vec));
G4_10_m2
```

Out[68]:
```
[-6*e1*z3 - 3*e*z3 + 6*e4*z3 - 5*e4*lam2 + 6*z3*lam2]
```

In [69]:
```
gen_10_3 = (intersection_matrix.inverse()*vector(\
    [tor.integrate(((n + ALPHA +1) - Kb)*Z3*L1*E1*E4*bas_i[1]) for bas_i in myb
ase2])).dot_product(mybase2_vec);

G4_10_3 = 5*(gen_10_3 - \
           Z3*(Cartan.inverse()*vector([tor.integrate(HS1*HS2*gen_10_3*Z3*i) fo
r i in E_vec])).dot_product(E_vec));
G4_10_3
```

Out[69]:
```
[-3*e1*z3 + e*z3 - 2*e4*z3 + 5*e4*lam1 - 2*z3*lam2]
```

In [70]:
```
gen_10_3 = (intersection_matrix.inverse()*vector(\
    [tor.integrate(HS1*HS2*L1*E4*bas_i[1]) for bas_i in mybase2])).dot_product
(mybase2_vec);

G4_10_3 = 5*(gen_10_3 - \
           Z3*(Cartan.inverse()*vector([tor.integrate(HS1*HS2*gen_10_3*Z3*i) fo
r i in E_vec])).dot_product(E_vec));
G4_10_3
```

Out[70]:
```
[-3*e1*z3 + e*z3 - 2*e4*z3 + 5*e4*lam1 - 2*z3*lam2]
```

In [71]:
```
5*Cartan.inverse()*vector([tor.integrate(HS1*HS2*gen_10_3*Z3*i) for i in E_ve
c])/((n + ALPHA +1) - Kb)
```

Out[71]:
```
(3, 1, -1, 2)
```

In [72]:
```
gen_5_m6 = (intersection_matrix.inverse()*vector(\
    [tor.integrate(HS1*(n*Z3)*E1*U*bas_i[1]) for bas_i in mybase2])).dot_produc
t(mybase2_vec);

G4_5_m6 = 5*(gen_5_m6 - \
           Z3*(Cartan.inverse()*vector([tor.integrate(HS1*HS2*gen_5_m6*Z3*i) fo
r i in E_vec])).dot_product(E_vec));
G4_5_m6
```

Out[72]:
```
[-12*e1*z3 - 6*e*z3 + 12*e4*z3 - 5*e1*lam1 + 5*e4*lam1 + 5*e1*lam2 - 5*e4*lam2
- 3*z3*lam2]
```

In [73]:
```
gen_5_m6 = (intersection_matrix.inverse()*vector(\
    [tor.integrate(HS1*HS2*E1*U*bas_i[1]) for bas_i in mybase2])).dot_product(m
ybase2_vec);

G4_5_m6 = 5*(gen_5_m6 - \
           Z3*(Cartan.inverse()*vector([tor.integrate(HS1*HS2*gen_5_m6*Z3*i) fo
r i in E_vec])).dot_product(E_vec));
G4_5_m6
```

Out[73]:
```
[-12*e1*z3 - 6*e*z3 + 12*e4*z3 - 5*e1*lam1 + 5*e4*lam1 + 5*e1*lam2 - 5*e4*lam2
- 3*z3*lam2]
```

In [74]:
```
5*Cartan.inverse()*vector([tor.integrate(HS1*HS2*gen_5_m6*Z3*i) for i in E_ve
c])/n
```

Out[74]:
```
(4, 3, 2, 1)
```

In [75]:
```
gen_5_m1 = (intersection_matrix.inverse()*vector(\
    [tor.integrate(E*P1*P2*Q*bas_i[1]) for bas_i in mybase2])).dot_product(myba
se2_vec);

G4_5_m1 = 5*(gen_5_m1 - \
           Z3*(Cartan.inverse()*vector([tor.integrate(HS1*HS2*gen_5_m1*Z3*i) fo
r i in E_vec])).dot_product(E_vec));
G4_5_m1
```

Out[75]:
```
[15*e1*z3 - 5*e4*z3 + 5/2*s*lam1 - 5/2*e1*lam1 - 10*e*lam1 - 15/2*e4*lam1 + 25/
2*z3*lam1 - 5*lam1^2 - 5/2*s*lam2 - 15/2*e1*lam2 + 10*e*lam2 + 5/2*e4*lam2 + 25
/2*z3*lam2 - 5*lam2^2]
```

In [76]:
```
gen_5_m1 = (intersection_matrix.inverse()*vector(\
    [tor.integrate(HS1*HS2*((P1 - L2)*(P2 - L1) + S*P1)*bas_i[1]) for bas_i in
mybase2])).dot_product(mybase2_vec);

G4_5_m1 = 5*(gen_5_m1 - \
           Z3*(Cartan.inverse()*vector([tor.integrate(HS1*HS2*gen_5_m1*Z3*i) fo
r i in E_vec])).dot_product(E_vec));
G4_5_m1
```

Out[76]:
```
[15*e1*z3 - 5*e4*z3 + 5/2*s*lam1 - 5/2*e1*lam1 - 10*e*lam1 - 15/2*e4*lam1 + 25/
2*z3*lam1 - 5*lam1^2 - 5/2*s*lam2 - 15/2*e1*lam2 + 10*e*lam2 + 5/2*e4*lam2 + 25
/2*z3*lam2 - 5*lam2^2]
```

In [77]:
```
5*Cartan.inverse()*vector([tor.integrate(HS1*HS2*gen_5_m1*Z3*i) for i in E_ve
c])\
/(3*((n + ALPHA +1) - Kb) + 2*(2*Kb - (n + 2) + (2*Kb - (n + ALPHA +1))))
```

Out[77]: (-1, -2, 2, 1)

In [78]:
```
gen_5_4 = (intersection_matrix.inverse()*vector(\
    [tor.integrate(HS1*HS2*(E1*(P1 - L2 - E4) + L1*E4)*bas_i[1]) for bas_i in m
ybase2])).dot_product(mybase2_vec) - G4_10_m2;

G4_5_4 = 5*(gen_5_4 - \
           Z3*(Cartan.inverse()*vector([tor.integrate(HS1*HS2*gen_5_4*Z3*i) for
i in E_vec])).dot_product(E_vec));
G4_5_4
```

Out[78]:
```
[31*e1*z3 + 13*e*z3 - 26*e4*z3 + 20*z3^2 + 5*s*lam1 - 5*e1*lam1 - 20*e*lam1 + 2
0*z3*lam1 - 10*lam1^2 - 5*s*lam2 + 20*e*lam2 + 30*e4*lam2 - 41*z3*lam2 - 10*lam
2^2]
```

In [79]:
```
5*Cartan.inverse()*vector([tor.integrate(HS1*HS2*gen_5_4*Z3*i) for i in E_ve
c])/(3*Kb - 2 - ALPHA)
```

Out[79]: (1, -3, -2, -1)

Flux corresponding to the non-flat fiber

In [80]:
```
# Chern class of the normal bundle

c_N_nonflat = (1 + ALPHA*Z1)*(1 + (Kb - (2*Kb - n - 1 - ALPHA))*Z2)*(1 + E)/(1+
HS1)
```

In [81]:
```
G4_non_flat = (intersection_matrix.inverse()*vector(\
    [tor.integrate(HS1*HS2*(((n + ALPHA +1) - Kb)*Z3*(E - L2 - E1) + E1*(L1 -
S))*bas_i[1]) for bas_i in mybase2])).dot_product(mybase2_vec);
G4_non_flat
```

Out[81]:
```
[-e1*z3 + e4*z3 + z3^2 + 1/2*s*lam1 + 1/2*e1*lam1 - 2*e*lam1 - 1/2*e4*lam1 + 3/
2*z3*lam1 - lam1^2 - 1/2*s*lam2 + 1/2*e1*lam2 + 2*e*lam2 + 1/2*e4*lam2 - 5/2*z3
*lam2 - lam2^2]
```

Compute integrals over chosen four cycles to guess at the expression of the second Chern class in terms of fluxes

In [82]:
```
Ch2_vec = intersection_matrix.inverse()*vector([tor.integrate(Ch2*j[1]*HS1*HS2)
for j in mybase2]);
Ch2_vec
```

Out[82]: (39, 28, 18, -10, 7, -27, -17, 1, 2, -5, 2)

In [83]:
```
# print vector([tor.integrate(wX*Z3*j[1]*HS1*HS2) for j in mybase2])
wX_vec = intersection_matrix.inverse()*vector([tor.integrate(G4_U1*j[1]*HS1*HS
2) for j in mybase2]);
wX_vec
```

Out[83]: (-35, -5, 5, 4, 1, 2, 1, 0, 0, 0, 0)

In [84]:
```
intersection_matrix.inverse()*vector([tor.integrate(G4_10_m2*j[1]*HS1*HS2) for
j in mybase2])
```

Out[84]: (0, 0, 0, -6, 6, -3, 6, -5, 0, 0, 0)

In [85]:
```
intersection_matrix.inverse()*vector([tor.integrate(G4_10_3*j[1]*HS1*HS2) for j
in mybase2])
```

Out[85]: (0, 0, 0, -3, -2, 1, -17, 5, 0, 0, 5)

In [86]:
```
intersection_matrix.inverse()*vector([tor.integrate(G4_5_m6*j[1]*HS1*HS2) for j
in mybase2])
```

Out[86]: (0, 0, 0, -12, -3, -6, -3, 0, 0, 5, 0)

In [87]:
```
intersection_matrix.inverse()*vector([tor.integrate(G4_5_m1*j[1]*HS1*HS2) for j
in mybase2])
```

Out[87]: (5, 5, 5, 15, 25, -5, 0, -5, -10, 0, -5)

In [88]:
```
intersection_matrix.inverse()*vector([tor.integrate(G4_5_4*j[1]*HS1*HS2) for j
in mybase2])
```

Out[88]: (20, 5, 0, 31, -21, 13, -56, 30, -5, 0, 5)

In [89]:
```
intersection_matrix.inverse()*vector([tor.integrate(G4_non_flat*j[1]*HS1*HS2) f
or j in mybase2])
```

Out[89]: (0, 0, -1, -1, -1, 1, 0, 0, 1, -1, 1)

In [90]:
```
intersection_matrix.inverse()*vector([tor.integrate(\
(Ch2 + G4_U1 - G4_10_m2 - G4_5_4 + G4_non_flat)\
*j[1]*HS1*HS2) for j in mybase2])
```

Out[90]: (-16, 18, 22, -32, 22, -34, 34, -24, 8, -6, -2)

In [91]:
```
_/2
```

Out[91]: (-8, 9, 11, -16, 11, -17, 17, -12, 4, -3, -1)

In [92]:
```
#The four flux G4_non_flat localises only to the non-flat fiber

vector([tor.integrate(G4_non_flat*j[1]*HS1*HS2) for j in mybase2])
```

Out[92]: (0, 0, 0, 0, 0, 0, 0, 0, 1, 0, 1)

Finally show that remaining part of 2nd Chern class is even

In [93]:
```
c1B, c2B = [((1+Z3)^4).part_of_degree(i) for i in [1,2]]
```

In [94]:
```
Ch2_0 = 6*c1B*(c1B - n*Z3 + S + U) + (c2B - c1B^2) #- (n*Z3)*(S - U - c1B - n*Z
3)
```

In [95]:
```
intersection_matrix.inverse()*vector([tor.integrate((Ch2 - Ch2_0 + G4_U1 + G4_1
0_m2 + G4_5_4 + G4_non_flat)*bas_i[1]*HS1*HS2) for bas_i in mybase2])
```

Out[95]:
```
(10, 4, -2, 18, -8, -14, -66, 26, -2, -6, 8)
```

Appendix B

The accidental isomorphism

In this appendix we review one of the so-called accidental isomorphisms, namely $Spin(3,3;\mathbb{R}) \cong SL(4;\mathbb{R})$. This is done by showing that the following homomorphism is a double cover:

$$SL(4;\mathbb{R}) \to SO(3,3;\mathbb{R})^+ \tag{B.1}$$

To this end choose a basis

$$\mathbb{R}^4 = \langle e_1, ..., e_4 \rangle. \tag{B.2}$$

We can now choose basis elements of $\Lambda^2\mathbb{R}^4$:

$$\{e_{23}, -e_{13}, e_{12}, e_{14}, e_{24}, e_{34}\}, \tag{B.3}$$

where $e_{ij} = e_i \wedge e_j$. A scalar product is given by

$$\langle x, y \rangle e_1 \wedge ... \wedge e_4 = x \wedge y, \quad x, y \in \Lambda^2\mathbb{R}^4 \tag{B.4}$$

If we let $SL(4;\mathbb{R})$ act on e_i by matrix multiplication, this induces an action on $\Lambda^2\mathbb{R}^4$ which explicitly is

$$A \cdot (e_i \wedge e_j) = (Ae_i) \wedge (Ae_j). \tag{B.5}$$

Note that $-A$ has exactly the same action. Because

$$(Ae_1) \wedge (Ae_2) \wedge (Ae_3) \wedge (Ae_4) = \mathrm{Det}(A) e_1 \wedge ... \wedge e_4 = e_1 \wedge ... \wedge e_4, \tag{B.6}$$

the scalar product specified above is left invariant. To make the connection to $SO^+(3,3;\mathbb{R})$ we use the expansion

$$A \cdot e_{ij} = \sum_{kl} B_{ij,kl} e_{kl}. \tag{B.7}$$

We have introduced a 6×6 matrix B, which as it turns out is an element of $SO^+(3,3;\mathbb{R})$. Note that $\pm A$ lead to the same B, implying that the homorphism will be a double cover. Also $\Lambda^2\mathbb{R}^4$ is the fundamental representation of $SO^+(3,3;\mathbb{R})$. The scalar product is again invariant under this action. We calculate:

$$\langle e_{14}, e_{23} \rangle = 1 \quad \langle e_{24}, -e_{13} \rangle = 1 \quad \langle e_{34}, e_{12} \rangle = 1, \tag{B.8}$$

where all other possible values for $\langle e_{ij}, e_{kl}\rangle = 0$. In matrix notation

$$\eta = \left(\begin{array}{ccc|ccc} 0 & 0 & 0 & 1 & 0 & 0 \\ 0 & 0 & 0 & 0 & 1 & 0 \\ 0 & 0 & 0 & 0 & 0 & 1 \\ \hline 1 & 0 & 0 & 0 & 0 & 0 \\ 0 & 1 & 0 & 0 & 0 & 0 \\ 0 & 0 & 1 & 0 & 0 & 0 \end{array}\right) . \tag{B.9}$$

The statement that B leaves the scalar product invariant is simply

$$B^T \eta B = \eta, \tag{B.10}$$

thus $B \in O(3,3;\mathbb{R})$. Since it is conatined in the image of a homorphism from the connected Lie group $SL(4;\mathbb{R})$, we can say $B \in SO^+(3,3;\mathbb{R})$.
It is useful to display all generators of $SO^+(3,3;\mathbb{R})$:

$$\left(\begin{array}{c|c} R & \\ \hline & 1 \end{array}\right) \in SL(4;\mathbb{R}) , \tag{B.11}$$

with $R \in SL(3;\mathbb{R})$ maps to

$$\left(\begin{array}{c|c} (R^{-1})^T & 0 \\ \hline 0 & R \end{array}\right) . \tag{B.12}$$

On the other hand

$$\left(\begin{array}{ccc|c} 1 & 0 & 0 & a \\ 0 & 1 & 0 & b \\ 0 & 0 & 1 & c \\ \hline 0 & 0 & 0 & 1 \end{array}\right) \tag{B.13}$$

yields

$$\left(\begin{array}{c|c} \mathbb{1} & \omega \\ \hline 0 & \mathbb{1} \end{array}\right) , \tag{B.14}$$

where

$$\omega = \left(\begin{array}{ccc} 0 & c & -b \\ -c & 0 & a \\ b & -a & 0 \end{array}\right) . \tag{B.15}$$

Contrarily

$$\left(\begin{array}{ccc|c} 1 & 0 & 0 & 0 \\ 0 & 1 & 0 & 0 \\ 0 & 0 & 1 & 0 \\ \hline a & b & c & 1 \end{array}\right) \tag{B.16}$$

goes to

$$\left(\begin{array}{c|c} \mathbb{1} & 0 \\ \hline -\omega & \mathbb{1} \end{array}\right) . \tag{B.17}$$

Appendix C

The derived category of quasi-coherent sheaves

C.1 Origin of the derived category description

In this section we state some facts about branes in IIB theory viewed as elements of the derived category of quasi-coherent sheaves. We follow [73]. Many details are given can also be found in [14].

When writing down the general action for the (2,2) SCFT there are two natural ways to 'twist' it called A- and B-model [74, 75]. These have one supercharge Q. When computing correlation functions it suffices to consider operators in Q-cohomology. When considering the closed string one finds for the A-model this is equivalent to elements of $H^{\text{even}}(Y;\mathbb{C})$, where Y is the Calabi-Yau threefold in the target space. Upon including boundaries, i.e. D-branes one arrives at the Fukaya category of Y [1].

On the other hand for the B-model one finds Q-cohomology equivalent to Dolbeault cohomology valued in exterior powers of the tangent bundle

$$H^{0,q}_{\bar{\partial}}(X, \Lambda^p T_X), \tag{C.1}$$

with X the target Calabi-Yau manifold. Deformations of the action live in $H^{0,1}(X, T_X)$ which corresponds to complex structure deformations in the target space.

If we now include boundaries we find D-branes to be equivalent to submanifolds $L \subset X$ with gauge bundles E on them. Appropriate boundary states now lie in $H^q(X, \text{End}(E))$ for strings with two endpoints on the same brane. For strings stretched between (L_1, E_1) and (L_2, E_2) we find states in $H^q(X, \text{Hom}(E_1, E_2))$. There is however one problem with this description of D-branes: Mirror symmetry fails because the category of submanifolds with gauge bundles is too small. Thus Kontsevich proposed homological mirror symmetry [76]

[1] The objects are easy to describe, the morphisms extremely hard

which can only be achieved by expanding the category of B-branes to the derived category of quasi-coherent sheaves.

The BRST symmetry Q induces a grading of operators by ghost number. One can freely attach ghost numbers to (basic) D-branes as well, similarly to the Fukaya category[2]. The refined notion of D-branes in the B-model is an object in the derived category of quasi-coherent sheaves

$$\ldots \xrightarrow{d_{n-1}} \mathcal{E}_n \xrightarrow{d_n} \mathcal{E}_{n+1} \xrightarrow{d_{n+1}} \mathcal{E}_{n+2} \xrightarrow{d_{n+2}} \ldots , \tag{C.2}$$

where each $\mathcal{E}_i$ corresponds to a basic D-brane with ghost number i[3]. (C.2) is a complex meaning

$$d_{i+1} \circ d_i = 0. \tag{C.3}$$

A D-brane with only one ghost number is represented by a complex with infinitely many zeros

$$\ldots \xrightarrow{0} 0 \xrightarrow{0} \mathcal{E} \xrightarrow{0} 0 \xrightarrow{0} \ldots \tag{C.4}$$

In general all complexes are infinitely long, but we choose not to display any zeros.

Open string states[4] correspond to elements in

$$\mathrm{Ext}^q(\mathcal{F}_\bullet, \mathcal{G}_\bullet). \tag{C.5}$$

Very importantly we have in the derived category

$$\mathrm{Ext}^q(\mathcal{F}_\bullet, \mathcal{G}_\bullet) = \mathrm{Hom}(\mathcal{F}_\bullet, \mathcal{G}_\bullet[q]), \tag{C.6}$$

where $\mathcal{G}_i[q] = \mathcal{G}_{i-q}$. We will use this simple prescription to perform a sample computation in the case of the conifold later, but first some further remarks on derived categories.

Morphisms in the derived category correspond to an infinite collection of equivalence classes of maps $([f_i])$ such that

$$\begin{array}{ccccccccccc}
\ldots & \xrightarrow{e_{i-2}} & \mathcal{E}_{i-1} & \xrightarrow{e_{i-1}} & \mathcal{E}_i & \xrightarrow{e_i} & \mathcal{E}_{i+1} & \xrightarrow{e_{i+1}} & \ldots \\
 & & \downarrow{\scriptstyle f_{i-1}} & \swarrow{\scriptstyle k_i} & \downarrow{\scriptstyle f_i} & \swarrow{\scriptstyle k_{i+1}} & \downarrow{\scriptstyle f_{i+1}} & & \\
\ldots & \xrightarrow{g_{i-2}} & \mathcal{G}_{i-1} & \xrightarrow{g_{i-1}} & \mathcal{G}_i & \xrightarrow{g_i} & \mathcal{G}_{i+1} & \xrightarrow{g_{i+1}} & \ldots
\end{array}$$

commutes. In addition we have

$$f_i \sim f_i - g_{i-1}k_i + k_{i+1}e_i. \tag{C.7}$$

[2]Essentially the A-model can only compute relative ghost numbers for states mediating between different D-branes.

[3]The assignment of ghost number to D-branes comes from the A-model, where it is only possible to compute relative ghosts numbers of general states.

[4]Note that elements in $\mathrm{Ext}^q(\mathcal{F}_i, \mathcal{G}_j)$ are assigned ghost number $q + j - i$. This will not matter to us in the following.

The k morphisms are called homotopy. As mentioned above the identification

$$\mathrm{Ext}^q(\mathcal{F}_\bullet, \mathcal{G}_\bullet) = \mathrm{Hom}(\mathcal{F}_\bullet, \mathcal{G}_\bullet[q]), \tag{C.8}$$

allows us to compute the Ext groups quite nicely, as we demonstrate in the next section.

C.2 Non-commutative crepant resolution of the conifold

We follow the presentation in [39]. For the conifold one can compute the Ext-groups using its so-called non-commutative crepant resolution [77]. To explain what this means we first define a ring A

$$A = \mathrm{End}(M \oplus R), \tag{C.9}$$

where $R = \mathbb{C}[\xi, u, w, \sigma]/\langle \xi^2 - u^2 - \sigma w \rangle$ and M is

$$M = \mathrm{coker}\left(\psi : R^2 \longrightarrow R^2\right). \tag{C.10}$$

The map ψ is specified by

$$\psi = \begin{pmatrix} \xi + u & \sigma \\ w & \xi - u \end{pmatrix}. \tag{C.11}$$

Observe that similarly we could choose

$$M = \mathrm{coker}\left(\phi : R^2 \longrightarrow R^2\right), \tag{C.12}$$

with

$$\phi = \begin{pmatrix} \xi - u & -\sigma \\ -w & \xi + u \end{pmatrix}. \tag{C.13}$$

A crucial point in the theory of non-commutative resolutions is the identity

$$\phi\psi = \psi\phi = (\xi^2 - u^2 - \sigma w) \begin{pmatrix} 1 & 0 \\ 0 & 1 \end{pmatrix}. \tag{C.14}$$

This allows one to infer that A is (bounded) derived equivalent to $Y_\pm$, which means

$$D^b(\mathrm{Mod}(A)) \cong D^b(\mathrm{QCoh}(Y_\pm)), \tag{C.15}$$

cf. Theorem 5.1 in [77]. These categories are bounded implying that the complexes are of finite length. The category of A-modules (i.e. representations of A) is easily described using quivers.

Let

$$A \cong \mathrm{Hom}(M, M) \oplus \mathrm{Hom}(M, R) \oplus \mathrm{Hom}(R, M) \oplus \mathrm{Hom}(R, R)$$

$$\cong \langle e_1 \rangle \oplus \langle \beta_1, \beta_2 \rangle \oplus \langle \alpha_1, \alpha_2 \rangle \oplus \langle e_0 \rangle. \tag{C.16}$$

Pictorially

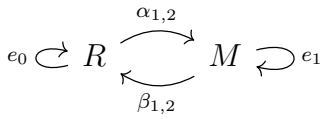

The two basic representations are

$$P_0 = e_0 A = \{\text{Paths ending on the left node}\} \tag{C.17}$$
$$P_1 = e_1 A = \{\text{Paths ending on the right node}\}. \tag{C.18}$$

Assigning

$$P_0 \mapsto \mathcal{O} \tag{C.19}$$
$$P_1 \mapsto \mathcal{O}(1), \tag{C.20}$$

we can convert these to sheaves.

The orientifold involution maps $P_i \to P_{1-i}$, i.e. it interchanges P_0 and P_1.

C.3 Sample computation of Ext groups

Let us compute all morphisms between

$$\begin{aligned} G_0 &= P_0 \xrightarrow{\alpha_1} P_1 \\ G_1 &= P_1 \xrightarrow{\beta_1} P_0 \end{aligned} \tag{C.21}$$

Firstly an element of $\mathrm{Hom}(G_0, G_1)$ is given by the equivalence class of maps f_1, f_2 such that

$$\begin{array}{ccc} P_0 & \xrightarrow{\alpha_1} & P_1 \\ \downarrow{\scriptstyle f_1} & \swarrow{\scriptstyle g} & \downarrow{\scriptstyle f_2} \\ P_1 & \xrightarrow{\beta_1} & P_0 \end{array}$$

commutes. In addtion we have the identification called homotopy

$$f_2 \sim f_2 - \beta_1 \circ g. \tag{C.22}$$

The diagram commuting means

$$f_2 \circ \alpha_1 = \beta_1 \circ f_1, \tag{C.23}$$

implying

$$f_1 = x\alpha_1, \quad f_2 = \beta_1 x, \tag{C.24}$$

for some $x \in \mathbb{C}$. This immediately forces $g = x$. Thus we obtain

$$f_2 \sim f_2 - \beta_1 x = 0, \tag{C.25}$$

that is

$$\mathrm{Ext}^0(G_0, G_1) = 0. \tag{C.26}$$

Proceeding to $\mathrm{Ext}^1(G_0, G_1)$ we consider

$$\begin{array}{ccc} P_0 & \xrightarrow{\alpha_1} & P_1 \\ {\scriptstyle g_1}\swarrow & \downarrow{\scriptstyle f_1} & \swarrow{\scriptstyle g_2} \\ P_1 & \xrightarrow{\beta_1} & P_0 \end{array}$$

Generically we have

$$\begin{aligned} f_1 &\in \mathbb{C}[\alpha_i \beta_j] \\ g_1 &\in \mathbb{C}[\alpha_1, \alpha_2] \\ g_2 &\in \mathbb{C}[\beta_1, \beta_2] \end{aligned} \tag{C.27}$$

Again we identify

$$f_1 \sim f_1 - \beta_1 g_1 + g_2 \alpha_1, \tag{C.28}$$

leading to

$$[f] \in \mathbb{C}[\alpha_2 \beta_2] = \mathrm{Ext}^1(G_0, G_1). \tag{C.29}$$

Obviously these complexes only have two non-zero entries, thus

$$\mathrm{Ext}^i(G_0, G_1) = 0, \quad \forall i \geq 2. \tag{C.30}$$

Appendix D

Weak coupling limit and orientifolds

In this appendix we give some more background on the weak coupling limit of F-theory, which is an orientifold compactification of IIB. Further we make some remarks regarding Chan-Paton factors in the orientifolded conifold.

D.1 Weak coupling limit

Let us study the weak coupling limit of F-theory [43], following [30]. Consider as base space $[u, v] \in \mathbb{P}^1$, i.e. as total space the K3 surface. The Weierstrass model is given by

$$y^2 = x^3 + f(u, v)xz^4 + g(u, v)z^6. \tag{D.1}$$

Restricting to the patch $z = 1, v = 1$ we have

$$y^2 = x^3 f(u)x + g(u), \tag{D.2}$$

as well as

$$\Delta = 27g^2 + 4f^3, \quad j(\tau) = \frac{4(24f)^3}{\Delta}. \tag{D.3}$$

If we choose a polynomial $p(u) = \Pi(u - u_i)$ of degree 4 and set

$$f = \alpha p^2, \quad g = p^3, \tag{D.4}$$

we obtain from (D.3)

$$\Delta = (4\alpha^3 + 27)\Pi(u - u_i)^6, \tag{D.5}$$

as well as

$$j(\tau) = \frac{4(24\alpha)^3}{27 + 4\alpha^3} \to \infty, \quad \alpha \to -\sqrt[3]{3/4}. \tag{D.6}$$

Thus in this limit we have $\tau \to i\infty$ corresponding to $g_{\text{IIB}} \to 0$, thus weak coupling limit. However we still have monodromies around the u_i. These are given by the $SL(2; \mathbb{Z})$ elements

$$\begin{pmatrix} -1 & 0 \\ 0 & -1 \end{pmatrix}. \tag{D.7}$$

These insertions can be seen to correspond to an orientifold seven plane of charge -4 with four D7-branes on top. This is reflected by the decomposition

$$\begin{pmatrix} -1 & 0 \\ 0 & -1 \end{pmatrix} = \mathbf{A}^4\mathbf{BC}, \tag{D.8}$$

where

$$\mathbf{A} = \begin{pmatrix} 1 & 1 \\ 0 & 1 \end{pmatrix}, \quad \mathbf{B} = \begin{pmatrix} 2 & 1 \\ -1 & 0 \end{pmatrix}, \quad \mathbf{C} = \begin{pmatrix} 0 & 1 \\ -1 & 2 \end{pmatrix}. \tag{D.9}$$

The product $\mathbf{BC} = -\mathbf{A}$ and corresponds to two D7-branes combining into an O7 plane.

Quantities such as the holomorphic top-form are not single valued around such a point. The solution is to move to the covering space of $\mathbb{P}^1$:

$$\xi^2 = p(u, v), \tag{D.10}$$

which with the scaling relations $(u, v, \xi) \sim (\lambda u, \lambda v, \lambda^2 \xi)$ can be seen to be Calabi-Yau. The orientifold involution is $\xi \leftrightarrow -\xi$ whence $\xi = 0$ is the location of the O7 planes.

It is now straightforward to generalize this to general Calabi-Yau fourfolds

$$y^2 = x^3 + fx + g, \tag{D.11}$$

with $f \in \mathcal{O}(4\bar{K}_B)$ and $g \in \mathcal{O}(6\bar{K}_B)$. Using polynomials h, η, χ of appropriate degree

$$f = 3h^2 + \epsilon\eta, \qquad g = 2h^3 + \epsilon h\eta\epsilon^2\chi/12, \tag{D.12}$$

we plug into (D.3). In the limit $\epsilon \to 0$ we obtain:

$$\Delta = -9\epsilon^2 h^2(\eta^2 - h\chi) \tag{D.13}$$

as well as

$$j(\tau) = \frac{24^4}{4} \frac{h^4}{\epsilon^2(\eta^2 - h\chi)}. \tag{D.14}$$

Again as $\epsilon \to 0$ we have

$$g_{\text{IIB}} \to 0, \tag{D.15}$$

except for $h = 0$. Thus we identify the orientifold locus as $h = 0$. The D7-branes wrap the remaining part of Δ

$$\eta^2 - h\chi = 0. \tag{D.16}$$

Again the double cover

$$\xi^2 = h \tag{D.17}$$

is Calabi-Yau, and can be used to consider the IIB theory. The orientifold action is $\xi \to -\xi$ as before.

D.2 Orientifold of the conifold

We now analze the conifold singularity

$$\xi^2 = u^2 + w\sigma \tag{D.18}$$

in more detail. Firstly notice that the homogeneous toric coordinates $\alpha_1, \alpha_2, \beta_1, \beta_2$ are given by

$$(\xi, u, w, \sigma) = (\frac{1}{2}(\alpha_1\beta_2 + \alpha_2\beta_1), \frac{1}{2}(\alpha_1\beta_2 - \alpha_2\beta_1), \alpha_2\beta_2, -\alpha_1\beta_1). \tag{D.19}$$

The (resolved) conifold is defined via the moment map

$$|\alpha_1|^2+|\alpha_2|^2-|\beta_1|^2-|\beta_2|^2= t, \tag{D.20}$$

where $|t|$ is related to the volume of the resolution $\mathbb{P}^1$ and the sign determines the complex structure.

The theory with D3-branes probing the conifold singularity was originally studied by Klebanov and Witten [78]. It can be summarized as a quiver

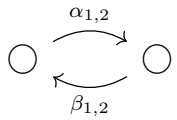

Each node carries gauge group $SU(N)$ for N coincident D3-branes. The α_i are elements of the representations $(\square, \bar{\square})$. The β_i live in $(\bar{\square}, \square)$.

The superpotential is

$$W \sim \epsilon^{ij}\epsilon^{lm}\mathrm{Tr}(\alpha_i\beta_l\alpha_j\beta_m). \tag{D.21}$$

The orientifold involution we are interested in acts as

$$\alpha_1 \leftrightarrow -\beta_1, \quad \alpha_2 \leftrightarrow -\beta_2, \tag{D.22}$$

which implies $\xi \leftrightarrow -\xi$. The resulting gauge theory is simply

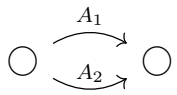

The potential is

$$W \sim \epsilon^{ij}\epsilon^{lm}\mathrm{Tr}(\gamma_G\alpha_i\gamma_G\alpha_l^T\gamma_G\alpha_j\gamma_G\alpha_m^T), \tag{D.23}$$

where $\gamma_k = \sigma_2^{\oplus n}$ and σ_2 the second Puali matrix. This corresponds to gauge group $USp(N)$ on the nodes.

This fact is important as $D(-1)$ instantons receive the opposite factors and therefore carry gauge group $SO(N)$ see chapter 2.2 of [79] and references therein. This allows us to cancel the two neutral fermionic zero modes associated with a broken supersymmetry usually denoted by τ_μ. The two remaining fermionic zero modes θ_α are associated with the surviving supersymmetry and allow for a superpotentatial contribution.

Appendix E

Calculation of the determinant of the metric

In this appendix we calculate the determinant of (3.38).

Observe that from the general structure of the metric

$$ds^2 = q(\alpha+\mu)ds^2_{FS} + \sum_{k=1}^{s-1} c_k(a_k+\mu)\pi_k^*(ds_k^2) + \frac{1}{|u|^2 H_{\mu\mu}}\,|du+uA|^2, \tag{E.1}$$

we immediately get

$$\det g = \frac{1}{|u|^2 H_{\mu\mu}} \frac{(q(\alpha+\mu))^{q-1}}{(1+|\vec{z}|^2)^q} \det\left(g^{(\mu)}_{\rm red}\right)\,, \tag{E.2}$$

with $g^{(\mu)}_{\rm red}$ given by

$$ds^2_{\mathscr{F}^2} = \sum_{k=1}^{s-1} c_k(a_k+\mu)\pi_k^*(ds_k^2)\,. \tag{E.3}$$

We now consider the coordinate patch on $GL(n;\mathbb{C})/P_{n_1,\ldots,n_s}$ where the matrix W can be brought into (block) lower triangular form. At the point $W=1$ we obtain

$$\begin{aligned}\pi_k^*(ds_k^2)|_{W=1} &= \sum_{k=1}^{s-1} c_k(a_k+\mu) \sum_{j=m_k+1}^{n}\sum_{i=1}^{m_k}|dw_{ji}|^2 \\ &= \sum_{i=1}^{s-1}\sum_{j=i+1}^{s}(\sum_{k=i}^{j-1} c_k(a_k+\mu)) \sum_{a=m_{j-1}+1}^{m_j}\sum_{b=m_{i-1}+1}^{m_i}|dw_{ab}|^2. \end{aligned}\tag{E.4}$$

Therefore the determinant at the identity is given by

$$\det g^{(\mu)}_{\rm red}|_{W=1} = \prod_{1\le i<j\le s}\left(\sum_{k=i}^{j-1}(a_k+c_k\mu)\right)^{n_i n_j} =: f(\mu) \tag{E.5}$$

In general the determinant is $SU(n)$ invariant and thus takes the form

$$\det g_{\mathrm{red}}^{(\mu)} = \xi(w_{ij}, \bar{w}_{ij}) f(\mu). \tag{E.6}$$

ξ can be further specified as follows: In the limit $\mu \to \infty$ we have $g_{\mathrm{red}}^{(\mu)} \to \mu\, g_{KE}$, with g_{KE} the Kähler-Einstein described in (3.34). Its Kähler potential is of the form $\sum c_k \log t_k$ and $Ric = g_{KE}$. Therefore up to some holomorphic κ:

$$\xi\left(w_{mi}, \bar{w}_{mi}\right) = \left|\kappa(w_{mi})\right|^2 e^{-\sum c_k \log t_k} = \left|\kappa(w_{mi})\right|^2 \frac{1}{\prod_k t_k^{c_k}}\,, \tag{E.7}$$

Bibliography

[1] I. Achmed-Zade, M. J. D. Hamilton, D. Lüst, and S. Massai, "A note on T-folds and T3 fibrations," *Journal of High Energy Physics* **2018** no. 12, (Dec, 2018) . http://dx.doi.org/10.1007/JHEP12(2018)020.

[2] R. Blumenhagen, D. Lüst, and S. Theisen, *Basic concepts of string theory*. Theoretical and Mathematical Physics. Springer, Heidelberg, Germany, 2013. http://www.springer.com/physics/theoretical%2C+mathematical+%26+computational+physics/book/978-3-642-29496-9.

[3] A. Giveon, M. Porrati, and E. Rabinovici, "Target space duality in string theory," *Phys.Rept.* **244** (1994) 77–202, arXiv:hep-th/9401139 [hep-th].

[4] P. Bouwknegt, J. Evslin, and V. Mathai, "T-duality: Topology change from h-flux," *Communications in Mathematical Physics* **249** no. 2, (Jun, 2004) 383415. http://dx.doi.org/10.1007/s00220-004-1115-6.

[5] D. Lüst, S. Massai, and V. Vall Camell, "The monodromy of T-folds and T-fects," *JHEP* **09** (2016) 127, arXiv:1508.01193 [hep-th].

[6] B. R. Greene, A. D. Shapere, C. Vafa, and S.-T. Yau, "Stringy Cosmic Strings and Noncompact Calabi-Yau Manifolds," *Nucl.Phys.* **B337** (1990) 1.

[7] J. A. Harvey and S. Jensen, "Worldsheet instanton corrections to the Kaluza-Klein monopole," *JHEP* **10** (2005) 028, arXiv:hep-th/0507204 [hep-th].

[8] H. Ooguri and C. Vafa, "Summing up D instantons," *Phys.Rev.Lett.* **77** (1996) 3296–3298, arXiv:hep-th/9608079 [hep-th].

[9] M. Gross and P. M. H. Wilson, "Large Complex Structure Limits of K3 Surfaces," *ArXiv Mathematics e-prints* (Aug., 2000) , math/0008018.

[10] D. Lüst, E. Plauschinn, and V. Vall Camell, "Unwinding strings in semi-flatland," *JHEP* **07** (2017) 027, arXiv:1706.00835 [hep-th].

[11] M. Gross, "Topological mirror symmetry," 1999. https://arxiv.org/abs/math/9909015.

[12] W.-D. Ruan, "Lagrangian torus fibration of quintic calabi-yau hypersurfaces i: Fermat quintic case," arXiv:math/9904012 [math.DG].

[13] D. R. Morrison, "On the structure of supersymmetric T3 fibrations," *ArXiv e-prints* (Feb., 2010) , arXiv:1002.4921 [math.AG].

[14] Aspinwall, Bridgeland, Craw, Douglas, Gross, Kapustin, Segal, Sendroi, and Wilson, *Dirichlet Branes and Mirror Symmetry*, vol. 4. American Mathematical Society, 2009.

[15] J. T. Liu and R. Minasian, "U-branes and T**3 fibrations," *Nucl.Phys.* **B510** (1998) 538–554, arXiv:hep-th/9707125 [hep-th].

[16] R. Donagi, P. Gao, and M. B. Schulz, "Abelian Fibrations, String Junctions, and Flux/Geometry Duality," *JHEP* **04** (2009) 119, arXiv:0810.5195 [hep-th].

[17] A. Malmendier and D. R. Morrison, "K3 surfaces, modular forms, and non-geometric heterotic compactifications," *Lett. Math. Phys.* **105** no. 8, (2015) 1085–1118, arXiv:1406.4873 [hep-th].

[18] A. Font, I. García-Etxebarria, D. Lüst, S. Massai, and C. Mayrhofer, "Heterotic T-fects, 6D SCFTs, and F-Theory," *JHEP* **08** (2016) 175, arXiv:1603.09361 [hep-th].

[19] Y. Namikawa and K. Ueno, "The complete classification of fibres in pencils of curves of genus two," *Manuscripta Math.* **9** no. 2, (1973) 143–186. http://dx.doi.org/10.1007/BF01297652.

[20] A. B. Altman and S. L. Kleiman, *The presentation functor and the compactified Jacobian*, pp. 15–32. Birkhäuser Boston, Boston, MA, 2007. http://dx.doi.org/10.1007/978-0-8176-4574-8_2.

[21] J. Kass, "Notes on compactified jacobian," 2008. http://people.math.sc.edu/kassj/Lecture%20Notes%20on%20Compactified%20Jacobians.pdf.

[22] B. Farb and D. Margalit, *A Primer on Mapping Class Groups*. Princeton University Press, 2011.

[23] P. Candelas, A. Constantin, C. Damian, M. Larfors, and J. F. Morales, "Type IIB flux vacua from G-theory II," *JHEP* **1502** (2015) 188, arXiv:1411.4786 [hep-th].

[24] I. Achmed-Zade, I. Garcia-Etxebarria, and C. Mayrhofer, "A note on non-flat points in the SU(5)x U(1)PQ F-theory model," *Journal of High Energy Physics* **2019** no. 5, (May, 2019) . http://dx.doi.org/10.1007/JHEP05(2019)013.

[25] C. Mayrhofer, E. Palti, and T. Weigand, "U(1) symmetries in F-theory GUTs with multiple sections," *JHEP* **1303** (2013) 098, arXiv:1211.6742 [hep-th].

[26] J. Marsano, N. Saulina, and S. Schafer-Nameki, "Compact F-theory GUTs with U(1)(PQ)," *JHEP* **1004** (2010) 095, arXiv:0912.0272 [hep-th].

[27] M. J. Dolan, J. Marsano, and S. Schfer-Nameki, "Unification and lhc phenomenology of f-theory guts with u(1) p q," *Journal of High Energy Physics* **2011** no. 12, (Dec, 2011) . http://dx.doi.org/10.1007/JHEP12(2011)032.

[28] C. Vafa, "Evidence for F theory," *Nucl.Phys.* **B469** (1996) 403–418, arXiv:hep-th/9602022 [hep-th].

[29] T. Weigand, "F-theory," *PoS* **TASI2017** (2018) 016, arXiv:1806.01854 [hep-th].

[30] F. Denef, "Les Houches Lectures on Constructing String Vacua," arXiv:0803.1194 [hep-th].

[31] K. Kodaira, "On compact analytic surfaces I-III," *Ann. of Math.,* **71** (1960), 111–152; **77** (1963), 563–626; **78** (1963), 1–40 .

[32] D. R. Morrison and D. S. Park, "F-Theory and the Mordell-Weil Group of Elliptically-Fibered Calabi-Yau Threefolds," *JHEP* **1210** (2012) 128, arXiv:1208.2695 [hep-th].

[33] P. Arras, A. Grassi, and T. Weigand, "Terminal Singularities, Milnor Numbers, and Matter in F-theory," *J. Geom. Phys.* **123** (2018) 71–97, arXiv:1612.05646 [hep-th].

[34] A. Grassi and T. Weigand, "On topological invariants of algebraic threefolds with ($\mathbb{Q}$-factorial) singularities," arXiv:1804.02424 [math.AG].

[35] T. Shioda, "Mordell-Weil Lattices and Galois Representation. I," *Proc. Japan Acad.* **A65** (1989) 268–271.

[36] R. Wazir, "Arithmetic on elliptic threefolds," *Compos.Math.* **140** (2001) 567–580, arXiv:math.NT/0112259.

[37] E. Witten, "On flux quantization in M theory and the effective action," *J.Geom.Phys.* **22** (1997) 1–13, arXiv:hep-th/9609122 [hep-th].

[38] D. S. Freed and E. Witten, "Anomalies in string theory with D-branes," arXiv:hep-th/9907189 [hep-th].

[39] A. Collinucci and I. Garca-Etxebarria, "E_6 Yukawa couplings in F-theory as D-brane instanton effects," *JHEP* **03** (2017) 155, arXiv:1612.06874 [hep-th].

[40] S. Krause, C. Mayrhofer, and T. Weigand, "Gauge fluxes in f-theory and type iib orientifolds," *Journal of High Energy Physics* **2012** no. 8, (Aug, 2012) . http://dx.doi.org/10.1007/JHEP08(2012)119.

[41] D. S. Park, "Anomaly Equations and Intersection Theory," *JHEP* **01** (2012) 093, arXiv:1111.2351 [hep-th].

[42] Tate J., "Algorithm for determining the type of a singular fiber in an elliptic pencil," pp. 33–52. Springer Berlin Heidelberg, 1975.

[43] A. Sen, "Orientifold limit of F theory vacua," *Phys.Rev.* **D55** (1997) 7345–7349, arXiv:hep-th/9702165 [hep-th].

[44] K. Hori, A. Iqbal, and C. Vafa, "D-branes and mirror symmetry," arXiv:hep-th/0005247 [hep-th].

[45] K. Hori and C. Vafa, "Mirror symmetry," arXiv:hep-th/0002222 [hep-th].

[46] V. Bouchard and P. Sulkowski, "Topological recursion and mirror curves," *Adv. Theor. Math. Phys.* **16** no. 5, (2012) 1443–1483, arXiv:1105.2052 [hep-th].

[47] B. Feng, Y.-H. He, K. D. Kennaway, and C. Vafa, "Dimer models from mirror symmetry and quivering amoebae," *Adv. Theor. Math. Phys.* **12** no. 3, (2008) 489–545, arXiv:hep-th/0511287 [hep-th].

[48] D. Forcella, I. Garca-Etxebarria, and A. Uranga, "E3-brane instantons and baryonic operators for D3-branes on toric singularities," *JHEP* **03** (2009) 041, arXiv:0806.2291 [hep-th].

[49] S. Franco and A. Uranga, "Bipartite Field Theories from D-Branes," *JHEP* **04** (2014) 161, arXiv:1306.6331 [hep-th].

[50] Y. Namikawa and J. H. M. Steenbrink, "Global smoothing of Calabi-Yau threefolds," *Inventiones mathematicae* **122** no. 1, (Dec, 1995) 403–419. https://doi.org/10.1007/BF01231450.

[51] W. Fulton, "Intersection Theory," *Princeton University Press 1993* .

[52] I. Achmed-Zade and D. Bykov, "Ricci-Flat Metrics on Vector Bundles Over Flag Manifolds," *Comm. Math. Phys.* **376** no. 3, (2020) 2309–2328, arXiv:1905.00412 [hep-th].

[53] A. Borel and F. Hirzebruch, "Characteristic Classes and Homogeneous Spaces, I," *American Journal of Mathematics* **80** no. 2, (1958) 458–538. http://www.jstor.org/stable/2372795.

[54] H. Azad, R. Kobayashi, and M. Qureshi, "Quasi-potentials and Kähler Einstein metrics on flag manifolds," *Journal of Algebra* **169** no. 2, (1997) 620–629.

[55] H. Azad and I. Biswas, "Quasi-potentials and Kähler Einstein metrics on flag manifolds II," *Journal of Algebra* **269** no. 2, (2003) 480–491.

[56] M. Bando, T. Kugo, and K. Yamawaki, "Nonlinear realization and hidden local symmetries," *Physics Reports* **164** no. 4 and 5, (1988) 217–314.

[57] E. Calabi, "On Kähler manifolds with vanishing canonical class," in *Algebraic geometry and topology. A symposium in honor of S. Lefschetz*, pp. 78–89. Princeton University Press, Princeton, N. J., 1957.

[58] S.-T. Yau, "Calabi's conjecture and some new results in algebraic geometry," *Proc. Natl. Acad. Sci. USA* **74** (1977) 1798–1799.

[59] S.-T. Yau, "On Ricci curvature of a compact Kähler manifold and complex Monge-Ampere equation I.," *Comm. Pure and App. Math.* **31** (1979) 339–411.

[60] C. van Coevering, "Regularity of asymptotically conical Ricci-flat Kähler metrics," `arXiv:0912.3946`.

[61] R. Goto, "Calabi-Yau structures and Einstein-Sasakian structures on crepant resolutions of isolated singularities," *J. Math. Soc. Japan* **64** no. 3, (2012) 1005–1052. `https://doi.org/10.2969/jmsj/06431005`.

[62] E. Calabi, "Métriques kählériennes et fibrés holomorphes," *Annales scientifiques de l'École Normale Supérieure* **4e série, 12** no. 2, (1979) 269–294.

[63] C. van Coevering, "Calabi-Yau metrics on canonical bundles of flag varieties," `arXiv:1807.07256 [math.DG]`.

[64] L. A. Pando Zayas and A. A. Tseytlin, "3-branes on spaces with $R \times S^2 \times S^3$ topology," *Phys.Rev.* **D63** (2001) 086006, `arXiv:hep-th/0101043 [hep-th]`.

[65] P. Candelas and X. C. de la Ossa, "Comments on Conifolds," *Nucl.Phys.* **B342** (1990) 246–268.

[66] K. Y. Lam, "A formula for the tangent bundle of flag manifolds and related manifolds," *Transactions of the American Mathematical Society* **213** (1975) 305–314. `http://www.jstor.org/stable/1998048`.

[67] V. A. Iskovskikh and Yu. G. Prokhorov, "Algebraic geometry V: Fano varieties.," in *Encyclopaedia of Mathematical Sciences, vol. 47*, A. N. Parshin, I. R. Shafarevich, and R. V. Gamkrelidze, eds. Springer, 1999.

[68] M. Brion, "Lectures on the geometry of flag varieties," in *Topics in Cohomological Studies of Algebraic Varieties: Impanga Lecture Notes*, P. Pragacz, ed., pp. 33–85. Birkhäuser Basel, Basel, 2005. `https://doi.org/10.1007/3-7643-7342-3_2`.

[69] V. Bouchard, "Toric geometry and string theory," 2006.

[70] S. H. Cox David, Little John, *Toric Varieties*, vol. 124. American Mathematical Society, 2011.

[71] V. Bouchard and H. Skarke, "Affine Kac-Moody algebras, CHL strings and the classification of tops," *Adv.Theor.Math.Phys.* **7** (2003) 205–232, arXiv:hep-th/0303218 [hep-th].

[72] V. Braun, T. W. Grimm, and J. Keitel, "Geometric Engineering in Toric F-Theory and GUTs with U(1) Gauge Factors," *JHEP* **1312** (2013) 069, arXiv:1306.0577 [hep-th].

[73] P. S. Aspinwall, "D-branes on Calabi-Yau manifolds," arXiv:hep-th/0403166 [hep-th].

[74] E. Witten, "Topological sigma models," *Comm. Math. Phys.* **118** no. 3, (1988) 411–449. https://projecteuclid.org:443/euclid.cmp/1104162092.

[75] E. Witten, "Mirror manifolds and topological field theory," 1991.

[76] M. Kontsevich, "Homological algebra of mirror symmetry," 1994.

[77] M. Van den Bergh, "Non-commutative crepant resolutions," *ArXiv Mathematics e-prints* (Nov., 2002) , math/0211064.

[78] I. R. Klebanov and E. Witten, "Superconformal field theory on threebranes at a calabi-yau singularity," *Nuclear Physics B* **536** no. 1-2, (Dec, 1998) 199218. http://dx.doi.org/10.1016/S0550-3213(98)00654-3.

[79] R. Blumenhagen, M. Cvetič, S. Kachru, and T. Weigand, "D-Brane Instantons in Type II Orientifolds," *Ann. Rev. Nucl. Part. Sci.* **59** (2009) 269–296, arXiv:0902.3251 [hep-th].

Acknowledgements

I would like to thank my supervisor Dieter Lüst for an excellent supervision over the past 5 years (including my master thesis)! This not only includes the technical side, but also his understanding during tough times. The size of the group has allowed me to foray into many different aspects of string theory.

Many thanks also go to Michael Haack for emotional support, as well as excellent lectures, on which he spends a lot of thought. I was privileged to see this process both from a students' and later an assistants' perspective and can only urge any student to attend them!

A special thank you goes to Mark Hamilton, who aquired fame in the TMP master program at the LMU, giving very interesting lectures at the intersection of math and physics. Thank you very much for all the interesting discussions, as well as the fruitful collaboration!

Even more thanks go to my day to day supervisors in chronological order: Stefano Massai, Christoph Mayrhofer, Dmitri Bykov. I can only say

- Mille Grazie!
- Merce Chef! (Bavarian pronunciation implied)
- Spassibo wam bolshoe!

Finally I thank the subgroup of the string theory group denoted by $\mathscr{N}$, for Nicos Hat. Thanks for all the good times guys!